



Cite this: *RSC Med. Chem.*, 2025, **16**, 561

## Natural peptides and their synthetic congeners acting against *Acinetobacter baumannii* through the membrane and cell wall: latest progress

Gautam Kumar 

*Acinetobacter baumannii* is one of the deadliest Gram-negative bacteria (GNB), responsible for 2–10% of hospital-acquired infections. Several antibiotics are used to control the growth of *A. baumannii*. However, in recent decades, the abuse and misuse of antibiotics to treat non-microbial diseases have led to the emergence of multidrug-resistant *A. baumannii* strains. *A. baumannii* possesses a complex cell wall structure. Cell wall-targeting agents remain the center of antibiotic drug discovery. Notably, the antibacterial drug discovery intends to target the membrane of the bacteria, offering several advantages over antibiotics targeting intracellular systems, as membrane-targeting agents do not have to travel through the plasma membrane to reach the cytoplasmic targets. Microorganisms, insects, and mammals produce antimicrobial peptides as their first line of defense to protect themselves from pathogens and predators. Importantly, antimicrobial peptides are considered potential alternatives to antibiotics. This communication summarises the recently identified peptides of natural origin and their synthetic congeners acting against the *A. baumannii* membrane by cell wall disruption.

Received 24th September 2024,  
Accepted 18th November 2024

DOI: 10.1039/d4md00745j

rsc.li/medchem

### 1. Introduction

*Acinetobacter baumannii* is a Gram-negative aerobic coccobacilli bacterium belonging to the *Moraxellaceae* family and *Acinetobacter* genus. The genus *Acinetobacter* came from the Greek word “akinetos”, meaning non-motile. It has characteristic features including non-motile, non-fastidious, and non-fermentative.<sup>1</sup> *A. baumannii* has a vast habitat, including soil, water, and food. There are more than 50 recognized *Acinetobacter* species, and most of them are non-pathogenic. The *Acinetobacter calcoaceticus*–*Acinetobacter baumannii* (Acb) complex comprises the phylogenetically most closely clinically relevant members of the *Acinetobacter* species, including *A. calcoaceticus*, *A. baumannii*, *A. nosocomialis*, *A. pittii*, *A. seifertii*, and *A. lactucae*.<sup>2</sup> Nevertheless, many *Acinetobacter* species are opportunistic human pathogens responsible for nosocomial infections. *A. baumannii* is responsible for 2–10% of hospital-acquired infections, including skin and soft tissue infections, pneumonia, urinary tract infection, bacteremia, endocarditis, and meningitis. On the other hand, *A. calcoaceticus* and *A. lwoffii* are responsible for fewer human-associated infections.<sup>3</sup> *A. baumannii* nosocomial infections are responsible for severe life-threatening complications and high morbidity and death rates. Patients with previous

illnesses such as diabetes, kidney disease, cancer, and chronic obstructive pulmonary disease are more prone to *A. baumannii* infections.<sup>4</sup> Also, a person with a habit of heavy smoking and excessive alcohol consumption frequently suffers from *A. baumannii* infections.<sup>5</sup> The most common mode of nosocomial infection transmission is frequently encountered due to medical devices used during surgical operations. *A. baumannii* colonizes medical surgical tools through biofilm formation over the surface of Foley catheters, cerebrospinal fluid shunts, and vascular catheters and becomes a source of new infections.<sup>6</sup>

#### 1.1. *A. baumannii* virulence factors

The genotypic and phenotypic analysis revealed *A. baumannii* virulence factors, including outer membrane porins, biofilm-associated protein (Bap), phospholipases, capsules, lipopolysaccharides (LPS), proteases, iron-chelating systems, penicillin-binding protein, and protein secretion systems.<sup>7</sup> The genomic studies of *Acinetobacter baylyi* led to identifying genes responsible for pilus biogenesis, iron scavenging, quorum sensing, and the type IV secretion system.<sup>8</sup> The virulence factors of *A. baumannii* allow it to survive under adverse environmental conditions and protect itself from being exposed to antimicrobials.<sup>8</sup> The virulence factors of *A. baumannii* are discussed below.

Porins present in the outer membrane of *A. baumannii* are responsible for cellular permeability in the bacteria. OmpA is a  $\beta$ -barrel porin abundantly present in the outer membrane

Department of Pharmacy, Birla Institute of Technology and Science Pilani, Pilani Campus, Rajasthan 333031, India. E-mail: gautam.kumar@pilani.bits-pilani.ac.in



of *A. baumannii*. In mammals, OmpA is responsible for the induction of apoptosis of epithelial cells by activating caspase 8 and 9. It also causes changes in cytochrome c and modulates mitochondrial activity in humans.<sup>8,9</sup> Meanwhile, the porins Omp34 and Ompw are highly immunogenic. Omp34 interacts with eukaryotic cells and induces apoptosis through a caspase-dependent mechanism. Moreover, Omp34 inhibits autophagy and promotes bacterial persistence in autophagosomes.<sup>10</sup> The concentration of glycosyltransferase (LpsB) increases during lipopolysaccharide biosynthesis in *A. baumannii* and is responsible for pathogenicity in mammals. The lipid anchor of LPS is hepta-acylated lipid A. Lipid A is the immunostimulatory component that stimulates toll-like receptor 4 (TLR4) in human cells. Also, lipid A is a crucial virulence component of the bacterial membrane and induces proinflammatory cytokine expression in humans.<sup>10,11</sup>

*A. baumannii* encodes two phospholipase C and three phospholipase D enzymes substrate-specific to the eukaryotic membrane component phosphatidylcholine. The enzymes phospholipase C and D displayed hemolytic activity against human erythrocytes. The phospholipase D

genes are also associated with serum resistance, epithelial cell invasion, and *in vivo*, pathogenesis in humans.<sup>10</sup> The *A. baumannii* capsule comprises L-rhamnose, D-glucose, D-glucuronic acid, and D-mannose, which promote its adhesion to epithelial cells and protect itself against phagocytosis.<sup>8</sup> A recent study revealed that *A. baumannii*'s thicker capsule is responsible for increased pathogenicity and antibiotic resistance. Also, thicker capsules are responsible for antimicrobial and disinfectant resistance in *A. baumannii*.<sup>12</sup> Moreover, *A. baumannii* pathogenicity depends upon the specific iron acquisition proteins, siderophores, and hemophores, which compete with host binding proteins for essential iron and are necessary for bacterial survival and growth under limited low-iron conditions.<sup>8</sup> A recent study demonstrated from their work that polymicrobial infections of *A. baumannii* and *K. pneumoniae* promote their co-existence and provide cross-protection against antibiotics.<sup>13</sup> *A. baumannii* virulence and its host response are depicted in Fig. 1.



Gautam Kumar

*Gautam Kumar is an Assistant Professor at the Department of Pharmacy, Birla Institute of Technology and Science Pilani, Pilani Campus, Rajasthan, India. He received his B. Pharm. and M. Pharm. degrees from Jamia Hamdard, Hamdard University, India. He did his PhD dissertation at the Department of Natural Products, National Institute of Pharmaceutical Education and Research (NIPER) S.A.S Nagar, Punjab, India.*

*During his PhD, he was involved in synthesizing heterocyclic compounds, including furan, thiophene, dihydroquinoline, and coumarin derivatives as potential anti-tubercular agents. He conducted post-doctoral research at the Indian Institute of Technology Bombay, India. During his post-doctoral research work, he was involved in designing and synthesising small bioactive molecules and chemical probes inspired by lipid molecules from Mycobacterium tuberculosis (M.tb), the causative agent of tuberculosis. He has developed “clickable” chemical probes based on the M.tb virulence-associated glycolipid, trehalose dimycolate, for real-time proteomics and imaging. Currently, he leads a lab in the area of Natural Products at the Department of Pharmacy, Birla Institute of Technology and Science Pilani, Pilani Campus, with a focus on bioassay-guided fractionation of extracts, isolation of natural products, phytopharmaceutical formulation development, and synthesis of biologically active molecules.*

## 1.2. *Acinetobacter baumannii* biofilm role in pathogenesis

The exopolysaccharide poly- $\beta$ -(1-6)-N-acetylglucosamine is responsible for biofilm formation in *A. baumannii*. A population of *A. baumannii* bacteria encased in the extracellular matrix on biotic or abiotic surfaces is called a biofilm, which plays a critical role in pathogenesis and provides protection from antimicrobials. The exopolysaccharide poly- $\beta$ -(1-6)-N-acetylglucosamine is also responsible for eukaryotic cell adhesion.<sup>14</sup> Biofilm-associated protein (BAP) significantly contributes to biofilm formation and is responsible for increased resistance to the immune host response. *A. baumannii*, despite lacking flagella, possesses uncharacterized surface-associated motility. The *Acinetobacter* genus produces polyamine 1,3-diamino propane, which is responsible for surface-associated motility and virulence. A GNAT-family acetyltransferase is conserved in *A. baumannii* and is responsible for regulating polyamines. Diaminopropane acetyltransferase (Dpa) performs the acetylation of polyamine 1,3-diaminopropane. It has been found that Dpa expression is upregulated in the bacteria, forming a pellicle, which helps in adhering to eukaryotic epithelial cells more than planktonic bacterial cells. Notably, deleting 1,3-diaminopropane acetyltransferase gene *dpa* enhances motility and negatively affects biofilm formation on plastic.<sup>15</sup> Moreover, the colonized *A. baumannii* biofilm is reported to cause post-neurosurgical meningitis and surgical wound infections.<sup>16</sup> The biofilm formation in *A. baumannii* is mediated by Csu pili, assembled through the “archaic” chaperone-usher pathway. The CsuC-CsuE chaperone-adhesin X-ray structure revealed hydrophobic finger-like loops at the tip of the pilus, which form attachments to the hydrophobic surface and, thus, biofilm formation can be a source of new infections.<sup>6</sup> Several findings have demonstrated the role of Csu pili in the spread of *A.*



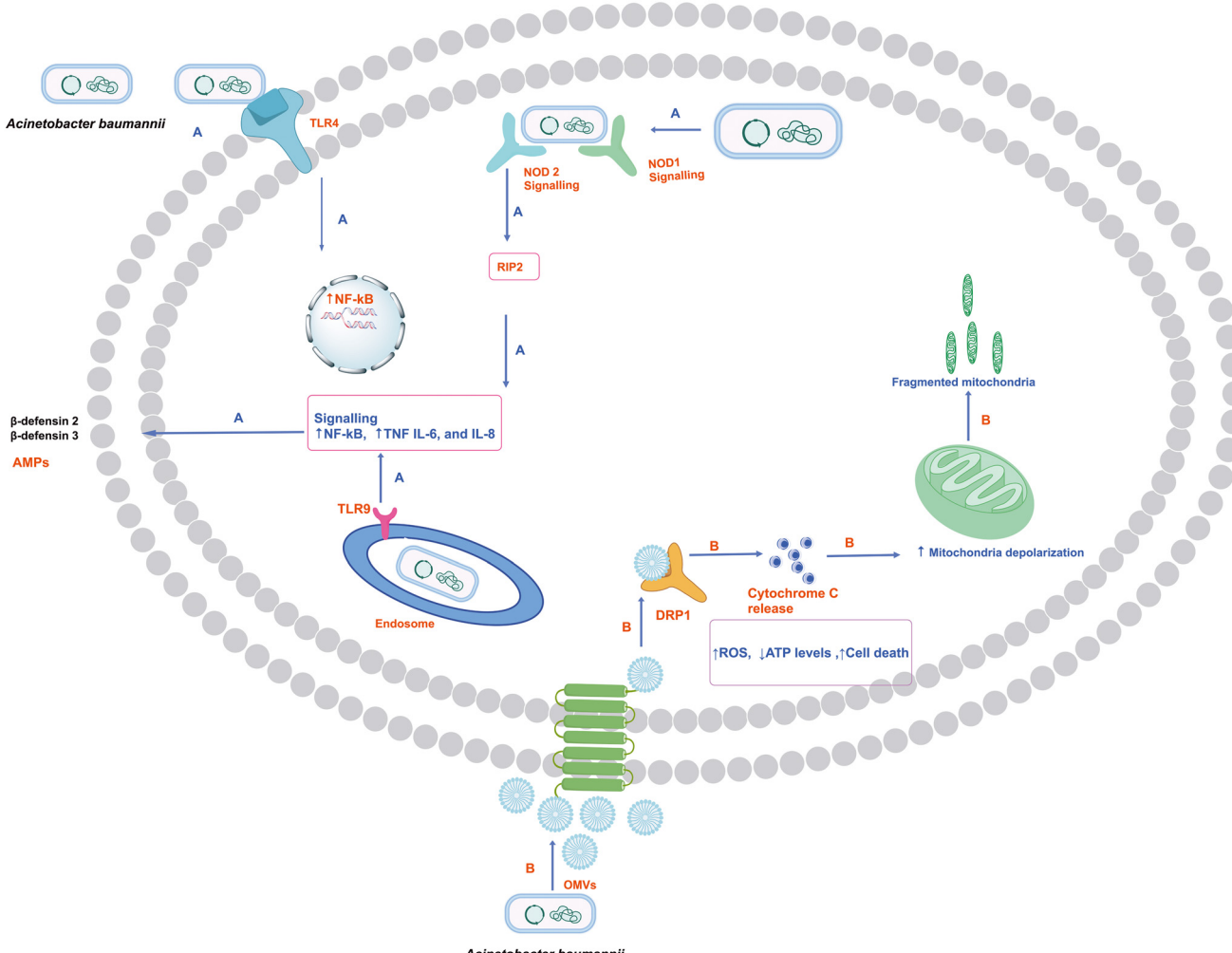


**Fig. 1** A diagrammatic representation depicting *A. baumannii* virulence and its host response. A. *A. baumannii* activates the host cell response by binding to plasma membrane-bound TLR4 and endosome-bound TLR9. Activating the TLR signaling activates the nuclear translocation of the NF- $\kappa$ B transcription factor. Also, NF- $\kappa$ B activates pattern recognition receptors NOD1 and NOD2. Furthermore, the activated NF- $\kappa$ B leads to the enhanced expressions of proinflammatory cytokines, including TNF, IL-6, and IL-8. Furthermore, NF- $\kappa$ B also increases the expressions of antimicrobial peptides (AMPs) like  $\beta$ -defensins, which inhibit the growth of *A. baumannii*. B. *A. baumannii* secretes outer membrane vesicles (OMVs) with outer membrane proteins that interact with the DRP1 host protein, causing the release of mitochondrial protein cytochrome C and fragmentation of mitochondria. OmpA enhances the release of ROS levels, decreases the ATP release, and increases the mitochondrial depolarization, and cytochrome C induces apoptotic cell death.<sup>10,11</sup>

*baumannii* through biofilm formation over the surface of medical surgical instruments.<sup>6</sup>

### 1.3. *A. baumannii* diagnosis

The conventional diagnosis of *A. baumannii* in most laboratories is carried out by cultures of pathogens. Additionally, biochemical assays and Gram staining techniques are used to identify *A. baumannii*. The detection of *A. baumannii* using a cultural method is time-consuming and laborious. Moreover, the polymerase chain reaction can identify *A. baumannii*, depending on DNA or complementary DNA amplification.<sup>17</sup> Also, antibody-based assays such as enzyme-linked immunosorbent assays (ELISA) are more specific in detecting pathogens.<sup>18</sup> In recent years, several

techniques have been evaluated to identify *A. baumannii*, including a phage-based real-time quantitative polymerase chain reaction (qPCR), dual aptamer-based.<sup>18,19</sup> A most important reliable biomarker is the *bla<sub>OXA-51</sub>* gene, which is responsible for the weak hydrolysis of carbapenems used to identify *A. baumannii*.<sup>20</sup>

### 1.4. *A. baumannii* cell wall

The membrane of the bacteria is composed of complex conserved structures. Membrane-targeting antibiotics are effective in killing slow-growing or dormant bacteria. Also, membrane-targeting antibiotics have pronounced and rapid bactericidal effects on bacteria.<sup>21</sup> Moreover, membrane-targeting antibiotics do not require to cross the membrane to

reach the targets, which is a significant hurdle in developing antibiotics. However, there is always a challenge associated with conventional antibiotics to cross the plasma membrane and reach intracellular targets. Also, antibacterial agents targeting the membrane are less likely to acquire resistance than those targeting intracellular systems, and thus, antibiotics will have prolonged clinical efficacy.<sup>22</sup> Membrane-targeting antibiotics must selectively target bacterial membranes, not mammalian cell membranes, as both membranes comprise lipid bilayers.<sup>22</sup> A diagrammatic representation of the *A. baumannii* cell wall is shown in Fig. 2.

*A. baumannii* is intrinsically resistant to toxic compounds and antibiotics because of the low permeability of its outer membrane. Notably, the outer membrane of *A. baumannii* is ~100-fold less permeable than that of *E. coli*.<sup>23</sup> *A. baumannii*'s outer membrane comprises an asymmetric bilayer with glycerophospholipids in the inner leaflet. The glycolipids are mainly constricted in the outer leaflet of the outer membrane and, depending upon the type of polysaccharide attached to glycolipids, are referred to as lipopolysaccharides and lipooligosaccharides (LOS).<sup>24</sup> Lipooligosaccharides are acylated disaccharides (lipid A) connected to an oligosaccharide. Also, lipopolysaccharides are acylated disaccharides linked to variable amounts of repeat units of polysaccharides called O-antigen.<sup>25</sup> The outer membrane proteins comprising  $\beta$ -barrel structures formed by 8 to 26 strands are anchored to the outer membrane. These large extended loops are present on the extracellular side and

shorter loops on the periplasmic side. Due to this complex structure, the outer membrane proteins give high stability to the membrane, thus making it capable of tolerating harsh environments.<sup>26</sup> The LPS provides structural roles such as a decrease in the membrane permeability and an increase in the rigidity of the bacterial cells.<sup>27</sup>

Next to the outer membrane, well-defined components of peptidoglycan layers are present. They comprise glycan layers of alternating *N*-acetylglucosamine (GlcNAc) and *N*-acetylmuramic acid (MurNAc) connected through MurNAc-attached peptides. Peptidoglycan provides cell-shape rigidity and mechanical strength to counteract osmotic stress. Also, the outer membrane asymmetry provides the membrane's impermeability due to the presence of LPS occupying the outer leaflet of the bacteria, as well as glycerophospholipids in the inner leaflet. The LPS comprises the lipid A anchor, core oligosaccharide, and O-antigen. Lipid A is a hydrophobic glycolipid and is a glucosamine-based phospholipid phosphorylated at the 1 and 4' positions. Notably, *A. baumannii* biosynthesizes hepta-acylated lipid A, while other GNBs, such as *E. coli*, produce hexa-acylated lipid A. Two 3-deoxy-D-manno-oct-2-uloseonic acid and oligomers of sugars form the core of LPS. Also, the antigens are attached to the core oligosaccharide LPS, generating an intact LPS. Notably, the lipid A and core moieties in *A. baumannii* are phosphorylated, generating an overall negative charge for the endotoxin molecules. The final step in the biosynthesis of lipid A involves the secondary acylation of lipid A precursors and is catalyzed by members of the superfamily enzymes

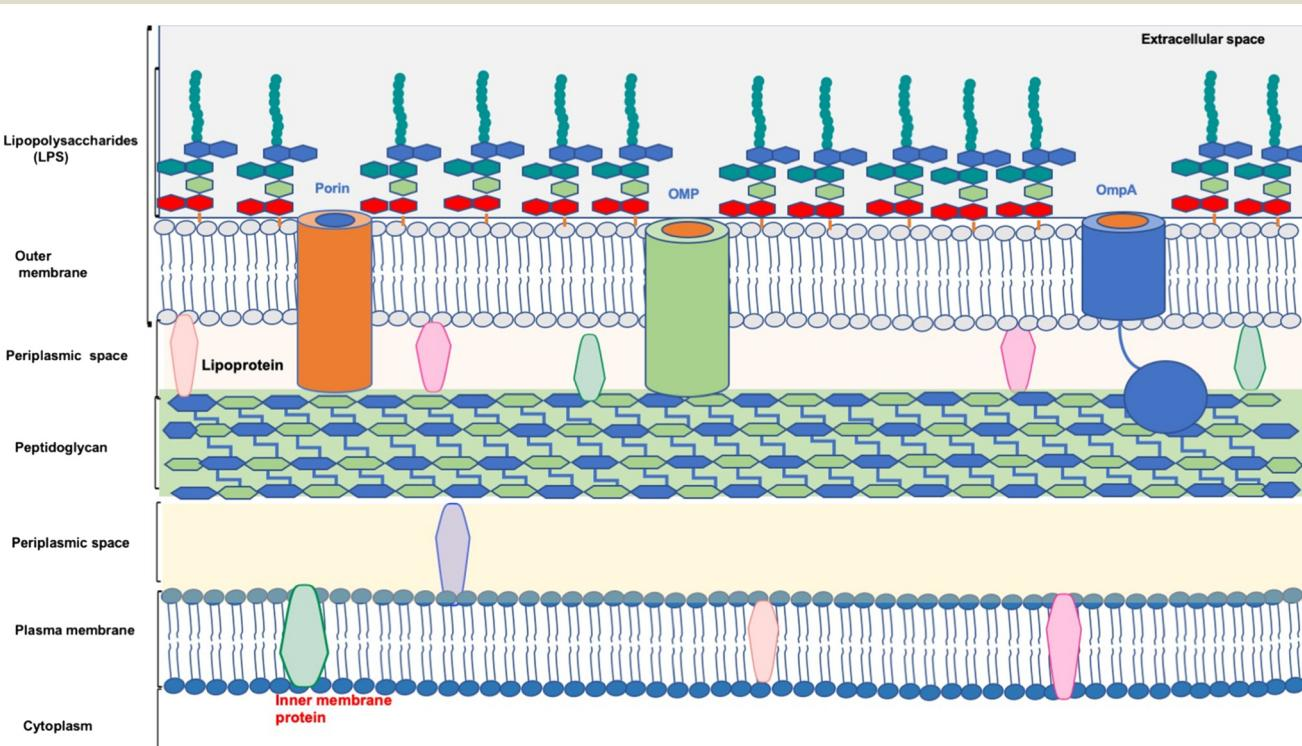


Fig. 2 A diagrammatic representation depicting the *A. baumannii* cell wall.



known as lysophospholipid acyltransferases (LPLATs).<sup>28,29</sup> Also, the LPS strengthens the outer membrane by balancing the electrostatic net charge.<sup>29</sup> It protects the cell from cationic peptides and cell lysis. Moreover, hepta-acylated lipid A is accountable for polymyxin resistance.

BamA, LptD, Omp33-36, and OmpW are outer membrane proteins identified in *A. baumannii*. BamA is responsible for allowing the other outer membrane proteins to be assembled. LptD enables the transportation of LPS to the outer membrane, while Omp33-36 is a porin channel for the passage of water. OmpW is a hydrophobic channel in the outer membrane and cytoplasm responsible for iron homeostasis.<sup>30</sup> Chemical structures of lipid A present in wild-type *A. baumannii* and colistin-resistant *A. baumannii* are shown in Fig. 3.

### 1.5. Conventional treatment of *A. baumannii* infections

*A. baumannii* survives for extended periods in the environment and thus can spread bacilli in the surroundings. The World Health Organization (WHO) has categorized and placed *A. baumannii* on the list of nosocomial ESKAPE (*Enterococcus faecium*, *Staphylococcus aureus*, *Klebsiella pneumoniae*, *Acinetobacter baumannii*, *Pseudomonas aeruginosa*, and *Enterobacter* spp.) pathogens and mentioned an urgent need for research and development of antibiotics to tackle *A. baumannii*.<sup>31</sup> *A. baumannii* infections can be treated by several classes of antibiotics including carbapenems, aminoglycosides, fluoroquinolones, cephalosporins, and  $\beta$ -lactamase inhibitors. In recent decades, there has been a decrease in the susceptibility of *A. baumannii* to antibiotics, leading to an increase in the minimum inhibitory concentrations (MICs) of the prescribed antibiotics.<sup>5</sup>

Sulbactam, clavulanic acid, and tazobactam belong to class A  $\beta$ -lactamase inhibitors. Sulbactam is a semisynthetic penicillanic acid sulfone derivative with intrinsic activity against carbapenem-resistant *Acinetobacter* strains.<sup>32</sup> It showed antibacterial activity through inhibition of the penicillin-binding protein (PBP) types 1a and 2, which results

in the interference of the cell wall synthesis. Sulbactam is given in combination with cefoperazone and ampicillin to prevent the hydrolysis of the  $\beta$ -lactam ring by  $\beta$ -lactamase enzymes.<sup>33</sup> Sulbactam, in combination with cefoperazone and ampicillin, has been approved for treating skin and soft tissue intra-abdominal and gynaecological infections caused by *A. baumannii*.<sup>34</sup> In a study, it has been found that spontaneous resistance to sulbactam in susceptible *A. baumannii* strains is rare. On the other hand, low-frequency and high-level resistance was observed in sulbactam and was associated with pbp3 mutants.<sup>32</sup> Avibactam, relebactam, and vaborbactam inhibit clinically relevant class A and C  $\beta$ -lactamases and a limited number of class D enzymes. ETX2514 is a broad-spectrum  $\beta$ -lactamase inhibitor. ETX2514, in combination with sulbactam, has shown potent *in vitro* and *in vivo* efficacy against MDR *A. baumannii*.<sup>35</sup>

Imipenem, meropenem, and doripenem belong to the carbapenem class and are considered the first-line treatment for the infection caused by *A. baumannii*.<sup>36</sup> Carbapenem antibiotics pass through porins to reach the targets and bind to the penicillin-binding proteins. PBPs, including PBP1a, 1b, 2, and 3, are responsible for peptidoglycan biosynthesis in the bacteria's cell wall. Notably, carbapenems structurally resemble acylated D-alanyl-D-alanine (the building block of peptidoglycan) and bind irreversibly to the PBP active sites. When  $\beta$ -lactam, like carbapenem, binds to the PBPs, it cannot further participate in the transpeptidation, preventing the cell wall formation and resulting in bactericidal activity.<sup>37</sup>

However, the rise in multidrug-resistant (MDR) *A. baumannii* strains reduced the effectiveness of  $\beta$ -lactams.<sup>38</sup> AmpC  $\beta$ -lactamase, known as Acinetobacter-derived cephalosporinase (ADC), is naturally produced by *A. baumannii*.<sup>39</sup> Carbapenemase enzymes, especially oxacillinas, are responsible for the neutralization of the carbapenem and are the major contributor to carbapenem resistance.<sup>39</sup> OXA-23 is the most common class D carbapenemase reported to be present in all countries' strains and is associated with endemic clones CC113/CC79, CC104/CC15, CC110/ST25, and CC109/CC1.<sup>40</sup> The recent research suggested that there is a near-complete absence of

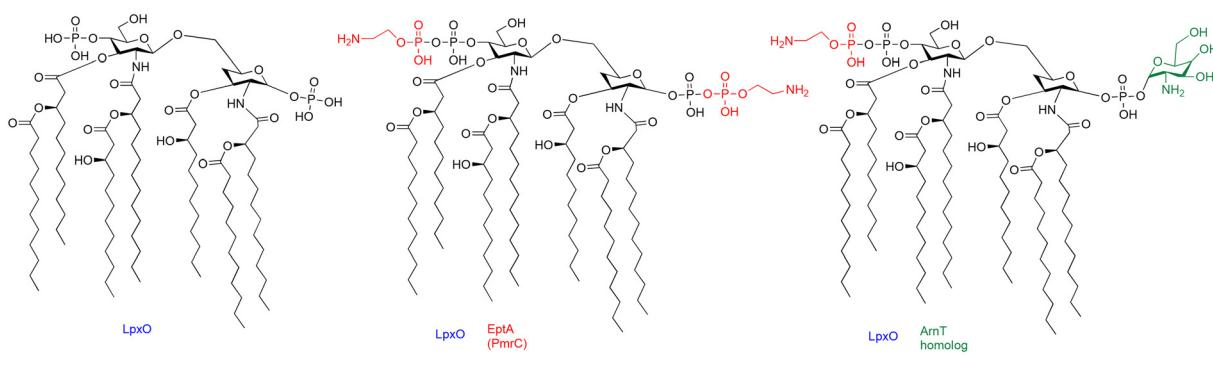


Fig. 3 Chemical structures of lipid A present in wild-type *A. baumannii* and colistin-resistant *A. baumannii*.



therapeutic options to treat infections caused by carbapenem-resistant *A. baumannii* (CRAB).<sup>41</sup>

Moreover, most of the clinical isolates of *A. baumannii* are resistant to cephalosporins, including third and fourth-generation (like ceftazidime and cefepime) agents. Cefiderocol is a novel siderophore cephalosporin that exhibits potent activity against MDR *A. baumannii*. Cefiderocol, in combination with antibiotics, is used to treat GNB infections. Time-kill analysis revealed that cefiderocol demonstrated synergistic activity with  $\beta$ -lactamase inhibitors. Also, cefiderocol, in combination with  $\beta$ -lactamase inhibitors, showed increased antibacterial activity against *A. baumannii* isolates.<sup>42</sup>

Tigecycline is a semisynthetic 9-*t*-butylglycylamido derivative of minocycline, belonging to a glycylcycline class. It is bacteriostatic and exhibits antibacterial activity by binding to the 30S ribosomal subunit. Tigecycline has been recommended for treating infections such as complicated skin and intra-abdominal infections and community-acquired pneumonia.<sup>43</sup> Tigecycline showed resilience to several resistance mechanisms and demonstrated broad-spectrum antibacterial activity compared to its parent congener tetracyclines. Minocycline regimen therapy in combination with colistin or carbapenems showed clinical and microbiological success rates of 72.6% and 60.2% in patients suffering from pneumonia caused by *A. baumannii*.<sup>44</sup>

Aminoglycosides such as tobramycin and amikacin are used to treat MDR *A. baumannii*. Aminoglycosides are generally used in combination with other antimicrobials. Recent studies demonstrated that L-lysine potentiated the activity of aminoglycosides and killed clinically resistant MDR *A. baumannii*. The exogenous use of lysine increases the proton motive force through the transmembrane and causes the accumulation of aminoglycosides in the bacterial cells.<sup>45</sup>

Rifampin acts by binding to the bacterial RNA polymerase and prevents transcription in the bacteria. Rifampin demonstrated partial and synergistic effects in MDR *A. baumannii* in combination with biapenem, colistin, and tigecycline. Rifabutin, a semisynthetic derivative of rifampin, effectively cures patients suffering from *A. baumannii* infections.<sup>46</sup>

Fosfomycin showed antimicrobial activity by interfering with peptidoglycan biosynthesis. Fosfomycin, upon entering the bacterial cells, irreversibly binds to MurA (a UDP-GlcNAc enolpyruvyl transferase), which catalyzes the first step in peptidoglycan via the synthesis of UDP-GlcNAc-3-O-enolpyruvate from UDP-GlcNAc and phosphoenolpyruvate. A recent study suggested that peptidoglycan remodelling by the AmpD and Anmk pathway contributes to intrinsic resistance to fosfomycin in *A. baumannii*.<sup>47</sup>

Bacteriophages are made up of proteins and nucleic acids. They are amplified in the presence of susceptible bacteria and cause lysis of the cells. Bacteriophages inhibit biofilm formation and are active against resistant bacterial strains.<sup>3</sup> ISTD and NOVI bacteriophages were assessed against *A. baumannii* isolates.<sup>3</sup> In another study, phage  $\phi$ FG02, in

combination with ceftazidime, was evaluated in an *in vivo* model of *A. baumannii* AB<sub>900</sub> infection. The phage  $\phi$ FG02 treated *A. baumannii* AB<sub>900</sub> showed a loss of genes involved in the capsule biosynthesis, increasing the sensitivity to ceftazidime of *A. baumannii*. This finding suggests that phage therapy, in combination with antibiotics, can restore the activity in resistant *A. baumannii* strains.<sup>48</sup>

Drug repurposing is one of the effective strategies for developing new antimicrobials.

A study assessed anticancer drugs, including 5-fluorouracil, cisplatin, mitomycin C, and melphalan, against *A. baumannii* ATCC BAA-747. Among these drugs, mitomycin C effectively inhibited *A. baumannii* ATCC BAA-747 with a MIC<sub>50</sub> value of 7  $\mu$ g mL<sup>-1</sup> and completely inhibited the growth at a concentration of 25  $\mu$ g mL<sup>-1</sup>. Moreover, mitomycin C increased the survival of the insect larvae *Galleria mellonella* infected with sensitive *A. baumannii* ATCC BAA-747 and MDR A560 and A578 strains, respectively.<sup>49</sup>

Auranofin is an anti-rheumatic drug that exhibits antibacterial activity in GPB with a MIC value of 0.0625  $\mu$ g mL<sup>-1</sup> against methicillin-resistant *Staphylococcus aureus* MRSA.<sup>50</sup> It shows multiple modes of antibacterial action, including DNA, cell wall, and protein synthesis inhibition. Moreover, auranofin inhibits GNB, including *E. coli*, *A. baumannii*, and *K. pneumoniae*, with higher MIC values of 125, 15.6, and 125  $\mu$ g mL<sup>-1</sup>, respectively. Pentamidine is an antiprotozoal drug that inhibits GNB by interacting with lipopolysaccharides, disrupting the outer membrane and increasing the membrane permeability. Pentamidine inhibits *E. coli*, *A. baumannii*, and *K. pneumoniae* with higher MIC values of 125, 250, and 500  $\mu$ g mL<sup>-1</sup>, respectively. Yu *et al.* in their study demonstrated that the combination of both auranofin and pentamidine displayed a strong synergistic effect against GNB (*E. coli*, *A. baumannii*, and *K. pneumoniae*) with fraction inhibitory concentration index (FIC) values ranging from 0.094–0.506. Also, the combination decreased the MIC of auranofin in sensitive *A. baumannii* and MDR *A. baumannii* up to 1  $\mu$ g mL<sup>-1</sup>. The mode of action of the combination is through disruption of the membrane, leading to an increase in the permeability of auranofin inside the bacterial cell. This study demonstrates that combining non-antibiotic drugs with complementary antibacterial mechanisms can lead to the discovery of new medications that can delay drug resistance.<sup>50</sup>

## 1.6. Antibiotic resistance in *Acinetobacter baumannii* spp.

*A. baumannii* is intrinsically resistant to several classes of antibiotics. *A. baumannii* has environmental persistence ability and follows a “persist and resist strategy” in which bacteria keep off oxidative stress and resist complement-mediated killing.<sup>31</sup> *A. baumannii* has developed several modes of antibiotic resistance, including enzyme-mediated metabolism that leads to inactivation of the drug, reduction in the access of the drug to the target site, overexpression of efflux pumps, and change in the drug permeability through



the membrane.<sup>9</sup> For instance, the aminoglycoside class of antibiotics is reported to acquire resistance to all these mechanisms.<sup>51</sup> The community-acquired *A. baumannii* is more susceptible than hospital-acquired *A. baumannii* strains. The genome sequence of community-acquired *A. baumannii* revealed that it lacks antibiotic resistance islands (AbaR), which encode genes that make it resistant to multiple antibiotics, including aminoglycosides,  $\beta$ -lactams, sulphonamides, and tetracyclines. It could be reasoned that community-acquired *A. baumannii* is more susceptible to prescribed antibiotics.<sup>52</sup>

Recent studies suggested that there is an increase in the progression of *A. baumannii*-resistant strains, including multidrug-resistant (MDR), extensively drug-resistant (XDR), and pan-drug-resistant (PDR) *A. baumannii*. MDR *A. baumannii* strains are non-sensitive to any three classes of antibiotics prescribed for *A. baumannii*. In contrast, XDR *A. baumannii* strains resist three classes of antibiotics and carbapenems. Meanwhile, PDR *A. baumannii* strains showed resistance to three classes of antibiotics: beta-lactams, fluoroquinolones, and aminoglycosides.<sup>53</sup> The pan  $\beta$ -lactam-resistant bacteria are only sensitive to one or two potential active drugs, while they resist all antibiotics.

The porin channel and outer membrane of *A. baumannii* are essential for transporting antimicrobial agents to access bacterial targets. Several studies confirmed that the loss of protein and porin channels led to the development of carbapenem resistance in *A. baumannii*.<sup>54</sup> The point mutations could be responsible for antibiotic resistance in *A. baumannii*. For example, mutations in the bacterial targets *gyrA* and *parC* topoisomerase enzymes are responsible for quinolone resistance in *A. baumannii*.<sup>54</sup> Also, *A. baumannii* showed improved expression of chromosomal genes for efflux systems, which played a significant role in extruding a range of structurally dissimilar antibiotics. These pumps are responsible for reduced susceptibility to antibiotics, which leads to the generation of MDR.<sup>55</sup>

The use of  $\beta$ -lactam antibiotics has mainly contributed to the emergence and rapid progression of *A. baumannii*-resistant strains. *A. baumannii* possesses a series of  $\beta$ -lactamases that hydrolyze and acquire resistance to broad-spectrum  $\beta$ -lactam penicillins, cephalosporins, and carbapenems. It has been found that the use of colistin methanesulfonate to treat carbapenem-resistant *A. baumannii* led to the emergence of *A. baumannii*-resistant strains.<sup>56</sup> Importantly, colistin-resistant isolates have emerged and restricted chemotherapy choices.<sup>57</sup>

One of the most common resistance mechanisms to  $\beta$ -lactam antibiotics is enzymatic hydrolysis of antibiotics by  $\beta$ -lactamase enzymes. Based on their amino acid sequences,  $\beta$ -lactamases are classified into four Ambler classes (A–D). The  $\beta$ -lactamase enzymes A, C, and D types perform hydrolysis of  $\beta$ -lactam antibiotics by forming an intermediate acyl-enzyme complex with the serine residue, and class B carries out the hydrolysis of  $\beta$ -lactam antibiotics by using one or more zinc ions.<sup>53</sup> Also, the association of OXA-23 with OM

porins is responsible for carbapenemase activity. The topology of the OXA-23 with OM porin complex revealed that catalytic site Oxa-23-K82 concentrates near the inner surface of OM porins. Notably, this orientation of Oxa-23-K82 near the porins would benefit the hydrolysis of antibiotics immediately entering the cells before their diffusion in the cellular matrix. The increased concentration of OXA-23 in the periplasm causes increased carbapenem resistance.<sup>58</sup> Also, the increased overexpression of OXA-51, OXA-23, and metallo- $\beta$ -lactamases in *A. baumannii* is responsible for carbapenem resistance. While OXA-51 and OXA-40 belong to the D  $\beta$ -lactamase class, their overexpression is responsible for ceftazidime resistance.<sup>52</sup> Oxacillinases are specific  $\beta$ -lactamases in *Acinetobacter* spp. and *Pseudomonas aeruginosa*. In contrast,  $\beta$ -lactamases such as *bla*<sub>OXA-23-like</sub>, *bla*<sub>OXA-51-like</sub>, and *bla*<sub>OXA-134</sub> enzymes are identified in *A. radioresistens*, *A. baumannii*, and *A. lwoffii*. Oxacillinases are responsible for the hydrolysis of oxacillin, benzylpenicillin, methicillin, amoxicillin, and some antibiotics of the cephalosporin class, respectively.<sup>57</sup> Specifically, the *bla*<sub>OXA-23-like</sub> oxacillinase is responsible for carbapenem resistance, OXA-type  $\beta$ -lactamases and *bla*<sub>OXA-40-like</sub>  $\beta$ -lactamases can hydrolyze penicillin but showed weak hydrolytic activity against cephalosporins and carbapenems (imipenem and ceftazidime), and *bla*<sub>OXA-51-like</sub> enzymes can inactivate clavulanic acid, tazobactam, and NaCl, respectively. In contrast, *bla*<sub>OXA-58-like</sub> enzymes can hydrolyze penicillin, imipenem, and oxacillin, while they are not active against extended-spectrum cephalosporins.<sup>57</sup>

Moreover, the polymyxin-dependent resistant *A. baumannii* strains possess mutations in the *lpxC* (lipopolysaccharide biosynthesis) and *katG* (reactive oxygen species scavenging) genes. The multi-omics study revealed that there is a remarkably abundant increased proportion of phosphatidylglycerol in the outer membrane of polymyxin-dependent resistant *A. baumannii*.<sup>59</sup>

The above reports suggest the loss of antibacterial activity of conventional antibiotics in *A. baumannii*; thus, there is a need for novel alternative treatments to address *A. baumannii*. Antibiotics with unique modes of action can overcome the existing resistance mechanisms in *A. baumannii*. This review discusses natural peptides, their synthetic congeners acting against *A. baumannii*, their modes of action, and their potential benefits and shortcomings.

## 2. Antimicrobial peptides (AMPs)

AMPs are produced from multiple organisms, including bacteria, reptiles, plants, and mammals, as part of their defense mechanism to protect themselves from pathogens and predators. AMPs are short-chain peptides with amino acids ranging from 10 to 100. AMPs are generally amphiphilic and positively charged (usually +2 to +9). The hydrophobic domains acquired approximately 50% of the amino acid residues of the AMP. In addition to positive charges, AMPs can have neutral or negative charges.<sup>60</sup> AMPs' physicochemical properties and antimicrobial activity depend



upon the length of the peptide, amino acid composition, cationic charge residues, hydrophobicity of the lipid constituents, overall net charge on the molecule, and the helicity of the spatial arrangement.<sup>61,62</sup> Importantly, AMPs display remarkable diversity in their structure and are considered potential alternatives to antibiotics. It is generally believed that developing microbial resistance against AMPs is unlikely since AMPs attack multiple low-affinity targets rather than a single high-affinity target like conventional antibiotics.<sup>63</sup> AMPs display various modes of action through interactions with intracellular targets and disruption of critical cellular processes.<sup>64</sup> Most of the AMPs have membrane-permeabilizing and disrupting abilities. Moreover, they inhibit the cytoplasmic membrane septum formation and cell wall synthesis. At the same time, some AMPs inhibit DNA and protein synthesis, chaperone-assisted protein folding, and enzymatic activity.<sup>64,65</sup> The nucleic acids, DNA, and RNA are considered intracellular targets of AMPs.<sup>66</sup> Mostly, AMPs are cationic and preferentially bind to the negatively charged bacterial cytoplasmic membranes rather than the zwitterionic membrane of mammalian cells. The peptide-to-lipid ratio influences the AMP interaction with the cell membrane. When the peptide-to-lipid ratio is low, the peptide orients parallel to the plasma membrane and vertical

to the hydrophobic center of the membrane as the peptide-to-lipid ratio rises. The binding of AMPs to the bacterial membrane causes leakage of intracellular ions, metabolites, and cytoplasmic contents, leading to bacterial cell death.<sup>67</sup>

Despite continuous efforts to combat MDR pathogens, only a few compounds entered the clinical evaluation and received approval for treating human MDR infections. At the same time, drug repurposing and antibiotic adjuvant combination therapy have received attention for treating MDR infections.<sup>68,69</sup> The AMPs are considered one of the promising alternatives to antibiotics, and they showed activity against both susceptible and MDR bacterial strains. Moreover, several studies have shown that AMPs as adjuvants exhibited potent synergistic activity with antibiotics. The synergistic combination of AMPs and antibiotics increases the therapeutic effects of the antibiotics, and it further allows the reduction of antibiotic dosage and toxicity effects, preventing antibiotic resistance development. Moreover, combining AMPs with antibiotics can help tackle MDR bacteria and prevent the further development of antibiotic-resistant strains.<sup>70</sup>

The AMP activity has been defined by theoretical models for the membrane-centric activity, which include barrel-stave, toroidal-pore, carpet, and aggregate models. In the barrel-

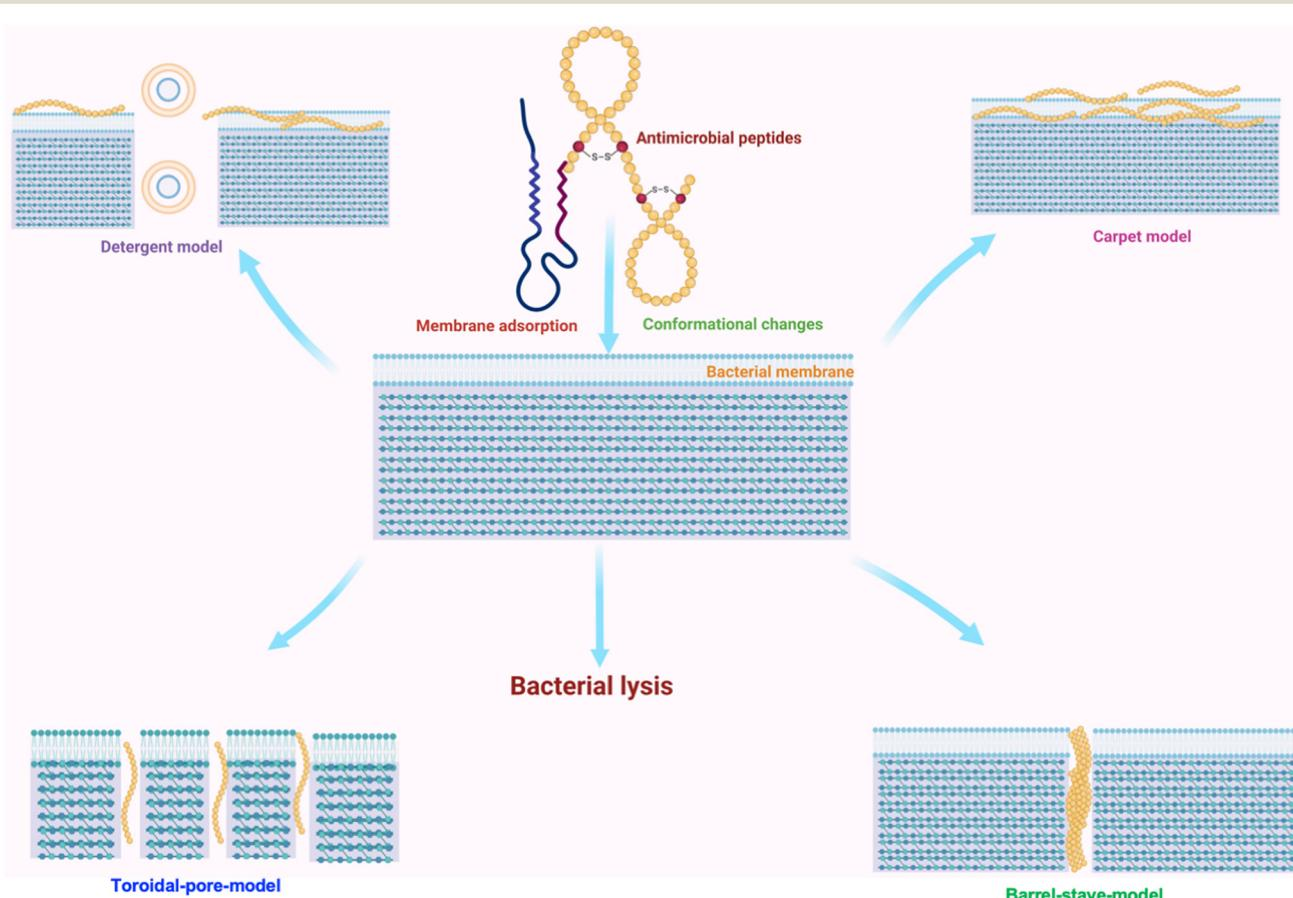


Fig. 4 A schematic representation depicting the AMP modes of action, *i.e.*, detergent, carpet, toroidal-pore, and barrel-stave models.<sup>71</sup>

stave model, the peptides with a specific orientation are sandwiched between membranes. Then, peptide monomers are aggregated to form transmembrane pores within the hydrophobic membrane core. In the barrel stave model, the AMPs will have a linear structure aligned with the shape of the pore to maximize their interaction with the membrane.<sup>71</sup> In the toroidal pore model, the AMPs are adsorbed to the bilayer, and after internalizing between the lipid bilayer, the phospholipid molecules bend inward to form pores. In this model, the hydrophilic domain of the AMP orients to the bilayer membrane to form the outer part of the pore, and the hydrophobic domain acts as the internal part. The peptide chain is positioned within the lipid bilayer, heads inside the pore, and embeds in the hydrophilic and hydrophobic interface. Notably, the transmembrane pore is broadened by the interaction between lipid head groups and the AMPs, allowing the water core to be lined. Toroidal pores are more common and are formed by a broader range of peptides than barrel-stave pores.<sup>71</sup> In the carpet model, the AMPs are electrostatically attached to the anionic phospholipid head groups and carpet the surface of the membrane. When the concentration of AMPs exceeds a certain threshold, they induce the formation of pores, causing severe membrane perturbation following the release of mixed peptide-lipid complexes.<sup>72</sup> The carpet mechanism, or detergent model, impacts the integrity of the membrane molecular structure.<sup>71</sup> In the aggregate model, the AMPs bind to the anionic cytoplasmic membrane, leading to transient peptide-lipid micelles. The AMPs, lipids, and water channels allow ions and cellular contents to leak, leading to cell death.<sup>72</sup> The AMP modes of action with their types of models are given in Fig. 4.

The pharmacodynamics of AMPs is complex, and several AMPs demonstrate multiple effects on the body, such as immunomodulatory activities, including enhanced chemotaxis of immune cells, activation of immune cells, and their cell differentiation and maturation.<sup>73</sup> Cationic host defense peptides exhibit various immune functions and modulate innate and adaptive immune responses. For example, IDR-1002 is bovine bactenecin, a host defense peptide that decreases TNF- $\alpha$ , IL-6, IL-8, and nitric oxide production triggered by toll-like receptor ligands and increases the expression of the anti-inflammatory cytokine IL-10.<sup>63</sup> The human cathelicidin LL-37 exhibited multiple immunomodulatory activities, including macrophage activation, upregulation of chemokines and chemokine receptor production, and promotion of wound healing.<sup>74</sup> Additionally, LL-37 acts on monocytes and induces chemokines such as CXCL8, CCL2, and CCL7 and anti-inflammatory cytokine expression, promoting differentiation to proinflammatory macrophages.<sup>75</sup> Host defense peptides are short-cationic peptides with diverse sequences produced by several cells and tissues in all complex life forms and play an essential role in the body's response to infection and inflammation.<sup>76</sup>  $\alpha$ -Defensins, including HNP1, HNP2, HNP3, and HNP4, act on lung epithelial cells and stimulate cytokine release such as CXCL8, CCL2, and GM-CSF. In contrast,  $\alpha$ -defensins such as HD5 and HD6 act on intestinal epithelial cells, activate NF- $\kappa$ B, and induce chemokine production such as CXCL8.  $\beta$ -Defensins HBD1, HBD2, HBD3, and HBD4 act on intestinal epithelial cells and promote migration and wound healing, and through epidermal keratinocytes stimulate chemokine and cytokine production such as IL-6,

**Table 1** AMPs with targets and their therapeutic indications

S. no.	Peptide	Target	Therapeutic indication	Ref.
1.	Colistin	Colistin binds to LPS and phospholipids in the outer cell membrane of GNB	GNB infections	77
2.	Polymyxins	They interact with the lipid A component of LPS	GNB infections	78
3.	Bacitracin	It inhibits dephosphorylation of the lipid carrier and obstructs the process of cell wall synthesis	GPB infections	79
4.	Gramicidin D	It increases the permeability and disrupts the inner cellular content	GPB infections	80
5.	Daptomycin	It disrupts the multiple aspects of the cell membrane function	GPB infections	81
6.	Teicoplanin	It inhibits the cell wall peptidoglycan synthesis	GPB infections	82
7.	Telavancin	It disrupts the peptidoglycan synthesis and cell membrane function	GPB infections	83
8.	Oritavancin	It binds to the $\alpha$ -alanyl- $\alpha$ -alanine terminus of the peptidoglycan precursor linked to the C55-lipid transporter (collectively referred to as lipid II)	GPB infections	84
9.	Dalbavancin	Dalbavancin interacts with terminal $\alpha$ -alanyl- $\alpha$ -alanine residues of peptidoglycan precursors. It prevents peptidoglycan cross-linking, thereby destroying the integrity of the cell wall	GPB infections	85
10.	Vancomycin	It inhibits the peptidoglycan synthesis of the cell wall	GPB infections	86
11.	Micafungin	It is a non-competitive inhibitor of 1,3- $\beta$ -D-glucan synthesis, an essential fungal cell wall component	Fungicidal activity against <i>Candida</i> species	87
12.	Caspofungin	It is a non-competitive inhibitor of 1,3- $\beta$ -D-glucan synthesis	Fungicidal activity against <i>Candida</i> species	88
13.	Enfuvirtide	T-20 effectively impedes the gp41-mediated fusion between the viral and host cell membranes	It is used for treating HIV-1 infections	89
14.	Cobicistat	It is inactive and selectively inhibits CYP3A isoenzymes and the number of transmembrane drug transporters at different blood-target tissue barriers	It is used in combination with other anti-retroviral drugs as a pharmacoenhancer	90



IL-10, and CCL2, and CCL20.<sup>76</sup> AMPs used for treating bacterial, viral, and fungal infections are given in Table 1.

The efficacy of AMPs is often questionable due to their limited contribution as clinical agents.<sup>91</sup> Most of the AMPs' experimental *in vitro* and *in vivo* results correlate little. Also, AMPs are sensitive to environmental conditions, including pH, serum, and salt. Moreover, some AMPs lost their activities under physiological salt conditions due to electrostatic attraction between peptides and the cell membrane, and some of the AMPs bind to serum protein, including albumin and lipoproteins, which leads to a decrease in their activity.<sup>91</sup>

## 2.1. Natural peptides and their analogs

**2.1.1. Bacteria.** Lipopeptides are amphiphilic hydrophobic fatty acid chains with hydrophilic cyclic peptides. Polymyxins are non-ribosomal cyclic lipopeptides obtained from *Paenibacillus polymyxa*.<sup>92</sup> Polymyxins possess a decapeptide core structure and an intramolecular cyclic heptapeptide amide linked loop formed between the side chain of the diaminobutyric acid (Dab) residue at the 4th position and the carboxyl group of the C-terminal threonine residue. Notably, polymyxins possess five nonproteogenic Dab residues, which acquire a positive charge at the physiological pH. They also contain conserved hydrophobic residues at positions 6 and 7 and an N-terminal fatty acyl group.<sup>93</sup> The polymyxin molecule binds to lipid A in folded conformation, wherein the octanoyl fatty-acyl group, D-Phe<sup>6</sup>, and Leu<sup>7</sup> at the N-terminal position are responsible for hydrophobic interactions with the hydrocarbon tails of lipid A. The L-2,4-diaminobutyric acid

(Dab) side-chain is cationic and displays ionic interactions with the phosphates of lipid A and the ketodeoxyoctanoic acid (Kdo) group. Dab<sup>3</sup> is responsible for making hydrophilic interactions with the Kdo sugars of lipid A. In contrast, Dab<sup>1</sup>, Dab<sup>5</sup>, Dab<sup>8</sup>, and Dab<sup>9</sup> are responsible for critical interactions with the 1-and 4'-phosphate, and these electrostatic interactions are the primary drivers for the association of the polymyxin with lipid A. These hydrophobic and ionic interactions ultimately disrupt the membrane lipid packing and permeate the outer membrane.<sup>93–95</sup> It has detergent effects on the membrane, causing enhanced permeability, loss of bacterial membrane integrity, and cell death.<sup>94</sup> Polymyxins displayed broad antibacterial activity against GNB. They kill *A. baumannii* by a concentration-dependent mechanism.<sup>5</sup> Colistin methanesulfonate (also known as polymyxin E) is a prodrug and is given through intravenous administration. It changes to its active form upon reaching blood. Colistin is generally prescribed with carbapenems, rifampicin, tigecycline, and sulbactam. Also, colistin has been recommended for treating infections caused by MDR *A. baumannii*.<sup>96,97</sup> In a clinical study, colistin, in combination with sulbactam, exhibited superior therapy in terms of the microbiology profile and a similar high safety profile to that of colistin monotherapy for treating MDR and XDR *A. baumannii* infections.<sup>98</sup> Polymyxins' mode of action is depicted in Fig. 5.

Roberts *et al.* evaluated polymyxin B (1), polymyxin B<sub>1</sub> (2, Fig. 6), polymyxin B<sub>2</sub> (3, Fig. 6), colistin (4), colistin A (5, Fig. 6), and colistin B (6, Fig. 6) against a panel of GNB, including *P. aeruginosa*, *A. baumannii*, *K. pneumoniae*, and *E. cloacae*. Here, polymyxin B represents 53% of the content of

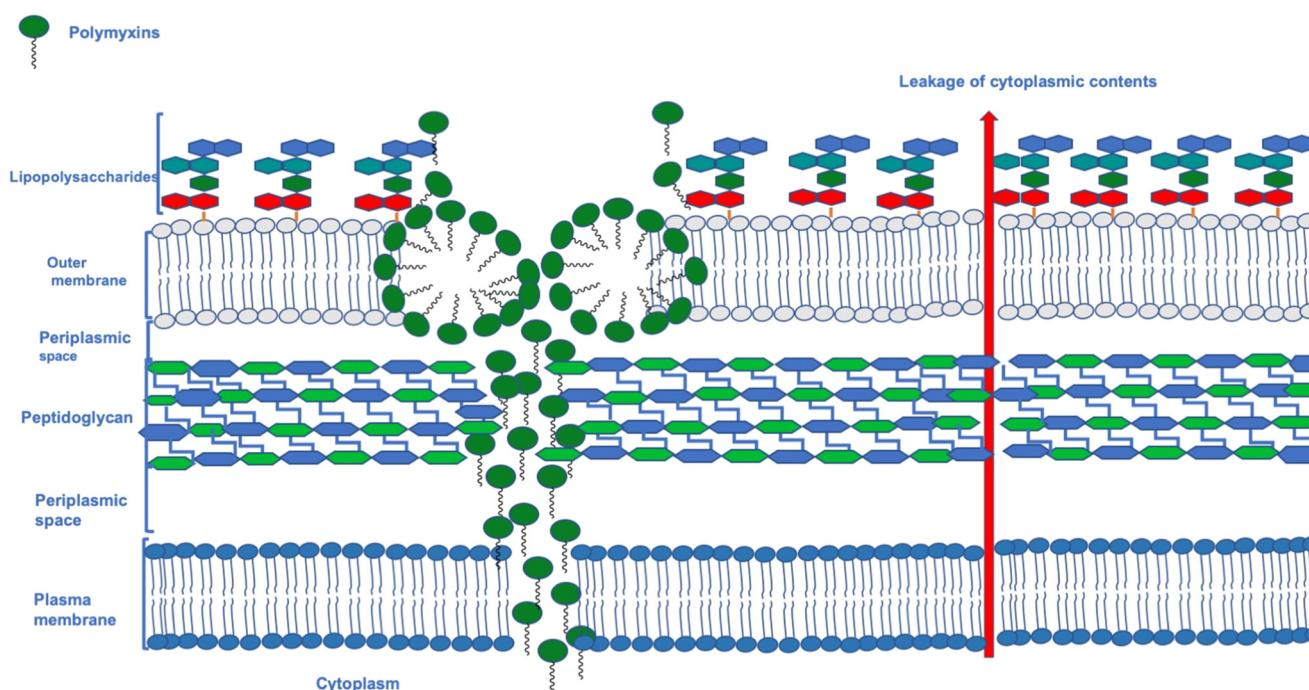


Fig. 5 A diagrammatic representation depicting the polymyxins' mode of action.



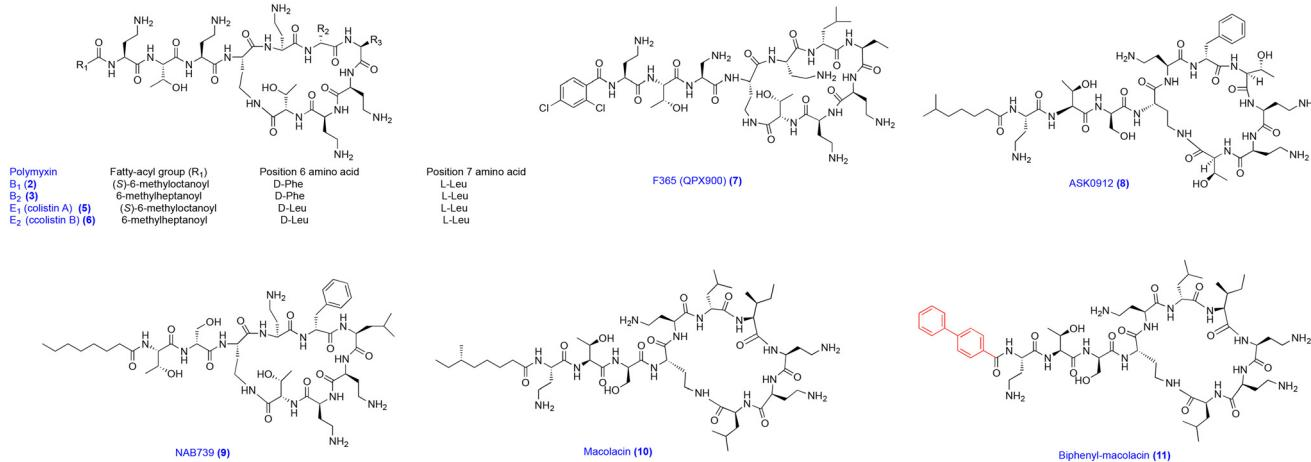


Fig. 6 Chemical structures of lipopeptides.

polymyxin B<sub>1</sub> and 23% of polymyxin B<sub>2</sub>, and colistin represents 58% of the content of colistin A and 19% of the content of colistin B, respectively. Currently, colistin and polymyxin B are the only AMPs used in the clinic for treating infections caused by GNB. Polymyxin B, polymyxin B<sub>1</sub>, B<sub>2</sub>, colistin, colistin A, and colistin B showed antibacterial activity against sensitive and resistant *A. baumannii* strains. Also, these compounds were found to be active in the *in vivo* model of GNB infections compared to the commercial polymyxin and colistin.<sup>99</sup> To retain essential interactions of polymyxins with lipid A and to reduce their toxicity, Roberts *et al.* synthesized polymyxin analogs in that all Dab<sup>1</sup>, Dab<sup>5</sup>, Dab<sup>8</sup>, and Dab<sup>9</sup> residues were conserved in the native polymyxins. At the same time, the modifications were carried out in the N-terminus and in positions 6 and 7 to reduce the hydrophobicity at the binding site. The removal of positive charge, the change in stereochemistry and the increase or reduction in the side chain length were carried out at position 3. This work led to the identification of potent polymyxin compound F365 (QPX9003) (7, Fig. 6), which inhibits GNB, including *A. baumannii* ATCC19606, *A. baumannii* FADDI-AB030\*, and *A. baumannii* FADDI-AB034\* with MIC values of 0.25, 0.25, and 2  $\mu\text{g mL}^{-1}$ , respectively. Moreover, F365 was superior to polymyxin B and colistin in terms of therapeutic efficacy and safety. Additionally, it showed superior safety and effectiveness in lung infections caused by MDR pathogens, including *A. baumannii*, *P. aeruginosa*, and *K. pneumoniae*.<sup>95</sup>

Polymyxin S2 (ASK0912) (8, Fig. 6) is a cyclic peptide derived from polymyxin B2 by substituting basic amino acid L-Dab3 with polar amino acid D-Ser3 and hydrophobic amino acid L-Leu7 with polar amino acid L-Thr7. Polymyxin S2 demonstrated broad-spectrum antibacterial activity against susceptible and resistant *E. coli*, *K. pneumoniae*, and *A. baumannii*. Polymyxin S2 inhibited *A. baumannii* with a MIC value of 0.25  $\mu\text{g mL}^{-1}$  and was nontoxic to Vero cells up to the concentration of  $>500$   $\mu\text{g mL}^{-1}$ .<sup>100,101</sup> Polymyxin S2 increased the survival rate of mice infected with sepsis

(induced by *A. baumannii*) by lowering the bacterial loads in organs and blood.<sup>101</sup>

NAB739 (9, Fig. 6) is a polymyxin derivative with three positive amino acid residues. It showed potential efficacy in treating *E. coli* in a murine model of infections. Also, NAB739 was less nephrotoxic to cynomolgus monkeys than polymyxin B. It has been established in several studies that polymyxins increase the permeability of the outer membrane and allow the entry of other drugs. Considering the importance of NAB739, Tyrrell *et al.* evaluated NAB739 in combination with several antibiotics against polymyxin-resistant (PMR) strains. Notably, NAB739 demonstrated synergistic activity with antibiotics against most GNB strains. For instance, the combination of NAB739 with rifampin or retapamulin demonstrated synergistic activity against polymyxin-resistant strains, including *E. coli* and *K. pneumoniae*. Also, NAB739, in combination with rifampin, demonstrated synergistic activity against *A. baumannii*. Notably, the antibiotics acting on GPB are generally ineffective on GNB. However, this study suggested that polymyxin and its derivatives, combined with other antibiotics (acting against GPB), can treat GNB infections.<sup>102</sup>

The plasmid-borne mobilized colistin-resistance (*mcr-1*) gene and its relatives significantly contribute to colistin-resistance in *A. baumannii*. The gene *mcr-1* encodes a phosphoethanolamine transferase that ligates phosphoethanolamine to a phosphate group in lipid A, thus reducing the electrostatic interactions between colistin and lipopolysaccharides, responsible for bacterial resistance to colistin.<sup>103</sup> Wang *et al.* performed the bioinformatic analysis of the sequenced bacterial genomes and used biosynthetic gene clusters to identify and predict a structurally divergent colistin congener macolacin (10, Fig. 6). Macolacin inhibits *K. pneumonia* 10031 and *A. baumannii* 17978, with the same MIC value of 1  $\mu\text{g mL}^{-1}$ . Colistin and polymyxin B showed a 32-fold higher MIC to *K. pneumonia* and *A. baumannii* expressed with the *mcr-1* gene. In contrast, macolacin showed only a two- to four-fold increase in MIC against these strains.



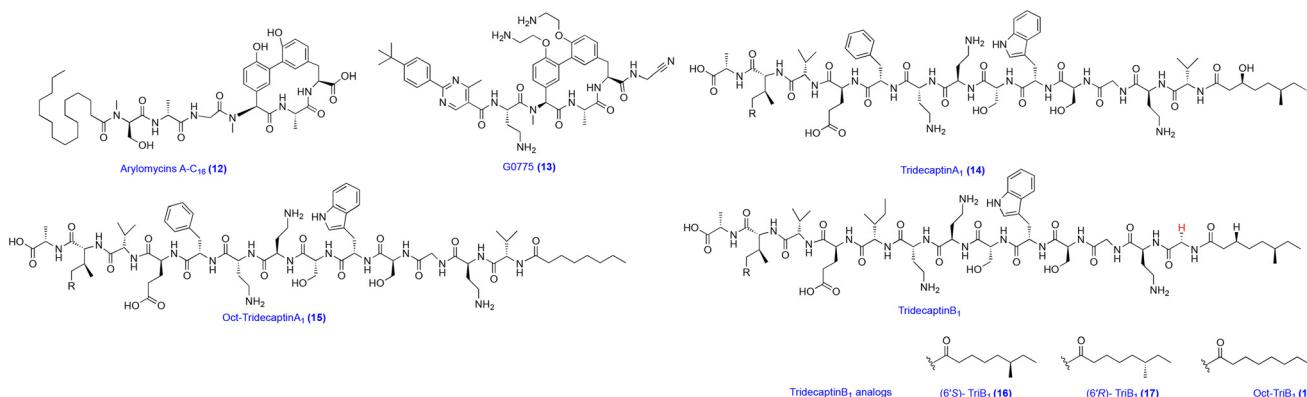


Fig. 7 Chemical structures of arylomycins A–C<sub>16</sub>, G0775, tridecaptin A<sub>1</sub>, Oct-TriA<sub>1</sub>, and tridecaptin B<sub>1</sub> analogs.

Further optimization of the macolacin structure generated a biphenyl analog of macolacin (11, Fig. 6) that was more effective in treating a mouse neutropenic infection model of extensively drug-resistant *A. baumannii*. The mode of action of 10 and 11 is by binding to the lipid A of *A. baumannii*.<sup>103</sup>

Arylomycins belong to macrocyclic lipopeptides obtained from *Streptomyces* culture, which inhibit the bacterial type I signal peptidase (SPase), an essential membrane-bound protease. The signal peptidase is present in the periplasmic space between the cytoplasm and outer membranes. Arylomycins do not exhibit antibacterial activity against ESKAPE pathogens because of their high molecular weight and lipophilicity. Recent research revealed that arylomycins are capable of penetrating the outer membrane. Also, they are inactive against GNB due to naturally occurring mutations in Gram-negative SPase LepB, which reduces the binding affinity of arylomycins in the membrane. The chemical optimization of arylomycins A–C<sub>16</sub> (12, Fig. 7) led to the identification of compound G0775 (13, Fig. 7) with increased target affinity and improved penetration in the

outer membrane. The access of G0775 to LepB in the bacteria does not require a porin mode of transportation. Arylomycins A–C<sub>16</sub> and G0775 inhibited *A. baumannii* ATCC 17978, with MIC values of >64 and 1  $\mu\text{g mL}^{-1}$ , respectively. Moreover, G0775 showed potential efficacy in treating several GNB infection *in vivo* models of mice infected with *E. coli*, *P. aeruginosa*, *K. pneumoniae*, and *A. baumannii*. Also, it was nontoxic to mammalian cells.<sup>104</sup>

Tridecaptins are produced from the *Bacillus* and *Paenibacillus* species belonging to the lipopeptide class. Tridecaptins exhibit antibacterial activity against GNB.<sup>105</sup> Tridecaptins are linear non-ribosomal peptides comprising 13 amino acids, acylated N-terminal fatty acid chains, and more than half of non-proteinogenic amino acid residues. Tridecaptins kill GNB by binding to lipid II and disrupting the inner membrane.<sup>106</sup> Tridecaptin A<sub>1</sub> (14, Fig. 7) is a member of the tridecaptin family and demonstrated potent antimicrobial activity against *A. baumannii* ATCC19606, with a MIC value of 12.5  $\mu\text{g mL}^{-1}$ .<sup>107,108</sup> The structure–activity relationship suggests that the tridecaptin stereochemistry and structure of

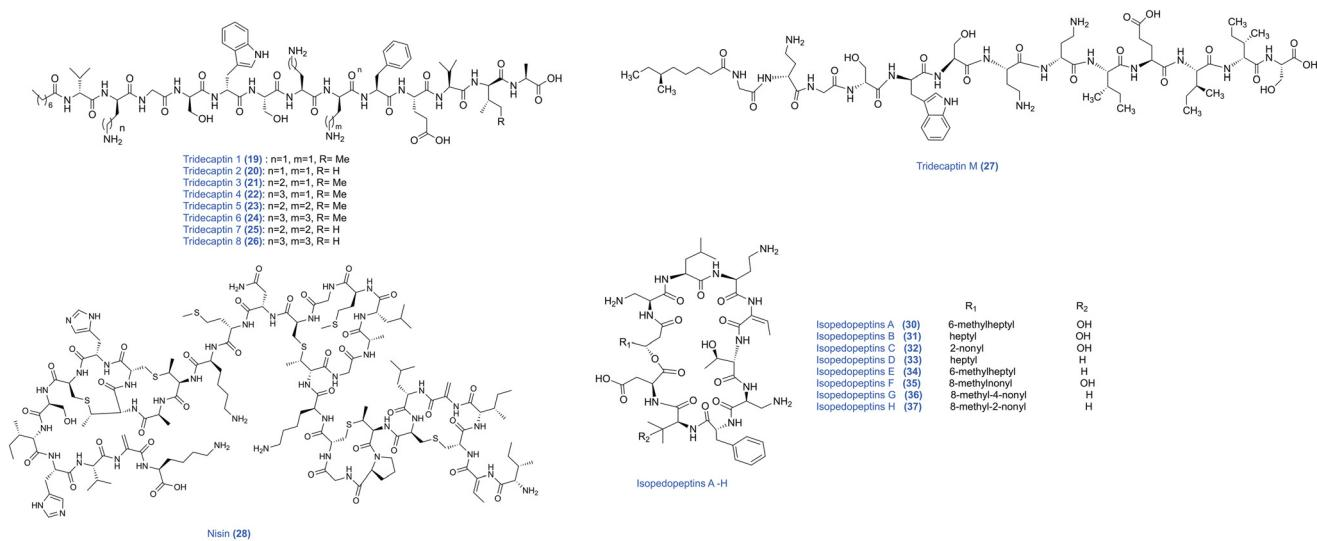


Fig. 8 Chemical structures of tridecaptin and its analogs 1–8, tridecaptin M, nisin, and isopedopeptins A–H.



the lipid tail are essential for antibacterial activity.<sup>109</sup> The removal of the N-terminal lipid from tridecaptin abolishes its antimicrobial activity. At the same time, replacing an octanol chain gives Oct-TriA<sub>1</sub> (15, Fig. 7) that can kill GNB.<sup>110</sup>

SRM 37 was derived from *Paenibacillus* NRRL B-30507, and to confirm the chemical structure, Cochrane *et al.* performed its synthesis. Also, they synthesized new variants of tridecaptin B<sub>1</sub>, including (6'S)-TriB<sub>1</sub> (16, Fig. 7), (6'R)-TriB<sub>1</sub> (17, Fig. 7), and Oct-TriB<sub>1</sub> (18, Fig. 7), and assessed them for antimicrobial activities. (6'S)-TriB<sub>1</sub>, (6'R)-TriB<sub>1</sub>, and Oct-TriB<sub>1</sub> showed broad-spectrum antibacterial activity and inhibited *E. coli*, *Salmonella enterica*, *Pseudomonas aeruginosa*, and *Klebsiella pneumoniae*. Moreover, (6'S)-TriB<sub>1</sub>, (6'R)-TriB<sub>1</sub> and Oct-TriB<sub>1</sub> inhibited *A. baumannii* ATCC19606 and *A. baumannii* ATCC BAA 1605 with MIC values of 25, 50, and 50  $\mu$ g mL<sup>-1</sup> and 25, 25, and 50  $\mu$ g mL<sup>-1</sup>, respectively.<sup>109</sup>

Oct-TriA<sub>1</sub> is a tridecaptin analog consisting of D,L-diaminobutyric acid and D-allo-isoleucine. It is synthesized from costlier amino acid residues. Ballantine *et al.* synthesized eight tridecaptin analogs that were cheaper in synthetic cost and evaluated them against MDR GNB. Tridecaptin analogs 1–8 (19–26, Fig. 8) demonstrated activity against sensitive and resistant *A. baumannii* strains. Among the synthesized compounds, tridecaptin-7 (25) displayed potent activity against MDR strains (clinical and environmental isolates) of *A. baumannii*, *K. pneumoniae*, and *E. cloacae*. Also, the tridecaptin-7 was four-fold more active against *P. pseudoalcaligenes* than canonical Oct-TriA<sub>1</sub> and was least in causing hemolysis to RBC.<sup>111</sup>

Tridecaptin M (27, Fig. 8) was isolated from the mud bacterium *Paenibacillus jamilae*.<sup>106</sup> Tridecaptin M is in preclinical development for treating XDR *Enterobacteriaceae* infections. In a study, Jangra *et al.* evaluated tridecaptin M in combination with other antibiotics against *A. baumannii* strains. Tridecaptin M sensitizes *A. baumannii* to vancomycin, ceftazidime, and rifampicin. The tridecaptin M and

rifampicin combination was the most promising against *A. baumannii*. Tridecaptin M killed the bacteria in an *ex vivo* model of *A. baumannii* and was superior to rifampicin monotherapy.<sup>112</sup>

*Lactococcus lactis* and some *Streptococcus* spp. produce nisin (28, Fig. 8). It belongs to the bacteriocin class and displayed antimicrobial activity in GPB by binding to the lipid II complex. This increases membrane permeability through pore formation and by inhibiting peptidoglycan synthesis. It is mainly used in the food industry as a natural preservative because of its low toxicity to humans and high effectiveness against GPB. However, it is inactive against GNB. A recent study revealed that nisin, in combination with polymyxin B, demonstrated synergistic activity against pan-drug-resistant and extensively resistant *A. baumannii*. Thus, these findings suggest that nisin can be combined to decrease the adverse effects of polymyxin B by lowering its dose.<sup>113</sup>

Synthetic modifications of nisin were carried out to enhance its antibacterial activity against GNB. Several short peptides active against GNB were fused as a tail to the C terminus of either the entire or truncated nisin species. Among these, tail T2 [DKYLPRPRPV], T6 [NGVQPKY], and T8 [KIAKVALKAL] were attached to nisin, which displayed improved activity against GNB. Further, work on this led to the identification of T16m2 (29, Fig. 8) (ABCDE rings + SV+ PRPPHPRLK), which inhibits *A. baumannii* with a MIC value of 0.5  $\mu$ M.<sup>114</sup>

Lipopeptides contain a peptide skeleton with one or more additional ester bonds. *Pedobacter cryoconitis* UP508 bacterial strain was isolated from the soil samples. Nord *et al.* isolated isopedopeptins A–H (30–37, Fig. 8) by bioassay-guided fractionation of *Pedobacter cryoconitis* UP508 extracts. Among the isolated compounds, isopedopeptins B showed promising antibacterial activity against Gram-negative carbapenem-resistant *A. baumannii* with a MIC value of 1  $\mu$ g

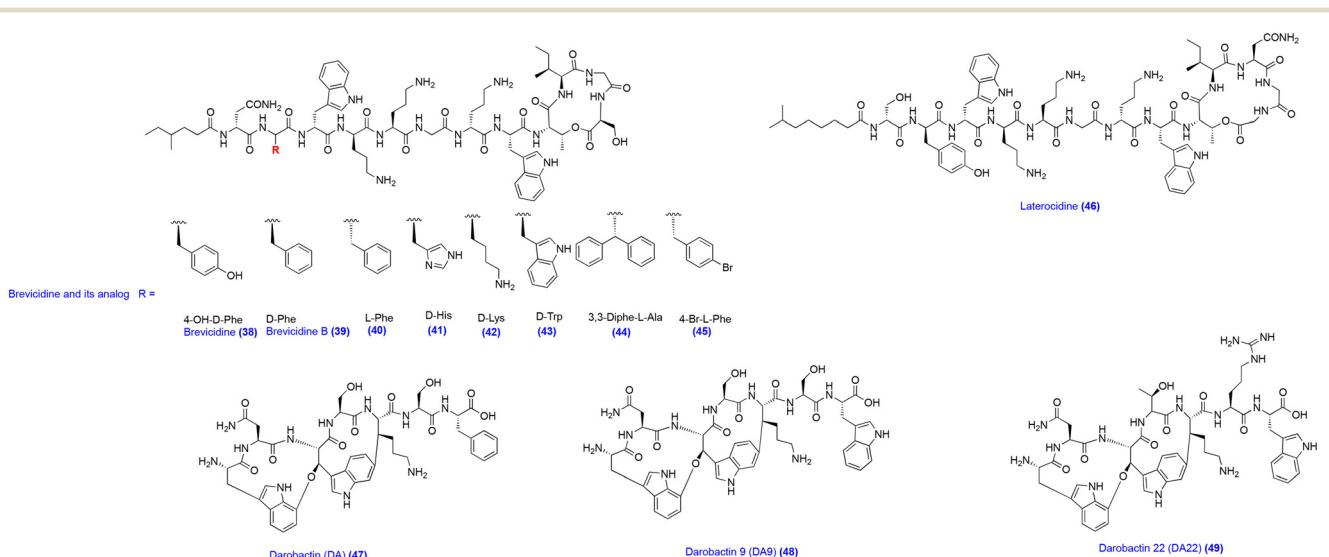


Fig. 9 Chemical structures of brevicidine B and its analogs, laterocidine and darobactins.



$\text{mL}^{-1}$ , and against colistin-resistant strains *A. baumannii*, with a MIC value of  $8 \mu\text{g mL}^{-1}$ , respectively. The isopodopeptins B exhibited an antibacterial mode of action in the *E. coli* liposome system by causing a significant leakage and disruption in the bacterial membrane.<sup>115</sup>

Brevicidine (38, Fig. 9) is a non-ribosomal cyclic lipopeptide isolated from the fermentation of *Brevibacillus laterosporus* DSM25. Earlier studies revealed that brevicidine exhibits broad-spectrum antibacterial activity against *Enterobacter cloacae*, *Escherichia coli*, *Pseudomonas aeruginosa*, and *Klebsiella pneumoniae*. Brevicidine demonstrated potent antibacterial activity against *Escherichia coli* by interacting with lipopolysaccharides on the outer membrane and phosphatidylglycerol and cardiolipin on the inner membrane, resulting in the dissipation of proton motive force and membrane disruption. Zhong *et al.* evaluated brevicidine with antibiotics for combination antibacterial studies. Notably, brevicidine ( $1 \mu\text{M}$ ) decreased the MIC of several antibiotics, including erythromycin, azithromycin, and rifampicin, against *A. baumannii* strains by 32–128-fold. Among them, the potent synergistic activity was achieved for brevicidine and erythromycin combination against *A. baumannii*. Moreover, this combination showed potent antibacterial activity in the *A. baumannii*-induced mouse peritonitis–sepsis models. Brevicidine demonstrated antibacterial activity against *A. baumannii* by disrupting the bacterial membrane. Also, the brevicidine and erythromycin combination showed enhanced killing of *A. baumannii* by adenosine triphosphate biosynthesis inhibition and by accumulation of reactive oxygen species, resulting in the pronounced death of *A. baumannii*.<sup>116</sup>

Brevicidine B contains a single substitution from D-Tyr to D-Phe in the exocyclic linear segment compared to brevicidine. In another study, brevicidine analogs (39–45, Fig. 9) were assessed for antibacterial activity. Interestingly, a single amino acid substitution led to a broader spectrum antimicrobial activity toward *E. coli*, *P. aeruginosa*, and *K. pneumoniae*, with MIC values ranging from  $4\text{--}8 \mu\text{g mL}^{-1}$ . Brevicidine B inhibits *A. baumannii* ATCC 19606 and *A. baumannii* AB5075 with the same MIC value of  $16 \mu\text{g mL}^{-1}$ . Brevicidine B was inactive against GPB, including MRSA strains.<sup>117</sup> The Li *et al.* group analyzed 7395 bacterial genomes and assessed their potential to synthesize cationic non-ribosomal peptides considering activity against GNB. This work identified two novel compounds, brevicidine and laterocidine (46, Fig. 9), which exhibit broad-spectrum activity against GNB. Laterocidine inhibited *A. baumannii*, with a MIC value of  $4 \mu\text{g mL}^{-1}$ . Moreover, brevicidine and laterocidine showed efficacy in mouse models of *E. coli* infections.<sup>118</sup>

Darobactins are produced by entomopathogenic *Photorhabdus khaini*. Darobactins are ribosomal synthesized and post-translationally modified peptides. They mimic the outer membrane protein (OMP) signaling peptide. They bind to the  $\beta$ -barrel of the outer membrane protein BamA, interfering with the integration of the OMP into the membrane. Due to this, BamA cannot close the lateral gate, affecting the entire complex's mechanical, kinetic, and energetic properties in the membrane of the bacteria. Using a biosynthetic engineering pathway, Seyfert *et al.* synthesized analogs of darobactin (DA) (47, Fig. 9). Among the synthesized analogs, DA9 (48, Fig. 9) and DA22 (49, Fig. 9)

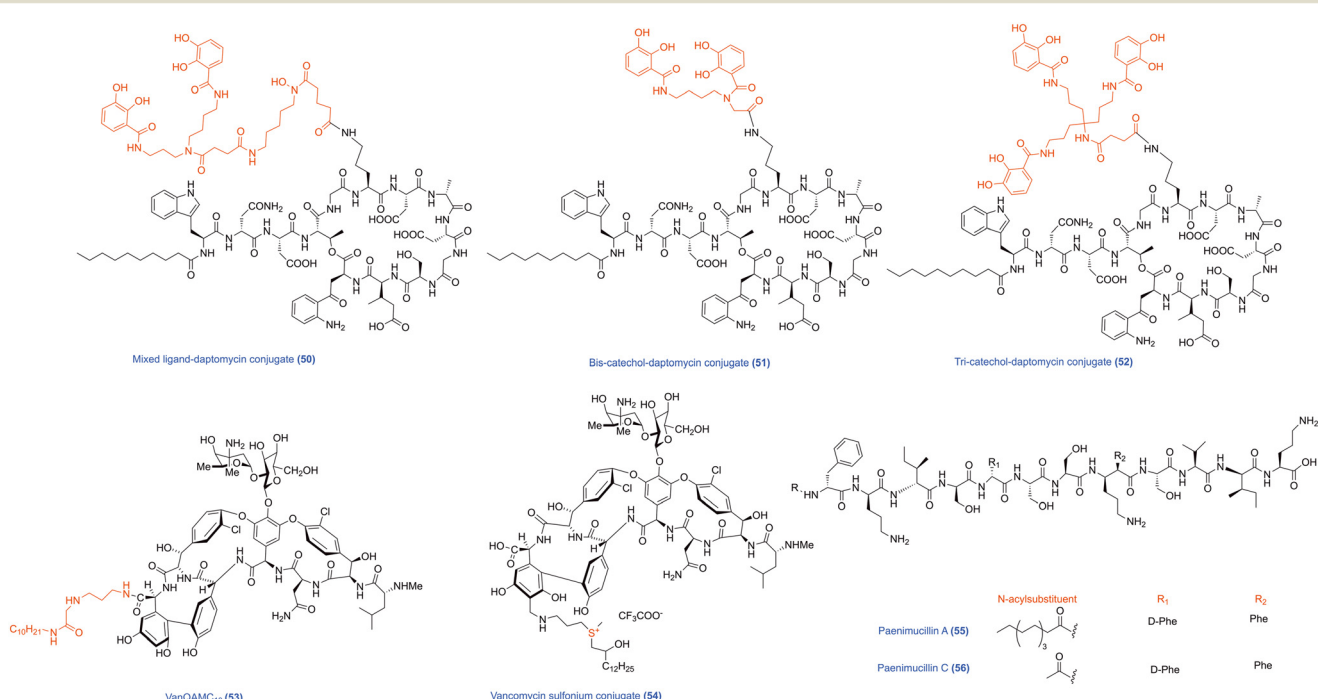


Fig. 10 Chemical structures of daptomycin–siderophore, daptomycin–catechol, vancomycin analogs, paenimucillin A, and paenimucillin C.



were the most superior analogs exhibiting antibacterial activity. DA and its analog DA22 demonstrated broad-spectrum antibacterial activity against *A. baumannii* DSM-30007 and *A. baumannii* DSM-30008 with MIC values of 16 and 4  $\mu\text{g mL}^{-1}$  and 2 and 0.25  $\mu\text{g mL}^{-1}$ , respectively. D22 was nontoxic to HepG2 cells and the zebrafish larvae model.<sup>119</sup>

Specific outer membrane receptor (OMR) transporters in the GNB recognize the siderophore complex and internalize the iron complex in the periplasm. Natural sideromycins are the covalent combination of siderophores and antibiotics, which are recognized by the OMR and allow antibiotics to be delivered inside the cells. In recent years, synthetic sideromycins have been synthesized to mimic the Trojan horse, allowing it to deliver antibiotics inside the cells. Daptomycin is a cyclic lipopeptide produced by the fermentation of *Streptomyces roseosporus*.<sup>120,121</sup> Daptomycin belongs to the class of calcium-dependent antibiotics and has an anionic charge. It is active against broad-spectrum GPB, including *Staphylococcus aureus*, *Streptococcus pyogenes*, *Streptococcus agalactiae*, *Streptococcus dysgalactiae* subsp. *equisimilis* and *Enterococcus faecalis*.<sup>122</sup> It acts against GPB by bacterial membrane disruption, causing rapid membrane depolarization and leaking of ions from the cell.<sup>123</sup> However, it is inactive against GNB because of its polyanionic character and its considerable size, thus it can't penetrate the outer membrane of GNB. In a study by Ghosh *et al.*, they synthesized a hybrid of siderophores and daptomycin, which can solve the issue of daptomycin membrane permeabilization in GNB. The resultant mixed-ligand daptomycin conjugate (50, Fig. 10) was active against GNB and GPB strains. Notably, the mixed-ligand daptomycin conjugate inhibited susceptible and MDR strains, including *A. baumannii* ATCC 17961, with a MIC value of 0.4  $\mu\text{M}$ . Moreover, the daptomycin conjugate increases the survival rate of mice infected with the *A. baumannii* ATCC 17961 sepsis model.<sup>124</sup> In contrast, other siderophore-based conjugates, including bis-catechol daptomycin (51, Fig. 10) and tri-catechol daptomycin conjugates (52, Fig. 10) showed potent antibacterial activity against *A. baumannii* strains. The above study suggests that combining siderophores with daptomycin facilitates the entry of conjugates into *A. baumannii* demonstrating its potential antibacterial activity against GNB.<sup>124,125</sup>

Vancomycin belongs to a glycopeptide obtained from *Amycolatopsis orientalis*. It possesses a sugar-containing heptapeptide structure.<sup>126</sup> The long-chain fatty acid of vancomycin is responsible for its lipophilicity character. Vancomycin and its derivatives showed antibacterial activity by acting on the cell wall precursors containing the D-Ala-D-Ala sequence.<sup>127</sup> It is active against GPB but does not possess activity against GNB. Recent work revealed that a vancomycin lipophilic cationic derivative can eradicate GNB *in vitro* and *in vivo* models.<sup>128</sup> Sarkar *et al.* synthesized vancomycin derivative VanQAmC<sub>10</sub> (53, Fig. 10), and its efficacy was assessed in GPB and GNB. VanQAmC<sub>10</sub> demonstrated activity against *A. baumannii* strains with MIC values ranging from

3.9 to 15.5  $\mu\text{M}$ . It demonstrated bactericidal activity against the carbapenem-resistant *A. baumannii*. It exhibited antibacterial activity by disruption of biofilm formation in *A. baumannii*. Moreover, VanQAmC<sub>10</sub> promoted the intracellular degradative mechanism autophagy in mammalian cells, which helps in the clearance of intracellular pathogens such as *S. aureus* and *Salmonella typhimurium*.<sup>129</sup> In another study by Guan *et al.*, they modified vancomycin with sulfonium ions. The synthesized sulfonium-vancomycin analogs were assessed for their activity in GPB and GNB. The sulfonium-vancomycin analogs showed enhanced antibacterial activity, a good pharmacokinetic profile, stability, and toxicity. The sulfonium-vancomycin conjugate demonstrated antibacterial activity by disrupting the bacterial membrane. The representative vancomycin sulfonium conjugate (54, Fig. 10) inhibited *A. baumannii* with MIC values ranging from 4–8  $\mu\text{g mL}^{-1}$ . This finding suggests that vancomycin having sulfonium modification enhanced the interaction with the bacterial membrane and promoted the disruption of membrane integrity in GNB.<sup>130</sup>

Sanderink *et al.* evaluated a combination of colistin with glycopeptide antibiotics vancomycin or teicoplanin against *A. baumannii*. The colistin-teicoplanin combination increased the survival of mice infected with carbapenem-resistant *A. baumannii* pneumonia by 74%. However, colistin in combination with vancomycin showed similar efficacy compared to colistin alone. This finding suggests that teicoplanin can be combined with colistin to lower the dose of colistin and can decrease the adverse effects associated with colistin.<sup>131</sup>

Paenimucillin A (55, Fig. 10) was initially identified using a culture-independent synthetic-bioinformatic natural product (syn-BNP). It was synthesized based on the bioinformatic prediction of the NRPS gene cluster of *Paenibacillus mucilaginosus* K02. Importantly, paenimucillin A shares similarities in five of their 13 residues and an acyl substituent at the N-terminal of tridecaptin. Paenimucillin A exhibited broad-spectrum antibacterial activity against GPB and mild antibacterial activity against *A. baumannii*. Vilafarres *et al.* carried out the bioinformatics-guided synthesis of paenimucillin A analogs. Among the synthesized compounds, paenimucillin C (56, Fig. 10) was cationic and inhibited the growth of MDR *A. baumannii* 1788 with a MIC value of 4  $\mu\text{g mL}^{-1}$ . Moreover, in rat cutaneous wound models infected with *A. baumannii*, paenimucillin C sterilized the wound infections completely, with no sign of rebound infection. Paenimucillin C demonstrated antibacterial activity against *A. baumannii* by pore formation and promoting cytoplasmic contents' leakage. In contrast, the closest similar structure, tridecaptin, showed antibacterial activity by binding to the target lipid II. Furthermore, paenimucillin C was the least toxic to HT-29 cells.<sup>132</sup>

X33 (57) is an oligopeptide isolated from *Streptomyces lavendulae* X33. It is active against *Penicillium digitatum* and *Candida albicans*. X33 showed moderate antibacterial activity against *A. baumannii* with MIC and MBC values of 78.13 and



312.50  $\mu\text{g mL}^{-1}$ , respectively. It causes changes in the cell wall permeability, induces changes in the cell morphology, and promotes leakage of cell contents. Moreover, X33 interfered with the tricarboxylic acid (TCA) cycle, glycolysis, oxidative phosphorylation, and pyruvate metabolism and induced oxidative stress in the bacterial cells.<sup>133</sup>

Lynronne-1 (58) is a 19 amino acid cationic peptide isolated from the bovine rumen microbiome. It inhibited *A. baumannii* ATCC 19606 with MIC values ranging from 16–8  $\mu\text{g mL}^{-1}$ , respectively. It displayed more selectivity to bacterial cells and exhibited the least hemolysis of the RBC cells. The biophysical models confirmed that the lynronne-1 mode of action is by membrane lysis. However, this has to be confirmed on the bacterial cells.<sup>134</sup>

**2.1.2. Humans.** Humans possess three types of AMPs: defensins, cathelicidins, and histatins. Cathelicidins are canonical peptides found in humans and other species, including cattle, reptiles, horses, and pigs. hCAP-18 belongs to the cathelicidin AMP family of humans, comprising an N-terminal, a cathelin, and a C-terminal LL-37 domain. LL-37 (LLGDFFRKSKEKIGKEFKRIVQRIKDFLRNLVPRTES) (59) is a 37 amino acid AMP produced from hCAP-18 by the catalyzing effects of proteinase. LL-37 showed broad-spectrum activity, including antibacterial, antiviral, and antifungal activity. It killed *A. baumannii* by binding to the OmpA (AbOmpA) protein membrane of *A. baumannii*.<sup>135</sup> LL-37 and its analogs LL/CAP18 (60) (FRKSKEKIGKLFKRVQRILDFLRNLV) and FF/CAP18 (61) (FRKSK EKIGK FFKRI VQRIF DFLRN LV) inhibited the growth of pan-drug-resistant *A. baumannii* (PDRAB) with MIC values of 32–64, 32–64, and 8–16  $\mu\text{g mL}^{-1}$ , respectively. Moreover, LL/CAP18 and FF/CAP18 exhibited biofilm inhibition and demonstrated rapid killing of the bacteria.<sup>136,137</sup> The combination of LL-37 and oncorhyncin II showed synergistic activity and demonstrated rapid killing of *A. baumannii*.<sup>138</sup> P-10 (62) is a cationic AMP and a synthetic derivative of LL-37 with a broad spectrum of antimicrobial activity. P-10, in combination with nisin, demonstrated synergistic activity against extensively drug-resistant *A. baumannii* and colistin-resistant *P. aeruginosa*.<sup>139</sup>

HLF (1–11) (63) belongs to the cathelicidin family and is derived from an N-terminal fragment of human lactoferrin. HLF showed promising antibacterial activity against MDR bacteria, including *Staphylococcus aureus* and *A. baumannii*, *in vitro* and *in vivo* models of infections. HLF (1–11) (GRRRRSVQWCA, C-terminal amide) contains N-terminal arginine 2 and 3, essential for bactericidal activity. Additionally, HLF (1–11) improves the survival of mice infected with *A. baumannii*-induced pneumonia by suppressing the pyroptosis of macrophages and inflammatory cytokine production of activated macrophages.<sup>140</sup> In a study, cathelicidin-related antimicrobial peptide (CRAMP) was evaluated in a murine model for immune response to multidrug-resistant *A. baumannii*. Wild-type and CRAMP knockout mice were infected intranasally with the multidrug-resistant *Acinetobacter baumannii*. These studies demonstrated that CRAMP<sup>−/−</sup> mice exhibited an

increase in the colony-forming units of the bacteria, and levels of IL-6 and CXCL1 were lower, and IL-10 was more in the BAL fluid compared to wild-type mice. The above results suggest that the cathelicidin-related antimicrobial peptide is essential in providing host defense against pulmonary infection with bacteria by activating neutrophils and the innate immune response.<sup>141</sup>

Defensins are derived from human peptides. They are cationic amphipathic with a  $\beta$ -sheet-rich group. They form a network of disulfide bridges leading to a conserved structural fold, an important characteristic of defensins. Defensins exhibit antibacterial activity by creating pores, leading to the loss of cellular contents. They have three types, *i.e.*,  $\alpha$ -,  $\beta$ -, and  $\theta$ -defensins. The  $\alpha$ -defensin and  $\beta$ -defensin peptides can be differentiated based on their disulfide bridge. In  $\alpha$ -defensin peptides, the intramolecular bonding occurs between cysteines 1–6, 2–4, and 3–5, whereas in  $\beta$ -defensins, intramolecular bonding occurs between 1–5, 2–4, and 3–6 cysteine residues, respectively.<sup>142</sup> Further,  $\beta$ -defensins are sub-classified into  $\beta$ -defensin-1 (hBD-1),  $\beta$ -defensin-2 (hBD-2),  $\beta$ -defensin-3 (hBD-3) and  $\beta$ -defensin-4 (hBD-4). Among them,  $\beta$ -defensin-2 comprises 41 amino acids. The synthetic  $\beta$ -defensin-2 (64) (GIGDPVTCLKSGAICHHPVFCPRRYKQIGTCGLPGTKCCKKP) showed bactericidal activity against *A. baumannii*, *Pseudomonas aeruginosa*, *Enterococcus faecalis*, *Enterococcus faecium* and *Staphylococcus aureus*. MDR *A. baumannii* (vLD90 = 3.25–4.5  $\mu\text{g mL}^{-1}$ ) was more susceptible to  $\beta$ -defensin-2 than wild-type *A. baumannii* (vLD90 = 3.90–9.35  $\mu\text{g mL}^{-1}$ ). Interestingly,  $\beta$ -defensin-2 does not exhibit promising bactericidal activity in *Escherichia coli*, *Klebsiella pneumoniae*, and *Proteus mirabilis*. In contrast,  $\beta$ -defensin-2 showed enhanced activity in the bacterial strains resistant to  $\beta$ -lactam antibiotics.<sup>143</sup>

Apolipoprotein E (ApoE) is a glycosylated protein in humans. It regulates microglial activation and inflammatory response during acute and chronic nerve injury. The proteolytic fragments of apolipoprotein E demonstrated antimicrobial and other biological activities. For instance, ApoE (130–162) showed antibacterial activity against *Escherichia coli* and *Pseudomonas aeruginosa*. Notably, ApoE<sub>23</sub> is active in *A. baumannii*. Wang *et al.* evaluated the apolipoprotein E mimetic COG1410 (65) peptide for antibacterial activity. COG1410 mimics the residues located between 138 and 149 of the ApoE N-terminal domain and has substitutions at positions 140 and 145 with aminoisobutyric acid. COG1410 inhibited *A. baumannii* ATCC19606 and PDR *A. baumannii* YQ4 with the same MIC value of 16  $\mu\text{g mL}^{-1}$  and quickly eliminated a large inoculum of *A. baumannii*. COG1410 demonstrated antibacterial activity by disrupting the plasma membrane, leaking the cytoplasmic contents, and inhibiting biofilm formation. COG1410 exhibited synergistic activity with polymyxin B and cured *C. elegans* infected with PDR *A. baumannii*. This finding suggests that COG1410 can be combined with polymyxin B to reduce the dose of polymyxins.<sup>144</sup>

**2.1.3. Bovine.** Bovine myeloid antimicrobial peptide 28 (BMAP-28) (66) is an AMP belonging to the cathelicidin



family. BMAP-28 exerts potent activity against *Pasteurella multocida*, and its analogs are reported to possess inhibitory activity against *Staphylococcus aureus* (MRSA) and *Leishmania*, respectively. Guo *et al.* evaluated BMAP-28 (GGLRSLGRKILRAWKKYGPPIVPIIRI) and its analogues A837 (GGLRKLGRKILRAWKKYGPPIVPIIRI), A838 (KGLRKLGRKI LRAWKKYGPPIVPIIRI), A839 (GGLRSLGRKILRAWKKGGPPIVPIIRI), and A840 (KGLRK LGRKILRAWKKGGPPIVPIIRI) for antibacterial activities. BMAP-28 and its analogs A837 (67), A838 (68), A839 (69), and A840 (70) demonstrated antibacterial activity against pan-drug-resistant *A. baumannii* strains with MIC values of 5, 10, 5–10, 5–10, and 5–10  $\mu\text{g mL}^{-1}$ , respectively. BMAP-28 and its analogs depicted rapid killing of pan-drug-resistant *Acinetobacter baumannii* by binding to its outer membrane protein OmpA (AbOmpA).<sup>145</sup>

Proline-rich peptides (Pr-AMPs) possess potent antimicrobial activities against bacterial species, including *K. pneumoniae*, *A. baumannii*, and *E. coli*. Pr-AMPs showed antimicrobial activity by acting on targets other than bacterial membranes. Bac7 (1–35) (71) is a proline-rich peptide that exhibits potent antimicrobial activity against many GNB species, including *A. baumannii*, with a MIC value of  $\leq 8 \mu\text{M}$ . Notably, at the sub-MIC values of Bac7, it decreased the biofilm formation and motility.<sup>146</sup> Bac5 (1–17) is a bovine proline-rich cathelicidin, and its fragments possess antibacterial activity against GNB, including *E. coli*, *A. baumannii*, and *K. pneumoniae*. Notably, the N-terminal 1–17 fragment of Bac5 is mainly responsible for antimicrobial activity and protein synthesis inhibition. Mardirossian *et al.* modified Bac5 to identify the critical residues for antimicrobial activity. Among the synthesized compounds, the representative derivatives Bac5-258 (72) (RFRPIRPPIRPPFYR), Bac5-272 (73) (RFRWPPIRPPIRPPFYR), Bac5-278 (74) (RWRWPPIRPPIRPPFYR), Bac5-281 (75) (RWRRPPIRRRPIRPPFYW), and Bac5-291 (76) (RWRRPPIRRRPIRPPFWR) showed broad spectrum activity against GNB. Bac5-258, Bac5-272, Bac5-278, Bac5-281, and Bac5-291 inhibited *A. baumannii* ATCC19606 with MIC values of  $> 64$ , 64, 8, 4, 2, and 8  $\mu\text{M}$ , and MBC values of  $> 64$ , 64, 16, 8, 8, and 16  $\mu\text{M}$ , respectively. Only Bac5-281 demonstrated protein synthesis inhibition among these peptides, mainly due to its membrane permeabilization. The other peptides showed dual modes of action, including protein synthesis inhibition and bacterial membrane destabilization. Notably, the Bac5 derivatives, which have more arginine and tryptophan residues, demonstrated enhanced antimicrobial activity and broader spectrum activity while retaining low cytotoxicity to eukaryotic cells.<sup>147</sup>

**2.1.4. Snake.** Cathelicidin-BF is a broad-spectrum AMP. However, it has instability *in vivo* and toxic effects such as hemolysis and immunoregulation.<sup>148</sup> To improve cathelicidin-BF stability, decrease its toxicity, and maintain its antibacterial activity, Mawangi *et al.* synthesized cathelicidin-BF analogs, including cathelicidin-BF15 (77) (VKRFKKFFRKLKKS), cathelicidin-BF15-a1 (78) (VKRFKKFFRKFKFV-NH<sub>2</sub>), cathelicidin-BF-a2 (79) (VKRWKKWFRKWKWV), and cathelicidin-BF-a3 (80) (VKRWKKWFRKWKWV-NH<sub>2</sub>). The introduction of cysteine in cathelicidin-BF-a3 led to the formation of cathelicidin-BF-a4 (ZY4)

(81), increasing its stability by cyclization and introducing a disulfide bridge formation. The increase in stability increases its  $t_{1/2}$  of 1.8 h *in vivo*. ZY4 demonstrated antibacterial activity in *A. baumannii* isolates with MIC ranging between 4.6 and 9.4  $\mu\text{g mL}^{-1}$ . ZY4 showed antibacterial activity through membrane permeabilization, disruption, and pore formation. It also inhibited biofilm formation in the bacteria and decreased the susceptibility of mice infected with *P. aeruginosa* and *A. baumannii* septicemia models.<sup>149</sup>

**2.1.5. Alligator and crocodile.** In a study, five new crocodylian  $\beta$ -defensin variants from *Alligator mississippiensis* and *Crocodylus porosus* were selected based on their preliminary investigation peptides, including Am2HR (82), Am11RR (83), Am17RV (84), Am23SK (85), and Cp13QK (86), and were synthesized in the lab. Among them, Am23SK (85) (SCRFGGGYCIWNWERCRSGHFLVALCPFRKRCCK) from *Alligator mississippiensis* displayed antibacterial activity against *A. baumannii* Ab5075 with a MIC value of 2  $\mu\text{g mL}^{-1}$ . Also, Am23SK was active against both planktonic cells and inhibited biofilm production. Moreover, Am23SK showed no toxicity towards mammalian cells and *in vitro* exhibited immunogenicity and moderately suppressed the production of proinflammatory mediators from stimulated human bronchial epithelial cells.<sup>150</sup>

Barksdale *et al.* characterized and evaluated the antimicrobial activity of peptides Apo5 (87), Apo6 (88), and A1P (89) derived from *Alligator mississippiensis*. Apo5 and Apo6 are related peptides, nested fragments of a purported apolipoprotein, and A1P is the C-terminal fragment of the alpha-1-proteinase inhibitor of the serpin family. Apo5 (FSTKTRNWFSEHFKVKEKLKDTFA), Apo6 (KTRNWFSEHFKVKEKLKDTFA), and A1P (PPPV IKFNRPFLMWIVERDTRSILFMGKIVNPKAP) exhibited broad-spectrum antibacterial activity. They inhibited *A. baumannii* ATCC 9955 and *A. baumannii* ATCC BAA-1794 with EC<sub>50</sub> values of 0.644 and 0.234  $\mu\text{g mL}^{-1}$ , 0.233 and 0.126  $\mu\text{g mL}^{-1}$ , and 224.0 and 23.6  $\mu\text{g mL}^{-1}$ , respectively. Additionally, these peptides inhibited the growth of *S. aureus*, *Escherichia coli*, and *P. aeruginosa*. The mode of action of Apo5 and Apo6 is by depolarisation of the bacterial membrane. However, A1P was unable to depolarise the bacterial membrane at low concentrations. This suggests that Apo5 and Apo6 modes of antibacterial action are by membrane disruption. Importantly, these peptides do not cause hemolysis of sheep red blood cells.<sup>151</sup>

**2.1.6. Frog.** Temporin-1CEc is a natural peptide obtained from frog *Rana chensinensis* skin secretion. Ji *et al.* synthesized temporin-1CEc analogs and labeled them 2K4L (90) (IILLLKKFLKKL-NH<sub>2</sub>) and 2K2L (91) (IIPPLPLKKFLKKL-NH<sub>2</sub>). 2K4L and 2K2L adopt an  $\alpha$ -helical secondary structure in a membrane-mimetic environment. 2K4L and 2K2L displayed bactericidal activity against *A. baumannii* MRAB 0227 and *A. baumannii* 22933 with MIC values of 6.25 and 3.13  $\mu\text{M}$  and 25 and 12.5  $\mu\text{M}$ , respectively. 2K2L and 2K4L have the same net charge, with high mean hydrophobic values of 14.94 and 17.14, respectively, suggesting that the peptide's hydrophobicity plays a vital role in antibacterial activity. The increase in the hydrophobicity remarkably



increases the permeability of the peptides in the membrane. Due to its strong positive charge on the 2K4L peptide, it promotes interaction with lipopolysaccharides and disrupts membrane integration, leading to leakage of cell contents. Moreover, 2K4L inhibited biofilm formation. Interestingly, 2K4L showed protection activity in mice infected with *A. baumannii*-induced sepsis.<sup>152</sup>

Hylin a1 (92) (IFGAILPLALGALKNLIK-NH<sub>2</sub>) was obtained from the arboreal South American frog *Hypsiboas albopunctatus*. It is an eighteen-amino acid peptide and demonstrates antimicrobial activity by acting on the bacterial membrane. However, hylin a1 exhibits hemolytic activity against red blood cells. Park *et al.* designed and synthesized hylin a1 analog peptides to decrease hemolytic activity. The hylin a1 analogs, including hylin a1-11K (93) (IAKA ILPLALKALKNLIK-NH<sub>2</sub>) and hylin a1-15K (94) (IAKA ILPLALKALKKLIK-NH<sub>2</sub>), exhibited broad-spectrum antimicrobial and anti-biofilm activity against carbapenem-resistant *A. baumannii* and showed lower hemolytic effects and lower selectivity to mammalian cells. Hylin a1-11K and hylin a1-15K showed antibacterial activity against *A. baumannii* by binding to lipopolysaccharides and causing the disruption of the bacterial membrane. Moreover, these analogs decreased the inflammation by suppressing the proinflammatory response generated due to *A. baumannii* infections and also ameliorated carbapenem resistance in mice infected with *A. baumannii*.<sup>153</sup>

Aurein is an antibacterial peptide secreted from the granular dorsal gland of *Litoria aurea*. P0 is a 45 amino acid  $\alpha$ -helical peptide belonging to the cathelicidin class, and A0 is an 11 amino acid  $\alpha$ -helical aurein derived peptide. P0 and A0 were modified to P7 and A3 derivatives by truncating the peptide chain and substituting amino acids with hydrophobic and positively charged amino acids tryptophan and arginine. From these two parent peptides,  $\alpha$ -helical cathelicidin (P7) and aurein (A3), a hybrid peptide was synthesized and designated as A3P7. Jariyattanarach *et al.*

modified the hybrid peptide A3P7 by flipping methodology. The parent compound A3P7 exhibits potent antibacterial activity against GNB and GPB but has hemolytic activity. To reduce the toxicity of A3P7, a series of eight compounds (AP12-AP19) were synthesized by truncating the C-terminal amino acids. Among them, AP19 (RLFRRVKKVAGKIAKRIWK-NH<sub>2</sub>) (95) demonstrated potent activity against *A. baumannii* with minimal hemolytic and cytotoxic activities against RBCs and mammalian cells. Further, to enhance the stability of AP19, the D-form of amino acids was incorporated to give D-AP19, which demonstrated antibacterial activity against MDR and XDR clinical isolates of *A. baumannii* and rapidly killed the bacteria. The mode of action of D-AP19 is by membrane disruption and leakage of the cytoplasmic intracellular contents. The bacteria treated with D-AP19 showed rough and shrunk surfaces, with blebbing and distortion of the membrane.<sup>154</sup>

Esculetin-1a (Esc) (96) is a 21-amino residue peptide from frog skin. It is a broad-spectrum AMP active against GPB and GNB. Amp Esc (1-21), in combination with colistin, showed synergistic activity against MDR *A. baumannii* clinical isolates. Esc (1-21), in combination with colistin, demonstrated antibacterial action by potentiating the membrane perturbation effects.<sup>155</sup>

**2.1.7. Insects.**  $\Delta$ -Myrtxin-Mp1a (Mp1a) was isolated from the venom of jack-jumper bull ant *Myrmecia pilosula*. It comprises 49 amino acid residues and two chains, *i.e.*, a 26-mer A chain and a 23-mer B chain connected by two disulfide bonds in an antiparallel arrangement. Mp1a A and B chains were synthesized in their reduced forms using solid-phase peptide synthesis. The chains were joined by cysteine oxidation to form Mp1a as a significant product along with other synthetic analogs. Mp1a (97, Fig. 11) and its analogs Mp 1b-3b (98-104, Fig. 11) showed potent activity against GPB and GNB, including *E. coli*, *K. pneumoniae*, *A. baumannii*, *P. aeruginosa*, *S. aureus*, and *S. pneumoniae*. Mp1a and its analogs (1b-3b) (98-104, Fig. 11) inhibited *A. baumannii*

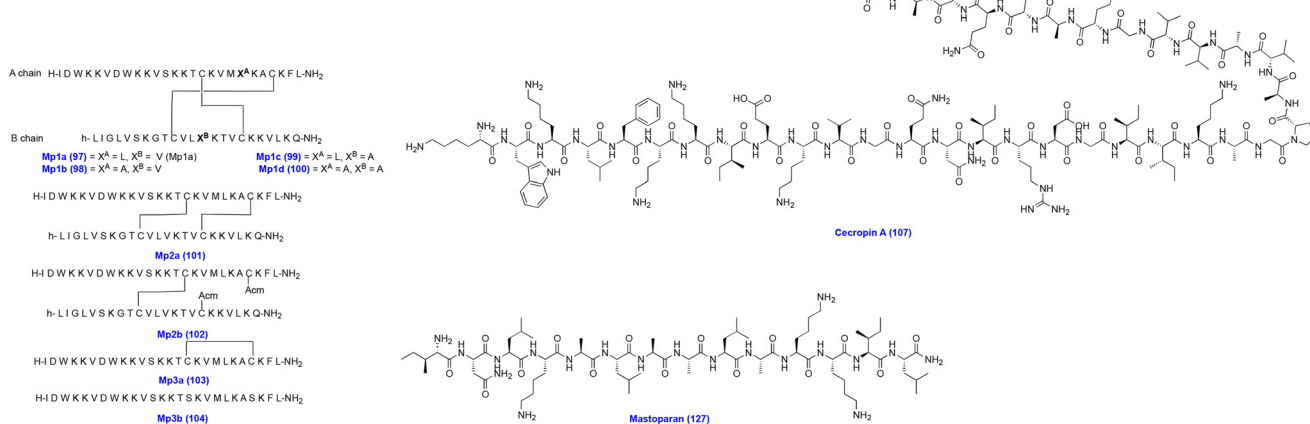


Fig. 11 Chemical structures of Mp1a analogs, cecropin A, and mastoparan.



ATCC 19606 with MIC values of 0.025, 0.015–0.03, 0.015–0.03, 0.015–0.03, 0.05–0.1, 0.025–0.1, 0.2, and 0.4–0.8  $\mu\text{M}$ , respectively. Mp1a and its derivatives demonstrated potent cell membrane binding and disrupted the cytoplasmic membrane. However, Mp1a causes the induction of calcium ions in mammalian cells, which results in toxicity to human kidney cells. For the same reason, the intraplantar injection of Mp1a (10  $\mu\text{M}$ ) into mice causes spontaneous pain.<sup>156</sup>

LyeTx I (105) (H-IWL TALKFLGKNLGKHLAKQQLAKL-NH<sub>2</sub>) is an AMP obtained from *Lycosa erythrogynatha* spider venom and exhibits broad-spectrum antimicrobial activity, including GPB and GNB, and fungi. Lima *et al.* modified the C-terminal portion of the LyeTx I peptide to generate LyeTx I mn $\Delta$ K (106) (H-IWLTKALKFLGKNLGK-NH<sub>2</sub>), a short peptide comprising 16 amino acids. LyeTx I mn $\Delta$ K showed antibacterial activity against carbapenem-resistant *A. baumannii* AC10, *A. baumannii* AC37, *A. baumannii* AC30, *A. baumannii* AC31, *A. baumannii* AC35, and *A. baumannii* AC03, with MIC and MBC values of 2 and 2  $\mu\text{M}$ , 4 and 4  $\mu\text{M}$ , 8 and 8  $\mu\text{M}$ , 16 and 16  $\mu\text{M}$ , 4 and 4  $\mu\text{M}$ , and 4 and 4  $\mu\text{M}$ , respectively. Moreover, intranasal dosing of LyeTx I mn $\Delta$ K reduced the bacterial load in the mouse model of carbapenem-resistant *A. baumannii*. Also, it showed synergistic activity with meropenem and colistin against carbapenem-resistant *A. baumannii*. It demonstrated significantly low cytotoxicity and hemolytic activity in Vero cells and RBCs. LyeTx I mn $\Delta$ K exhibits an antibacterial mode of action by disrupting the bacterial cell membrane, causing leakage of cell contents and reducing the preformed biofilms.<sup>157</sup>

Cecropins are amphipathic peptides secreted by insects. Cecropin A (107, Fig. 11) was first isolated from the giant silk moth *Hyalophora cecropia*. Cecropin A is a hydrophobic cationic AMP, which exhibits antibacterial activity by facilitating membrane permeabilization and inhibiting proton gradient formation. However, it suffers from stability issues due to abundant lysine and arginine in the structure, a common recognition sequence for protease enzymes. Several synthetic modifications were carried out to address the inherent instability issue of cecropin A.<sup>158,159</sup> The insect *Musca domestica* cecropin showed antibacterial activity by acting on the cell membrane integrity of *Escherichia coli* and *A. baumannii*. Cec4 (108) (GWLKKIGKKIERVGQNTRDATIQAIQVAQQAANVAATLKG) is an  $\alpha$ -helix peptide, which exhibited antibacterial activity against *A. baumannii* (ATCC 19606), MDR *A. baumannii* (ID: 4367661), and extensive drug-resistant *A. baumannii* (PRAB) with the same MIC value of 4  $\mu\text{g mL}^{-1}$  and showed minimum biofilm inhibition concentration (MBIC<sub>90</sub>) values of 64, 64 and 128  $\mu\text{g mL}^{-1}$  and minimum biofilm eradication concentration (MBEC) values of 128, 128, and 256  $\mu\text{g mL}^{-1}$ , respectively. Importantly, Cec4 showed no toxicity to hemolytic effects on human cells. Cec4 treatment of *A. baumannii* led to the destruction of the bacterial membrane and caused leakage of the cytoplasmic contents.<sup>160</sup> In another study, Cec4 demonstrated activity against carbapenem-resistant *A. baumannii* with a MIC value of 4  $\mu\text{g mL}^{-1}$ , a MBIC value of 64–128  $\mu\text{g mL}^{-1}$ , and a MBEC value of 256–512  $\mu\text{g mL}^{-1}$ ,

respectively. Scanning electron microscopy (SEM) and confocal laser scanning microscopy (CLSM) revealed that Cec4-treated *A. baumannii* cells showed biofilm disruption. Meanwhile, transcriptome analysis revealed that multiple metabolic pathways were affected in *A. baumannii*.<sup>161</sup>

Papiliocin is an antimicrobial peptide of 37 amino acid residues belonging to a class of cecropins. It is present in the swallowtail butterfly larvae. It is active against MDR GNB. However, it is responsible for immunogenic potential. Kim *et al.* designed a short 12-meric antimicrobial peptide by substituting 12 papiliocin (pap12-1) peptide residues at the N-terminal end to increase the antibacterial activity and bacterial membrane interactions. Notably, the designed 12-meric peptides displayed enhanced antibacterial activity by destabilizing and increasing the membrane's permeability and causing leakage of cellular contents. Among these peptides, Pap12-6 (109) (RWKIFKKVVKW-NH<sub>2</sub>) inhibited *A. baumannii* with a MIC value of 4  $\mu\text{M}$ . Moreover, Pap12-6 significantly reduced the bacterial growth in a mouse sepsis model. Also, it significantly reduced inflammatory cytokines.<sup>162</sup>

Mandel *et al.* synthesized OMN6 (110, Fig. 11), a cyclic peptide of 40 amino acids. It displayed improved stability and a significant decrease in proteolytic degradation. OMN6 showed potent inhibitory activity against GNB, including *A. baumannii*, *Klebsiella pneumoniae*, and *Escherichia coli*. OMN6 showed antibacterial activity against *A. baumannii* ACC 00445, *A. baumannii* ACC 00527, *A. baumannii* ACC 00535, and *A. baumannii* ACC 01077 with the same MIC value of 4  $\mu\text{g mL}^{-1}$ , respectively. The mode of action of OMN6 was determined using *E. coli*. It disrupted the membrane and caused leakage of the cell contents. Moreover, OMN6 did not cause hemolysis of the red blood cells and was nontoxic to the HEK293T cells.<sup>163</sup>

Peptides D6 and D8 are derived from cecropin–melittin hybrids. D6 and D8 showed antimicrobial activity by binding to the LPS of the bacterial membrane. In combination with antibiotics, these peptides potentiated the effects of vancomycin against a murine model for abscess formation by *P. aeruginosa*. Also, D6 and D8 comprise D-amino acid residues, which are costlier and are not recognized by mammalian proteases, making them more stable *in vivo* models. Keeping this in view, Schouten *et al.* synthesized L forms of peptides L6 (111) (RRLFRRILRWL) and L8 (112) (KRIVQRIKKWLR). The peptides L6 and L8 demonstrated synergistic activity with vancomycin against *E. coli*, *A. baumannii*, and *K. pneumoniae*. Further, L6 potentiated the action of vancomycin in *A. baumannii*. However, the peptides L6 and L8 were unstable in human serum. Stapled peptides were generated by introducing hydrocarbons, which reduce flexibility in the peptides. The stapled peptide L8S1 potentiated the activity of vancomycin in the *in vivo* model of *A. baumannii* infections.<sup>164</sup>

Protaetiamycine (113) is an AMP present in insects belonging to the defensin class. Earlier studies have identified Pro9-3 (114) (RLWLAIWRR-NH<sub>2</sub>) and Pro9-3D



(rlwlairwrr-NH<sub>2</sub>) (**115**) peptides based on the chemical structure of defensins. Further, based on the defensin, 10-meric peptide Pro10-1 and its enantiomer, Pro10-1D, were synthesized by including an Arg residue at the N-terminus of Pro9-3. Krishnan *et al.* synthesized 9-meric peptides R-Pro9-3 (**116**) (RRWIALWLR-NH<sub>2</sub>) and R-Pro9-3D (**117**) (rrwialwlr-NH<sub>2</sub>). Pro9-3, Pro9-3D, R-Pro9-3, and R-Pro9-3D inhibited *A. baumannii* with MIC values of 16, 8, 16, and 8 μM, respectively. Moreover, these peptides showed inhibitory action against CRAB. Also, R-Pro9-3D protected mice infected with the *A. baumannii*-induced sepsis model. These peptides showed antibacterial activity by interacting with LPS in the outer membrane, causing permeabilization. Furthermore, R-Pro9-3D demonstrated good proteolytic stability and low toxicity.<sup>165</sup>

CM11 (**118**) (COOH-WKLFKKILKVL-NH<sub>2</sub>) is a cecropin A-melittin peptide hybrid. The modification of CM11 led to peptide mCM11 (**119**) (NH<sub>2</sub>-WRLFRRILRVL-NH<sub>2</sub>). The mCM11 peptide showed antibacterial and antibiofilm formation activity. It inhibited MDR *A. baumannii* 31, PDR *A. baumannii* 71, XDR *A. baumannii* 23, and XDR *A. baumannii* 59, with MIC values of <4, <4, 4, and 4 μg mL<sup>-1</sup>, respectively. Moreover, mCM11 disrupted the bacterial membrane due to its high arginine content, which enhanced its antimicrobial activity. Furthermore, it demonstrated low hemolytic activity on human RBCs.<sup>166</sup>

Eales *et al.* assessed the antibacterial activity of bicarinalin (**120**) and BP100 (**121**) against *A. baumannii* strains. Bicarinalin (**120**) (KIKIPWGKVKDFLVGGMKAV) is an amphipathic obtained from the venom of the myrmicine ant *Tetramorium bicarinatum*. It exhibits antibacterial activity against GPB and GNB. Melittin is an alpha-helical peptide isolated from the European honey bee, which is cytotoxic to the cells. To overcome the proteolytic degradation and melittin's toxicity, a peptide BP100 (**121**) (KKLFKKILKYL) was synthesized. BP100 is a hybrid of cecropin A and melittin. BP100 showed potent antibacterial activity against GNB. Bicarinalin and BP100 inhibited *A. baumannii* with MIC and MBC values of 4 and 4 μg mL<sup>-1</sup>, respectively. Bicarinalin and BP100 inhibited biofilm formation in *A. baumannii*. Notably, *A. baumannii* treated with bicarinalin and BP100 showed morphological changes in the cells, with pronounced blebbing with variable cell shape, shrinkage, and membrane disruption. Further liposome assays confirmed that these peptides cause membrane disruption by pore-formation.<sup>167</sup>

HP (2–20) (**122**) is a protein obtained from the N-terminal region of *Helicobacter pylori* ribosomal protein L1 (RPL1). The peptides cecropin A, melittin, magainin 2, and HP (2–20) are known for their antibacterial activity. Gopal *et al.* synthesized four chimeric peptides HPME (**123**) (AKKVFKRLGIGAVLKVLTTG, a combination of HP 2–9 and ME 1–12), HPMA (**124**) (AKKVF KRLGIGKFLHSAKKF-NH<sub>2</sub>, a combination of HP 2–9 and MA 1–12), CAME (**125**) (WKLFKKI GIGAVLKVLTTG-NH<sub>2</sub>, a combination of CA 1–8 and ME 1–12), and CAMA (**126**) (WKLFKK IIGIKFLHSAKKF-NH<sub>2</sub>, a combination of CA 1–8 and MA 1–12). Interestingly,

all these four peptides, HPME, HPMA, CAME, and CAMA, exhibited antibacterial activity with MIC values ranging from 3.12–12.5 μM in *A. baumannii* strains that were resistant to antibiotics, including ampicillin, cefotaxime, ciprofloxacin, tobramycin, and erythromycin. Importantly, these peptides exhibited synergistic activity with the commercial antibiotics and inhibited biofilm formation.<sup>168</sup>

Mastoparan (**127**, Fig. 11) (H-INLKALAALAKKIL-NH<sub>2</sub>) is an AMP that showed potent antibacterial activity against colistin-susceptible and colistin-resistant *A. baumannii*. However, mastoparan is unstable in serum. To enhance the stability and maintain the antimicrobial activity, Vila-Farrés *et al.* synthesized mastoparan analogs. Among the synthesized mastoparan analogs, H-inlkalaalakkil-NH<sub>2</sub> (**128**) and Gu-INLKALAALAKKIL-NH<sub>2</sub> (**129**) showed activity against *A. baumannii* Ab113 with MIC values of 2.7 and 2.6 μM, respectively. In contrast, mastoparan inhibited *A. baumannii* Ab113 with a MIC value of 2.7 μM. Importantly, mastoparan analogs H-inlkalaalakkil-NH<sub>2</sub> and Gu-INLKALAALAKKIL-NH<sub>2</sub> were stable for 24 h in human serum, whereas mastoparan was stable for six hours. Also, *A. baumannii* treated cells with mastoparan and its analogs showed structural damage to the membrane, depicting fractures and causing dye leakage in the dye-assay experiment. This finding suggests that the mode of action of these peptides is by disruption of the bacterial membrane.<sup>169</sup>

Lycosin-II (**130**) (VWLSALKFIGKHLAKHQLSKL) is a peptide isolated from the venom of the spider *Lycosa singoriensis*. It is a linear cationic amphipathic α-helical peptide. Lycosin-II inhibited *A. baumannii* with MIC values ranging from 3.1–6.3 μM. In the presence of magnesium ions, there is an increase in the MIC of lycosin-II against *A. baumannii*, which suggests that magnesium might compete with the bacterial cell membrane. However, lycosin-II is unstable *in vivo*, which limits further development.<sup>170</sup>

DvAMP (**131**) (EKKPWARLRFKFLLKGLAKKMK) is a novel antimicrobial peptide identified by pre-screening the uniport database. A typical α-helical peptide showed 100% homology to *Drosophila virilis*. It exhibits antifungal activity against *Cryptococcus neoformans*.<sup>171</sup> DvAMP inhibited *A. baumannii* ATCC19606, *A. baumannii* CRAB 01, *A. baumannii* CRAB 02, *A. baumannii* CRAB 03, *A. baumannii* CRAB 04, and *A. baumannii* CRAB 05, with the same MIC value of 8 μg mL<sup>-1</sup>. DvAMP binds to exogenous lipopolysaccharides and phospholipids of *A. baumannii*, which results in enhanced membrane permeability, causing the dissipation of proton motive force, reducing intracellular ATP, and increasing ROS levels, ultimately leading to bacterial death. Additionally, it showed antibiofilm activity in *A. baumannii*. Moreover, it increases the survival rates of mice infected with the *A. baumannii* pneumonia model by decreasing the bacterial load.<sup>172</sup>

**2.1.8. Worm.** Arenicins are AMPs obtained from the coelomocytes of marine polychaeta lugworm *Arenicola marina*. Arenicin-3 (**132**) (GFCWYVCYRNGVRVCYRCN) belongs to the arenicin family. Arenicin-3 comprises a 21 amino acid residue amphipathic β-hairpin and possesses two



disulfide bonds. It showed antibacterial activity against MDR and XDR *E. coli* with a MIC value of  $1 \mu\text{g mL}^{-1}$ . However, it is cytotoxic and induces hemolysis to erythrocytes. Elliott *et al.* performed a structure-based design on arenincin-3 that identified AA139 (133) (GFCWYVCARRNGARVCYRRCN). AA139 inhibited non-MDR *A. baumannii*, MDR *A. baumannii*, and XDR *A. baumannii* with MIC values of 2, 1, and  $0.5 \mu\text{g mL}^{-1}$ , respectively. Notably, arenincin-3 variants showed antibacterial activity by causing membrane disruption and leakage of cytoplasmic contents in *P. aeruginosa*. Moreover, AA139 caused a release of ATP from the *E. coli* bacterial cells. Also, AA139 displayed promising efficacy in several Gram-negative infection *in vivo* models. It exhibited lower mammalian toxicity than the native arenincin-3.<sup>173</sup>

**2.1.9. Scorpion.** Hp1404 (134) is a peptide obtained from the venomous gland of the scorpion *Heterometrus petersii*. Hp1404 (GILGKLWEGVKSIF-NH<sub>2</sub>) is an amphipathic  $\alpha$ -helical structure. It exhibits antibacterial activity against GPB *Staphylococcus aureus*. However, it has demonstrated cytotoxicity to mammalian cells by causing hemolysis of red blood cells. Hong *et al.* designed analogs of Hp1404 by substituting the amino acids to reduce toxicity and improve antibacterial activity. The Hp1404 analogues include Hp1404-A (135) (GILGKLWEGVKSIA-NH<sub>2</sub>), Hp1404-K (136) (GILGKLWEGVKSIIK-NH<sub>2</sub>), Hp1404-V (137) (GILGKLWEGVKSIV-NH<sub>2</sub>), Hp1404-L (138) (GILGKLWEGVKSIL-NH<sub>2</sub>), Hp1404-I (139) (GILGKLWEGVKSII-NH<sub>2</sub>), and Hp1404-W (140) (GILGKLWEGVKSIIW-NH<sub>2</sub>). Hp1404 and its analogs Hp1404-V, Hp1404-L, Hp1404-I, and Hp1404-W demonstrated antibacterial activity against *A. baumannii* strains. The mode of action of these peptides is through bacterial membrane destruction and inhibition of biofilm formation.<sup>174</sup>

Luo *et al.* screened peptides from different species of scorpion, including VsCT1 from *Vaejovis subcristatus*, BmKn1 from *Mesobuthus martensii* Karsch, spiniferin from *Heterometrus spinifer*, Hp1404 from *Heterometrus petersii*, ctriporin from *Chaerilus tricostatus*, and Im4 and Im5 from *Isometrus maculatus*, respectively. Peptides VsCT1 (141) (FLKGIIDTVSNWL), BmKn1 (142) (FIGAVAGLLSKIF), spiniferin (143) (ILGEIWKGKIDIL), Hp1404 (134) (GILGKLWEGVKSIF), ctriporin (144) (FLWGLIPGAISAVTSLIKK), Im4 (145) (FIGMIPGLIGGLISAIIK) and Im5 (146) (FLGSLFSIGSKLLPGVIKLFQRKKQ) showed activity against *Acinetobacter baumannii* ATCC19606 with MIC values of  $>40$ ,  $>40$ ,  $>40$ , 5, 20,  $>40$ , and  $2.5 \mu\text{g mL}^{-1}$ , respectively. Hp1404, ctriporin, and Im5 showed antibacterial activity against a series of *A. baumannii* clinical isolates resistant to carbapenem. Hp1404, Im5, and ctriporin showed activity against CRAB strains with MIC values of 6.4, 5.0, and  $29.1 \mu\text{g mL}^{-1}$ , respectively. Among these, Hp1404 was better compared to Im5 and ctriporin due to its extensive therapeutic index. It caused hemolysis of red blood cells at very high concentrations. Hp1404 caused dose-dependent disruption of the bacterial cell membrane and lysis of the bacterial membrane.<sup>175</sup>

**2.1.10. Octopus.** Octopromycin (147) (N-RRLIRTDTG-PIIYDYFKDQLLKGMVILRESMKNLKGM-C) was isolated from *Octopus minor*. It has 38 amino residues having an  $\alpha$ -helix secondary structure. It showed antibacterial activity

against *A. baumannii* with MIC and MBC values of 50 and  $100 \mu\text{g mL}^{-1}$ , respectively. Octopromycin-treated *A. baumannii* cells showed severe cell wall damage, including a rough membrane structure, irregular cell shape, and holes in the cell wall. Also, octopromycin enhanced the membrane's permeability and caused a concentration-dependent increase in reactive oxygen species (ROS) generation inside the cells. Furthermore, it increased the survival of *A. baumannii*-infected fish.<sup>176</sup> The antibiofilm activity of octopromycin involves ultrastructural damage to the extracellular matrix alteration in the membrane permeability of *A. baumannii*. Moreover, octopromycin inhibited alginate production, surface movements (swarming and swimming), and twitching motility of *A. baumannii*, confirming its anti-quorum-sensing activity.<sup>177</sup>

Octominin is a defensin protein-3-based AMP obtained from *Octopus minor*. In *O. minor*, the prohibitin-2 gene is responsible for the biosynthesis of prohibitin, which inhibits cellular proliferation. Jayathilaka *et al.* used the prohibitin-2 gene to synthesize octoprohibitin using charged amino acid residues, including arginine and lysine. Octoprohibitin (148) exhibited moderate antibacterial activity against *A. baumannii* with MIC and MBC values of 50 and  $100 \mu\text{g mL}^{-1}$ , respectively. The field emission electron microscopy analysis of *A. baumannii* cells treated with octoprohibitin showed prominent and severe damage with opening and shrinkage of the cells. It also inhibited the biofilm formation in *A. baumannii* and increased the survival of zebrafish infected with *A. baumannii*.<sup>178</sup>

**2.1.11. Fish.** Tilapia piscidin 2 (TP2) (149) is a peptide found in *Oreochromis niloticus* (Nile tilapia), with no antibacterial activity. The TP2 (GECIWDAIFHGAKHFLHRLVNP) peptide was modified to give TP2-5 (150) (KKCIAKAILKKAKKLLKKLVNP) and TP2-6 (151) (KKCIAKAILKKAKKLLKDLVNP), which are amphipathic with net positive charges of +9 and +7, respectively. TP2-5 and TP2-6 inhibited the growth of both sensitive and MDR isolates of *A. baumannii*. TP2-5 and TP2-6 showed antibacterial activity by membrane depolarization. The bacterial cells treated with TP2-5 and TP2-6 peptides showed a deformed membrane architecture and prevented biofilm formation. Notably, both these peptides were of negligible toxicity and did not cause hemolysis of RBC cells even at a concentration of  $100 \mu\text{g mL}^{-1}$ .<sup>179</sup>

**2.1.12. Bacteriophage-derived peptides.** Lysins are bacteriophage-derived antimicrobial agents. Exogenous endolysins showed differentiated susceptibility to GPB and GNB.<sup>180</sup> Endolysins are commonly known as lysins, which possess hydrolytic enzymes.<sup>181</sup> The bacteriophages use hydrolytic enzymes to degrade the host bacteria peptidoglycan and to release its phages (progeny). Lysins have several advantages, including high host specificity, rapid host lysis, and inactivity to normal microflora compared to other antibiotics and phages.<sup>182</sup>

The cecropin A (CecA) N terminus is responsible for antibacterial activity against *A. baumannii*. LysMK34 is



prepared from the lysis of *A. baumannii* phage MK34. Notably, LysMK34 showed a turgor pressure-dependent intrinsic antibacterial activity. Abdelkader *et al.* prepared a chimeric protein by fusing lysis (LysMK34) with the N-terminus of cecropin A via a linker of three Ala-Gly repeats to give engineered LysMK34 (eLysMK34) (152). eLysMK34 showed antibacterial activity against sensitive and resistant *A. baumannii* strains. Also, eLysMK34 was active against other GNB, including *P. aeruginosa*, *E. coli*, and colistin-resistant strains. Moreover, eLysMK34 was nontoxic to the HaCaT human epithelial cell line. The eLysMK34 antibacterial activity does not depend on high intracellular osmotic pressure. The mode of action of eLysMK34 is due to its combined actions of peptidoglycan degradation and pressure-induced osmotic lysis, eventually killing bacterial cells.<sup>183</sup>

Yang *et al.* prepared a peptide-modified lysis PlyA (153) using cecropin A peptide residues 1–8 (KWKLFKKI) and OBP<sub>gp279</sub>. Importantly, PlyA showed good antibacterial activity against *A. baumannii* and *P. aeruginosa* but reduced activity against bacterial cells in their stationary phase. It has been found that the addition of the outer membrane permeabilizers EDTA and citric acid enhances the antibacterial activity against stationary phase cells. However, PlyA gets deactivated in complicated media, including biomatrices, milk, and serum. This could limit its further development as a therapeutic drug candidate.<sup>184</sup>

Earlier studies demonstrated that AbEndolysin of phage Ab1656-2 (154) consists of N-terminal *N*-acetylmuramidase and C-terminal peptidoglycan binding domains. AbEndolysin showed antibacterial activity against clinical *A. baumannii* strains. Islam *et al.* synthesized a chimeric protein eAbEndolysin (155) by combining cecropin A with the N-terminus of AbEndolysin. Interestingly, cecropin A-fused AbEndolysin exhibited enhanced bactericidal activity by 2–8 fold against various MDR *A. baumannii* clinical isolates and more than its parent lysis. Moreover, eAbEndolysin showed synergistic activity with  $\beta$ -lactam antibiotics, including cefotaxime, ceftazidime, and aztreonam, and an additive effect with meropenem and imipenem against *A. baumannii*. Importantly, eAbEndolysin did not show any toxicity to A549 cell lines and cured mice infected with *A. baumannii*.<sup>185</sup>

LysAB2 (156) is endolysin obtained from *A. baumannii* phage  $\Phi$ AB2, which showed antibacterial activity against GPB and GNB. Notably, the detailed assessment of LysAB2 revealed that the sequence between 113 and 145 is essential for antimicrobial activity. Peng *et al.* synthesized four peptides (LysAB2 P0-P3) based on the amino acid sequence present between 113 and 145 of LysAB2. Among them, the representative LysAB2 P3 (157) (NPEKALEKLIAIQKAIKGMLNGWFTGVGVFRKR) showed antibacterial activity against MDR and colistin-resistant *A. baumannii* strains. LysAB2 P3 caused damage to the bacterial cell membrane, with the collapse of the cellular structure. Furthermore, it decreased the bacterial load in a mouse model infected with *A. baumannii* infections, and it cured 60% of the

mice infected with bacteremia induced by *A. baumannii*. However, it caused moderate hemolysis of RBCs.<sup>186</sup>

The C-terminal region of *A. baumannii* phage lysis LysAB2 has a cationic character and is involved in the permeabilization to the outer membrane. *A. baumannii* phage lysis PlyF307 and its amino acids between 108 to 138 partly resembled the LysAB2 peptide named P307 (158). Further, P307 was modified with eight amino acids, with a complete C-terminal part of native PlyF307 to give a peptide P307<sub>AE-8</sub> (159). Additionally, the fusion of eight amino acids gave P307<sub>SQ-8</sub>. The derivatives P307 and P307<sub>SQ-8</sub> exhibited antibacterial activity against *A. baumannii* and inhibited biofilm formation. Moreover, P307<sub>AE-8</sub> killed the bacteria by disrupting the bacterial plasma membrane. It did not cause hemolysis in human red blood cells.<sup>187</sup>

The lysis LysP53 (160) is derived from *A. baumannii* phage 53. It showed the highest similarity of 87% with the endopeptidase derived from *Acinetobacter* phage DMU1. The time-kill kinetic studies revealed that LysP53 (100  $\mu$ g mL<sup>-1</sup>) caused a 4-log reduction in *A. baumannii* in 15 minutes of exposure. Additionally, it is active against *P. aeruginosa*, *K. pneumoniae*, and *E. coli*. It contained an N-terminal domain of  $\alpha$ -helical fragments in the N-terminus of LysP53, especially the N-terminal 33 amino acid sequence. Further, two peptides were generated from LysP53, *i.e.*, P103 (1–17 aa) and P104 (1–33 aa), and these peptides did not show bactericidal activity compared to whole-length peptides. Notably, LysP53 showed no toxicity to A549 cells even at a very high concentration of 500  $\mu$ g mL<sup>-1</sup>. Moreover, LysP53 (57.6  $\mu$ M) upon topical application to a mouse model infected with *A. baumannii*-associated burn reduced the bacterial loads better than minocycline.<sup>182</sup>

Artilysins are prepared by an engineered fusion of endolysins with membrane-destabilizing peptides. Using a specific lipopolysaccharide destabilizing peptide facilitates the translocation of the endolysin moiety, which eventually leads to enzymatic degradation of peptidoglycan, resulting in the lysis of the cells. Artilysin Art-175 (161) comprises a modified variant of endolysin KZ144 and a giant *P. aeruginosa* bacteriophage  $\Phi$ KZ, linking to the N-terminal of SMAP-29, an antibacterial peptide derived from the sheep myeloid. Art-175 showed bactericidal activity against *A. baumannii* and *P. aeruginosa*. It inhibited MDR *A. baumannii* with MIC values ranging between 4 and 20  $\mu$ g mL<sup>-1</sup> and eliminated a large inoculant of *A. baumannii*  $\geq 10^8$  CFU mL<sup>-1</sup>. It also killed the actively dividing and persister cells. The antibacterial mode of action of Art-175 is by osmotic lysis and peptidoglycan degradation.<sup>188</sup>

**2.1.13. Sensitizer peptides.** The antibiotics used for GPB are generally ineffective for GNB infections. Sensitizer peptides are used to sensitize the outer membrane of GNB and allow the use of antibiotics targeting Gram-positive to be used in GNB. The sensitizer peptide causes the relocation of anionic lipopolysaccharides in the membrane, allows the membrane to be demixed, and thus potentiates the activity of antimicrobial agents or endolysins.<sup>189</sup> KL-L9P is a well-known



sensitizer that promotes bacterial membrane rearrangements and allows most Gram-positive antibiotics to pass through. LysSPN1S is an endolysin obtained from the *Salmonella* phage SPN1S, which showed antibacterial activity against *E. coli* by cleaving the glycosidic bond of the peptidoglycan. Son *et al.* synthesized fusion endolysin, Lys1S-L9P (162), by fusing the sensitizer peptide KL-L9P (KLLKLLKKPLKLLK) onto the endolysin LysSPN1S. Notably, Lys1S-L9P showed broad-spectrum antibacterial activity against GNB, including MDR strains, *E. coli*, *A. baumannii*, and *P. aeruginosa*. Moreover, it caused a significant decrease in the biofilm formation in *E. coli* and *A. baumannii*. It also increased the survival rate of *Galleria mellonella* larvae infected with *A. baumannii*. Importantly, Lys1S-L9P did not exhibit any toxicity to human cells.<sup>190</sup>

**2.1.14. Plants.** Plants are rich sources of diverse chemical scaffolds, including antimicrobial peptides. Porto *et al.* explored guava glycine-rich peptide Pg-AMP1 by using the genetic algorithm. Further, they used Pg-AMP1 as a template to generate guavanins peptides. The computationally designed guavanins were found to be rich in arginine residues. In comparison, some guavanins were rich in tyrosine residues. The designed AMPs, guavanins 2, 12, 13, and 14, do not exhibit hemolytic activity. The representative potent peptide guavanin 2 (163) (RQYMRQIEQALRYGYRISRR) showed a narrow-spectrum antibacterial activity. It showed antibacterial

activity against *Acinetobacter baumannii* ATCC 19606 with a MIC value of 6.25  $\mu\text{g mL}^{-1}$ . Guavanin 2 acts preferentially against GNB with a selectivity index of 23.93. Moreover, guavanin 2 showed antibacterial activity in a mice model induced with *P. aeruginosa* abscess skin infection. Guavanin 2 (6.25  $\mu\text{g mL}^{-1}$ ) caused a decrease in the 3-log reduction in bacterial counts after four days of application. Moreover, guavanin 2 exhibits antibacterial activity by allowing slow permeation through the cytoplasmic membrane, triggering hyperpolarization and causing membrane disruption in the bacterial cells.<sup>191</sup>

## 2.2. Synthetics and peptidomimetics

**2.2.1. Dendrimers.** The branched peptide dendrimers of specific amino acids are considered better antibacterial agents.<sup>192</sup> The dendrimer topology allows the multivalency of pre-existing AMP sequences or single amino acids, typically by attachment of particular amino acids to a dendritic tree. Recent research suggested that the antimicrobial activity of dendrimers is due to their dendritic effect, cationic residue within the dendrimer branches, and conformation flexibility at the water-membrane interface that allows the membrane's permeability. Moreover, the dendrimer protects its degradation from protease enzymes.<sup>192,193</sup> G3KL (164, Fig. 12) is a novel AMP dendrimer identified from high-

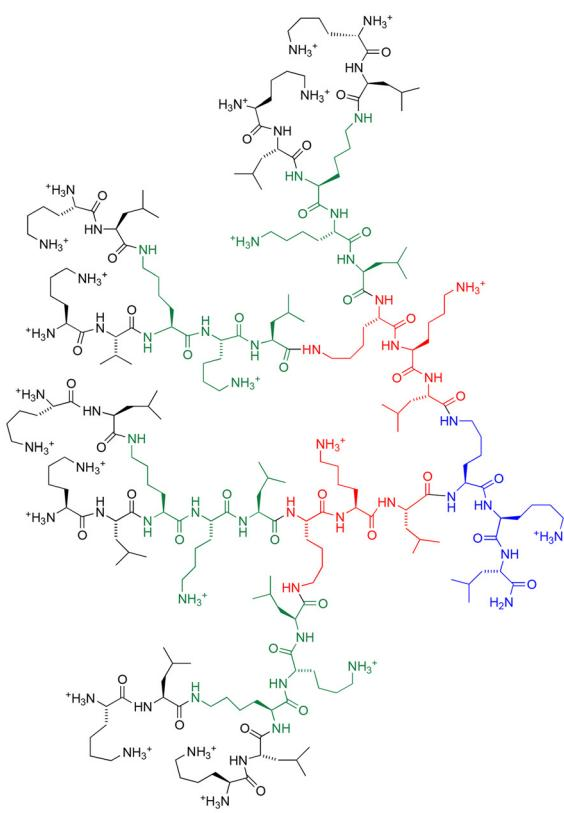
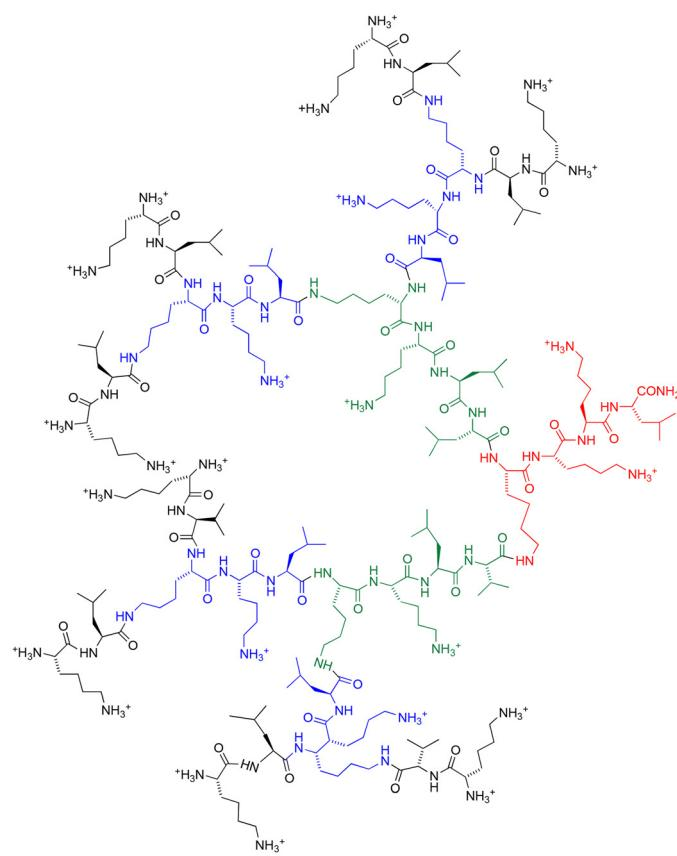


Fig. 12 Chemical structure of G3KL and T7 dendrimers.



throughput screening assays. In dendrimer G3KL ( $((KL)_8(KKL)_4(KKL)_2KKL)$ , K is lysine, *K* is branched lysine, and *L* is leucine. G3KL exhibited *in vitro* antibacterial activity against several GNB strains, including *A. baumannii* and *P. aeruginosa*.<sup>193</sup> Importantly, it demonstrated very low toxicity to human red blood cells at a very high concentration of  $>840 \mu\text{g mL}^{-1}$  and was stable in human serum with a  $t_{1/2}$  value of 9 h.<sup>194</sup> G3KL and its *D*-enantiomer did not show any antibacterial activity in an *in vivo* model of *A. baumannii* infections. Siriwardena *et al.* designed and synthesized dendrimers T4 ( $((KL)_8(KK)_4(KLKL)_2KLKL)$ ), T5 ( $((KL)_8(KKL)_4(KLL)_2KKKL)$  and T7 ( $((KL)_8(KKL)_4(KKLL)_2KKKL$ ) which were similar in activity to G3KL. Among the identified dendrimers, T7 (165, Fig. 12) showed broad spectrum activity against Gram-negative MDR strains, including *A. baumannii*, *E. coli*, *P. aeruginosa*, *E. cloacae*, and *K. pneumoniae*. Moreover, T7 demonstrated higher stability in serum with  $>24$  h. It also increased the survival of mice infected with MDR strain *A. baumannii* abax1605034. Interestingly, these dendrimers exist in a hydrophobically collapsed conformation in water and rearrange after coming in contact with the bacterial membrane to an extended partially  $\alpha$ -helical conformation, thus exposing hydrophobic leucine residue side chains and enabling interactions with the lipid membrane leading to the membrane disruption of the bacteria. In another study, Siriwardena *et al.* synthesized DC5 ( $((OF)_8(KBL)_4(KLKK)_2KKKL$ ) by combining the outer branches of TNS18 ( $((OF)_4(KBL)_2KKL(C_{10})$ ) and an inner branch core of T7 which retained activity against GNB.<sup>195</sup> The above studies on dendrimers symbolize that dendrimers' size does not limit their antibacterial activity.<sup>196</sup>

**2.2.2. Chimeric and synthetic peptides.** TAT-RasGAP<sub>317–326</sub> (166) is a chimeric peptide consisting of the cell-permeable HIV peptide TAT<sub>48–57</sub> (RRRQRRKKRG) linked to a ten amino acid sequence of the Src homology 3 domain (SH3 domain) (DTRLNTVWMW) of p120 RasGAP with two glycine residues. It possesses several positive charges due to multiple arginine residues. TAT-RasGAP<sub>317–326</sub> inhibited *A. baumannii* ATCC 19606 and *P. aeruginosa* PA14 with MIC values of 8 and  $32 \mu\text{g mL}^{-1}$ . It inhibited the biofilm formation in *A. baumannii* ATCC 19606 and *P. aeruginosa* PA14 with biofilm prevention concentration (BPC<sub>90</sub>) values ranging between 16 and  $32 \mu\text{g mL}^{-1}$ . The molecular mode of antibacterial action of TAT-RasGAP<sub>317–326</sub> has to be established.<sup>197</sup>

SA4 (167) (IOWAGOLFOLFO-NH<sub>2</sub>) is a cationic amphiphilic peptide.<sup>198</sup> It inhibits GPB and GNB strains with MIC values ranging between 1 and  $32 \mu\text{g mL}^{-1}$ . The calcein dye leakage and transmission electron microscopy studies confirmed that SA-4 acts on the bacterial membrane and causes perturbation in the membrane.<sup>198</sup> Sharma *et al.* synthesized a poly-N-substituted glycine congener of SA4 and named it SPO (168, Fig. 13). SA4 and SPO exhibited antibacterial activity against *A. baumannii* strains with MIC values ranging between 50 and  $100 \mu\text{g mL}^{-1}$  and demonstrated biofilm inhibition activity. Even SPO at a higher concentration of  $500 \mu\text{g mL}^{-1}$  did not cause hemolysis of the erythrocytes. *A. baumannii* cells treated with SA4 and SPO showed abnormalities like disrupted cell structures and cellular debris.<sup>199</sup>

Paenipeptin is a synthetically derived lipopeptide AMP, consisting of an N-terminal C<sub>8</sub> fatty acyl chain with three positive charge amino acids. From the initial study of

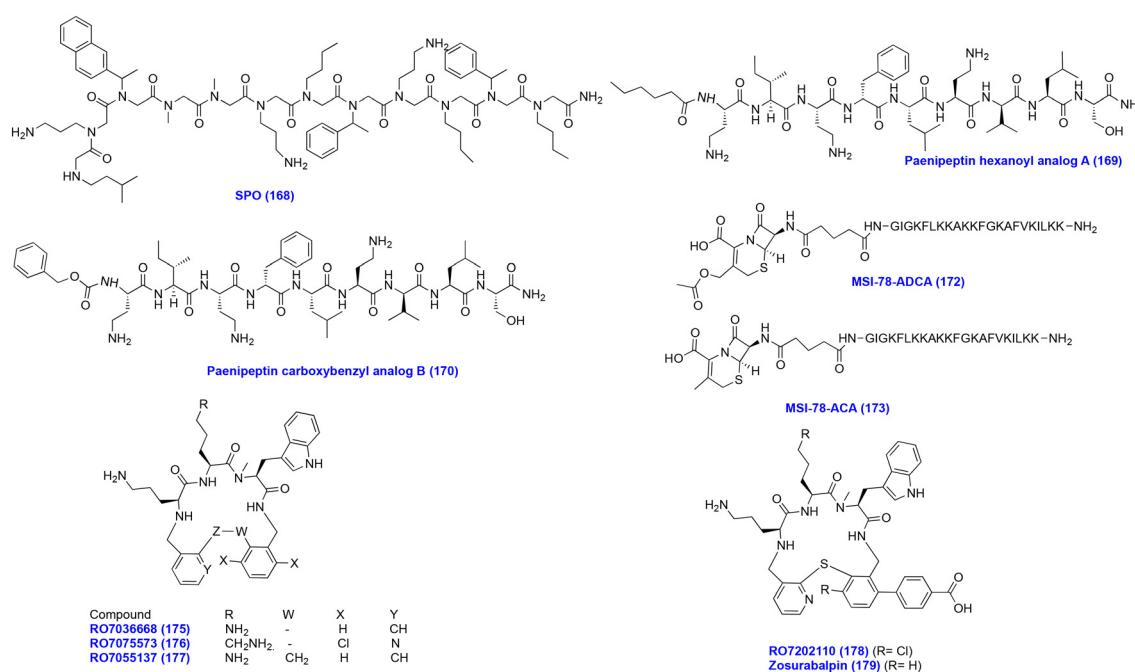


Fig. 13 Chemical structures of SPO, paenipeptin hexanoyl and carboxybenzyl analogs, MSI-78-ADCA, MSI-78-ACA, and macrocyclic tethered peptides.



paenipeptin analogs, two compounds, paenipeptin A and paenipeptin B (169 and 170, Fig. 13), were found to be non-hemolytic. Analog A has a shorter lipid chain of  $C_6$  than paenipeptin, whereas analog B has a lipid chain modified with the carboxybenzyl group. Importantly, these two analogs potentiated the activity of clarithromycin and rifampin against carbapenem-resistant *K. pneumoniae*, *A. baumannii*, and *A. baumannii* FDA-CDC AR 0063 strains. Both paenipeptin analogs A and B were stable in 95% human serum for 24 hours. Moreover, 169 and 170 analogs were nontoxic to kidney cells.<sup>200</sup>

Nagarajan *et al.* designed AMPs using computational graph optimization and a maximum common subgraph approach. This work led to the design and identification of five peptides,  $\Omega$ 03,  $\Omega$ 13,  $\Omega$ 17,  $\Omega$ 76, and  $\Omega$ 93.  $\Omega$ 76 (171) (FLKAIKKFGKEFKKIGAKLK) displayed antibacterial activity against carbapenem and tigecycline-resistant microorganisms.  $\Omega$ 76 displayed antibacterial activity against *E. coli* and *A. baumannii* with the same MBC<sub>50</sub> value of 4 mg per liter. In infected mice models of *A. baumannii*,  $\Omega$ 76 displayed high efficacy against carbapenem and tigecycline-resistant *A. baumannii*. Interestingly,  $\Omega$ 76 adopts an  $\alpha$ -helical structure in the membrane, causing rapid membrane disruption, leakage, and bacterial death.<sup>201</sup>

$\beta$ -Lactam antibiotics showed antibacterial activity by inhibiting the bacterial cell wall synthesis. However, the  $\beta$ -lactam antibiotics are deactivated by bacterial  $\beta$ -lactamases. In recent years, linking the core structure of the  $\beta$ -lactam ring and its synthetic modification allows the escape from the  $\beta$ -lactamase, and thus it retains antibacterial activity. 7-Aminodesacetoxycephalosporanic acid is a precursor to  $\beta$ -lactam and cephalosporin antibiotics. MSI-78, CA(1-7)M(2-9)NH<sub>2</sub>, and *des*-Chex1-Arg20 are cationic AMPs. Li *et al.* carried out the chemical modification of 7-aminodesacetoxycephalosporanic acid by linking it to MSI-78, CA(1-7)M(2-9)NH<sub>2</sub>, and *des*-Chex1-Arg20. MSI-78 is a modified AMP from the magainin family. Among these,  $\beta$ -lactam antibiotics linked to MSI-78 conjugates MSI-78-ADCA (172 Fig. 13) and MSI-78-ACA (173, Fig. 13) have shown significant antibacterial activity against GNB, including *K. pneumoniae*, *A. baumannii*, and *P. aeruginosa*. Moreover, these peptides were found to be nontoxic to mammalian cell lines.<sup>202</sup>

In a study, He *et al.* screened cyclic peptides acting against *Staphylococcus aureus*, *E. coli*, and *A. baumannii*. Among the screened peptides, the cyclic peptide B2 (174) (cyclo-RRWWRRW) showed activity against *A. baumannii* and MDR *A. baumannii* with the same MIC value of 6  $\mu$ g mL<sup>-1</sup>. The antibacterial activity of peptide B2 was retained in salt, including NaCl and CaCl<sub>2</sub>. However, the peptide B2 exhibited slight toxicity to sheep red blood cells and human lung fibroblast HLF-1 cells. The MDR *A. baumannii* treated with peptide B2 displayed membrane rupture, full perforations, and the leakage of cellular contents from lysed cells. Moreover, the peptide B2 showed significant therapeutic effects on lung infections in mice infected with MDR *A.*

Table 2 AMPs with their mode of action and their targeted bacteria

Category	Compound name	Source	Mode of action	Morphological changes	Targeted <i>A. baumannii</i>	Other targeted bacteria	Ref.
Lipopeptides	Polymyxin B (1)		The polymyxin molecule binds to lipid A	Polymyxin and colistin disrupt membrane lipid packing and make the outer membrane permeable	Polymyxin B (1) MIC A. <i>baumannii</i> ATCC19606 = 1 $\mu$ g mL <sup>-1</sup>	<i>P. aeruginosa</i> , <i>K. pneumoniae</i> , <i>E. cloacae</i>	99
					Polymyxin B (1) MIC A. <i>baumannii</i> FADDI-AB03 = 0.5 $\mu$ g mL <sup>-1</sup>		
					Polymyxin B (1) MIC A. <i>baumannii</i> ATCC17978 = 1 $\mu$ g mL <sup>-1</sup>		
					Polymyxin B <sub>1</sub> (2) MIC A. <i>baumannii</i> ATCC19606 = 0.5 $\mu$ g mL <sup>-1</sup>		
					Polymyxin B <sub>1</sub> (2) MIC A. <i>baumannii</i> FADDI-AB03 = 0.5 $\mu$ g mL <sup>-1</sup>		
					Polymyxin B <sub>1</sub> (2) MIC A. <i>baumannii</i> ATCC17978 = 1 $\mu$ g mL <sup>-1</sup>		
					Polymyxin B <sub>2</sub> (3) MIC A. <i>baumannii</i> ATCC19606 = 1 $\mu$ g mL <sup>-1</sup>		
					Polymyxin B <sub>2</sub> (3) MIC A.		



Table 2 (continued)

Category	Compound name	Source	Mode of action	Morphological changes	Targeted <i>A. baumannii</i>	Other targeted bacteria	Ref.
Colistin (4)					<i>baumannii</i> FADDI-AB03 = 1 $\mu\text{g mL}^{-1}$		
					Polymyxin B <sub>2</sub> (3) MIC <i>A. baumannii</i> ATCC17978 = 0.5 $\mu\text{g mL}^{-1}$		
					Colistin (4) MIC <i>A. baumannii</i> ATCC19606 = 1 $\mu\text{g mL}^{-1}$		
					Colistin (4) MIC <i>A. baumannii</i> FADDI-AB03 = 1 $\mu\text{g mL}^{-1}$		
Colistin A (5)					Colistin (4) MIC <i>A. baumannii</i> ATCC17978 = 0.5 $\mu\text{g mL}^{-1}$		
					Colistin A (5) MIC <i>A. baumannii</i> ATCC19606 = 2 $\mu\text{g mL}^{-1}$		
					Colistin A (5) MIC <i>A. baumannii</i> FADDI-AB03 = 1 $\mu\text{g mL}^{-1}$		
Colistin B (6)					Colistin A (5) MIC <i>A. baumannii</i> ATCC17978 = 1 $\mu\text{g mL}^{-1}$		
					Colistin B (6) MIC <i>A. baumannii</i> ATCC19606 = 2 $\mu\text{g mL}^{-1}$		
					Colistin B (6) MIC <i>A. baumannii</i> FADDI-AB03 = 1 $\mu\text{g mL}^{-1}$		
					Colistin B (6) MIC <i>A. baumannii</i> ATCC17978 = 1 $\mu\text{g mL}^{-1}$		
Lipopeptides	F365 (QPX9003) (7)	Synthetic polymyxin analogs			<i>P. aeruginosa</i> ATCC F365 (QPX9003) (7) MIC <i>A. baumannii</i> ATCC19606 = 0.25 $\mu\text{g mL}^{-1}$	95	
					<i>P. aeruginosa</i> FADDI-PA025, <i>P. aeruginosa</i> FADDI-PA038*, <i>K. pneumoniae</i> F365 (QPX9003) (7) MIC <i>A. baumannii</i> FADDI-AB030* = 0.25 $\mu\text{g mL}^{-1}$		
					<i>K. pneumoniae</i> F365 (QPX9003) (7) MIC <i>A. baumannii</i> FADDI-KP032*, <i>K. pneumoniae</i> FADDI-KP034* = 2 $\mu\text{g mL}^{-1}$		
Lipopeptides	Polymyxin S2 (ASK0912) (8)	Synthetic polymyxin analogs			Polymyxin S2 (ASK0912) (8) MIC <i>A. baumannii</i> = 0.25 $\mu\text{g mL}^{-1}$	101	
Lipopeptides	NAB739 (9)	Synthetic polymyxin analogs			NAB739 (9), in combination with rifampin, demonstrated synergistic activity against <i>A. baumannii</i>	102	



Table 2 (continued)

Category	Compound name	Source	Mode of action	Morphological changes	Targeted <i>A. baumannii</i>	Other targeted bacteria	Ref.
Lipoproteptides	Macolacin (10)	Colistin congener	It binds to lipid A		Macolacin (10) MIC <i>A. baumannii</i> 17.978 = 1 $\mu$ g mL <sup>-1</sup>	<i>P. aeruginosa</i> PA01, <i>E. cloacae</i> 0150	103
Lipoproteptides	Arylomycins A-C <sub>16</sub> (12)	<i>Streptomyces</i> culture	It inhibits essential bacterial type I signal peptidase		Arylomycins A-C <sub>16</sub> (12) MIC <i>A. baumannii</i> ATCC 43816, 17.978 = >64 $\mu$ g mL <sup>-1</sup>	<i>E. coli</i> ATCC 25922, <i>K. pneumoniae</i> ATCC 43816, <i>Enterobacter cloacae</i> ATCC 13407, <i>Enterobacter aerogenes</i> ATCC 13408, <i>Citrobacter werkmanii</i> ATCC 51114, <i>Serratia marcescens</i> CDC4385-74, and <i>P. aeruginosa</i> ATCC 27853	104
Lipoproteptides	G0775 (13)	Arylomycins A-C <sub>16</sub> derivative	They inhibit essential bacterial type I signal peptidase		G0775 (13) MIC <i>A. baumannii</i> ATCC 17978 = 1 $\mu$ g mL <sup>-1</sup>	<i>E. coli</i> ATCC 25922, <i>K. pneumoniae</i> ATCC 43816, <i>Enterobacter cloacae</i> ATCC 13407, <i>Enterobacter aerogenes</i> ATCC 13408, <i>Citrobacter werkmanii</i> ATCC 51114, <i>Serratia marcescens</i> CDC4385-74, and <i>P. aeruginosa</i> ATCC 27853	104
Lipoproteptides	Tridecaptin A <sub>1</sub> (14)		It binds to lipid II	It disrupts the inner membrane	Tridecaptin A <sub>1</sub> (14) MIC <i>A. baumannii</i> ATCC199606 = 12.5 $\mu$ g mL <sup>-1</sup>	<i>Klebsiella pneumoniae</i> ATCC 13883, <i>E. coli</i> ATCC 25922, <i>S. enterica</i> ATCC 13311, <i>P. aeruginosa</i> ATCC 27853, <i>C. jejuni</i> NCTC 11168	107, 108
Lipoproteptides	Tridecaptin analogs 1-8 (19-26)				Tridecaptin analogs 1-8 demonstrated activity against <i>A. baumannii</i> , <i>A. baumannii</i> ACM 29 with MIC values of 12.5, 25, and 25 $\mu$ g mL <sup>-1</sup> , and 25, 100, and 50 $\mu$ g mL <sup>-1</sup> , and 100, 50, and 50 $\mu$ g mL <sup>-1</sup> , and 50, 25, and 50 $\mu$ g mL <sup>-1</sup> , and 12.5, 50, and 50, $\mu$ g mL <sup>-1</sup> , and 6.25, 25, and 25, $\mu$ g mL <sup>-1</sup> , and 25, 25, and 50 $\mu$ g mL <sup>-1</sup> , and >100, >100, and >100 $\mu$ g mL <sup>-1</sup> , respectively	<i>E. cloacae</i> , <i>K. pneumoniae</i> , <i>K. pneumoniae</i> IMP 170, and <i>P. pseudotaiwanensis</i>	111
Lipoproteptides	Tridecaptin M (27)				Tridecaptin M (27) sensitizes <i>A. baumannii</i> to vancomycin, ceftazidime, and rifampicin against <i>A. baumannii</i> strains		112

Table 2 (continued)

Category	Compound name	Source	Mode of action	Morphological changes	Targeted <i>A. baumannii</i>	Other targeted bacteria	Ref.
Bacteriocins	Nisin (28)	<i>Lactococcus lactis</i>	It binds to the lipid-II complex	It increases the membrane permeability through pore formation and inhibits peptidoglycan synthesis	Nisin (28), in combination with polymyxin B, demonstrated synergistic activity against pan-drug-resistant and extensively resistant <i>A. baumannii</i>	<i>E. coli</i> LMG15862, <i>K. pneumoniae</i> LMG20218, <i>P. aeruginosa</i> LMG 6395, <i>E. aerogenes</i> LMG02094, <i>L. lactis</i> MG1363	114
Bacteriocins	T16m2 (29)	Nisin derivative			T16m2 (29) MIC A. <i>baumannii</i> LMG01041 = 0.5 $\mu$ M	<i>E. coli</i> , and <i>Klebsiella pneumoniae</i>	113
Lipopeptides	Isopedopeptins B (31)				They cause a significant leakage of cytoplasmic contents and disruption in the bacterial membrane	Isopedopeptins B (31) MIC carbapenem-resistant <i>A. baumannii</i> = 1 $\mu$ g mL <sup>-1</sup>	115
Lipopeptides	Brevicidine (38)	<i>Brevibacillus laterosporus</i> DSM25	It interacts with lipopolysaccharides on the outer membrane and phosphatidylglycerol and cardiolipin on the inner membrane of <i>E. coli</i>	It causes the dissipation of proton motive force and membrane disruption	Brevicidine (38) demonstrated synergistic activity with erythromycin against <i>A. baumannii</i>	Brevicidine B (38) MIC <i>A. baumannii</i> ATCC 19606 = 16 $\mu$ g mL <sup>-1</sup>	116
Lipopeptides	Brevicidine B (38)					Laterocidine (46) MIC <i>A. baumannii</i> = 4 $\mu$ g mL <sup>-1</sup>	117
Lipopeptides	Laterocidine (46)					<i>E. coli</i> TOPIQ, <i>P. aeruginosa</i> , <i>K. pneumoniae</i> NRRL-B-408, <i>Enterobacter cloacae</i> NRRL-B-413	118
Cyclopeptide	DA (47)				It interfered with the integration of the OMP into the membrane. Thus, BamaA cannot close the lateral gate, affecting the entire complex's mechanical, kinetic, and energetic properties	<i>Citrobacter freundii</i> DSM-30009, <i>E. coli</i> ATC-25922, <i>K. pneumoniae</i> DSM-30104, <i>P. aeruginosa</i>	119
Cyclopeptide	Darobactin analogue DA 9 (48) and DA22 (49)		It binds to the $\beta$ -barrel of the outer membrane protein (OMP) BamaA		DA (47), D9 (48), and D22 (49) inhibited CRAB isolates <i>A. baumannii</i> 038 (OXA-23), 045 (OXA-58), 046 (OXA-40), 047 (OXA-255), 070 (NDM-1), 054 (OXA-51-1SAB1) with MIC values of 16, 16-32, 8-16, 16-32, 8, and 16-32 $\mu$ g mL <sup>-1</sup> , and 4, 8, 4-8, 2, and 8 $\mu$ g mL <sup>-1</sup> , and 0.5, 0.5, 0.25, 0.0625, and 0.125 $\mu$ g mL <sup>-1</sup> , respectively	Mixed-ligand daptomycin conjugate (50) MIC A. <i>baumannii</i> ATCC 17961 = 0.4 $\mu$ M	120
Cyclic lipopeptide	Mixed-ligand daptomycin conjugate (50)		Daptomycin derivative		These conjugates allow membrane permeabilization in GNB		121



Table 2 (continued)

Category	Compound name	Source	Mode of action	Morphological changes	Targeted <i>A. baumannii</i>	Other targeted bacteria	Ref.
Bis-catechol daptomycin conjugate (51)	Daptomycin derivative			Bis-catechol daptomycin conjugate (51) and Tri-catechol daptomycin conjugate (52) inhibit <i>A. baumannii</i> ATCC 17961, <i>A. baumannii</i> ATCC 3484, <i>A. baumannii</i> ATCC 3486, <i>A. baumannii</i> ATCC 5079, <i>A. baumannii</i> ATCC 5081, <i>A. baumannii</i> ATCC 17978, <i>A. baumannii</i> ATCC 17978 PNT165 <sup>b</sup> , <i>A. baumannii</i> ATCC 17978 PNT221, <i>A. baumannii</i> ATCC 17978 PNT255, <i>A. baumannii</i> ATCC 17978 PNT320 <sup>c</sup> with MIC values of 0.4 and 0.2 $\mu$ M, 1.6 and 3 $\mu$ M, 0.8 and 3 $\mu$ M, 3 and 12.5 $\mu$ M, 50 and 12.5 $\mu$ M, 1.6 and 0.8 $\mu$ M, 1.6 and 0.4 $\mu$ M, 0.8 and 0.4 $\mu$ M, 1.6 and 0.8 $\mu$ M, and 1.6 and 0.4 $\mu$ M, respectively	<i>S. aureus</i> and <i>Salmonella typhimurium</i>	124, 125	
Glycopeptide	VanQAmC <sub>10</sub> (53)	Vancomycin derivative		VanQAmC <sub>10</sub> (53) MIC <i>A. baumannii</i> = 3.9 to 15.5 $\mu$ M	<i>S. aureus</i> and <i>Salmonella typhimurium</i>	129	
Glycopeptide	Vancomycin sulfonium conjugates (54)	Vancomycin derivative		Vancomycin sulfonium conjugates (54) MIC <i>A. baumannii</i> = 4–8 $\mu$ g mL <sup>-1</sup> inhibited MDR <i>A. baumannii</i> 1788, <i>A. baumannii</i> 1790, <i>A. baumannii</i> 1791, <i>A. baumannii</i> 1795, <i>A. baumannii</i> S3, and <i>A. baumannii</i> S5 with MIC values of 4, 4, 2, 4, 4, and 4 $\mu$ g mL <sup>-1</sup> , respectively	<i>E. coli</i> , <i>K. pneumoniae</i> , <i>P. aeruginosa</i> , and <i>M. catarrhalis</i>	130	
Linear peptide	Paenimucillin C (56)	<i>Paenibacillus mucilaginosus</i> K02		It showed antibacterial activity through pore formation and caused leakage of cytoplasmic contents		132	
Oligopeptide	X33 (57)	<i>Streptomyces lavendulae</i> X33		It causes cell wall permeability and morphology changes and promotes cell content leakage	X33 (57) MIC <i>A. baumannii</i> = 78.13 $\mu$ g mL <sup>-1</sup>	133	
Cationic peptide	Lynronne-1 (58)	Bovine rumen microbiome		It causes bacterial membrane lysis	Lynronne-1 (58) MIC <i>A. baumannii</i> ATCC 19606 = 16–8 $\mu$ g mL <sup>-1</sup>		<i>S. aureus</i> ATCC 29213, and <i>S. aureus</i> ATCC 6538



Table 2 (continued)

Category	Compound name	Source	Mode of action	Morphological changes	Targeted <i>A. baumannii</i>	Other targeted bacteria	Ref.
Cathelicidin	LL-37 (59)	Produced from hCAP-18	LL-37 binds to OmpA (AbOmpA) protein		LL-37 (59) MIC pan-drug-resistant <i>A. baumannii</i> = 32–64 $\mu\text{g}$ $\text{mL}^{-1}$		135–138
Cathelicidin	LL/CAP18 (60)	LL-37 derivative		LL-37, in combination with oncorhycin II, showed synergistic activity and demonstrated rapid killing of <i>A. baumannii</i>	LL/CAP18 (60) MIC pan-drug-resistant <i>A. baumannii</i> = 32–64 $\mu\text{g}$ $\text{mL}^{-1}$	LL/CAP18 (60) MIC pan-drug-resistant <i>A. baumannii</i> = 32–64 $\mu\text{g}$ $\text{mL}^{-1}$	136, 137
Cathelicidin	FF/CAP18 (61)	LL-37 derivative			FF/CAP18 (61) MIC pan-drug-resistant <i>A. baumannii</i> = 8–16 $\mu\text{g}$ $\text{mL}^{-1}$	FF/CAP18 (61) MIC pan-drug-resistant <i>A. baumannii</i> = 8–16 $\mu\text{g}$ $\text{mL}^{-1}$	136, 137
Cathelicidin	P-10 (62)	LL-37 derivative		P-10 (62), in combination with nisin, showed synergistic activity against extensively drug-resistant <i>A. baumannii</i>	P-10 (62) MIC with nisin, is also active against colistin-resistant <i>P. aeruginosa</i>	P-10 (62) in combination with nisin, is also active against colistin-resistant <i>P. aeruginosa</i>	139
Cathelicidin	HLF (1–11) (63)	Produced from human lactoferrin		HLF (63) is active against <i>in vitro</i> and <i>in vivo</i> models of <i>A. baumannii</i> infections	HLF (63) is active against <i>in vitro</i> and <i>in vivo</i> models of <i>A. baumannii</i> infections	MDR <i>Staphylococcus aureus</i>	140
Defensins	Synthetic $\beta$ -defensin-2 (64)			Synthetic $\beta$ -defensin-2 (64) MIC MDR <i>A. baumannii</i> vLD90 = 3.25–4.5 $\mu\text{g}$ $\text{mL}^{-1}$	Synthetic $\beta$ -defensin-2 (64) MIC MDR <i>A. baumannii</i> vLD90 = 3.25–4.5 $\mu\text{g}$ $\text{mL}^{-1}$	<i>Pseudomonas aeruginosa</i> , <i>Enterococcus faecalis</i> , <i>Enterococcus faecium</i> and <i>Staphylococcus aureus</i>	143
Cathelicidin	COG1410 (65)	Apolipoprotein E mimetic		It disrupts the plasma membrane, leaking the cytoplasmic contents and inhibiting biofilm formation	COG1410 (65) MIC <i>A. baumannii</i> ATCC19606 = 16 $\mu\text{g}$ $\text{mL}^{-1}$	COG1410 (65) MIC PDR <i>A. baumannii</i> YQ4 = 16 $\mu\text{g}$ $\text{mL}^{-1}$	3.90–9.35 $\mu\text{g}$ $\text{mL}^{-1}$
Cathelicidin	BMAP-28 (66)				COG1410 exhibited synergistic activity with polymyxin B and cured <i>C. elegans</i> infected with PDR <i>Acinetobacter baumannii</i> BMAP-28 (66) MIC pan-drug-resistant <i>A. baumannii</i> ATCC19606 = 5 $\mu\text{g}$ $\text{mL}^{-1}$	COG1410 exhibited synergistic activity with polymyxin B and cured <i>C. elegans</i> infected with PDR <i>Acinetobacter baumannii</i> BMAP-28 (66) MIC pan-drug-resistant <i>A. baumannii</i> ATCC19606 = 5 $\mu\text{g}$ $\text{mL}^{-1}$	145
Cathelicidin	A837 (67)				67, 68, 69, and 70 inhibited	BMAP-28 and its analogs bind to the outer membrane	145
Cathelicidin	A838 (68)				inhibited	protein OmpA	
Cathelicidin	A839 (69) and A840 (70)				pan-drug-resistant <i>A. baumannii</i> ATCC19606 10,		

Table 2 (continued)

Category	Compound name	Source	Mode of action	Morphological changes	Targeted <i>A. baumannii</i>	Other targeted bacteria	Ref.	
		(AbOmpA) of <i>A. baumannii</i>			5–10, 5–10, 5–10 $\mu\text{g mL}^{-1}$ , and clinical isolates of pan-drug-resistant <i>A. baumannii</i> strains with MIC values of 5–10, 20, 5–220, 5–20, and 5–20 $\mu\text{g mL}^{-1}$ , respectively			
Cathelicidin	Bac7 (71)	Bac5 analogues			Bac7 (71) MIC <i>A. baumannii</i> ATCC19606 = $\leq 8 \mu\text{M}$		146	
Cathelicidin	Bac5-258 (72), Bac5-272 (73), Bac5-278 (74), Bac5-281 (75), and Bac5-291 (76)			Peptides cause protein synthesis inhibition and bacterial membrane destabilization	72, 73, 74, 75 and 76 MIC <i>A. baumannii</i> ATCC19606 = $> 64, 64, 8, 4, 2$ , and 8 $\mu\text{M}$ , respectively		147	
Cathelicidin	Cathelicidin-BF-a4 (ZY4) (81)	Cathelicidin-BF derivative		It induces membrane permeabilization and disruption of the membrane, causing pore formation	Cathelicidin-BF-a4 (81) demonstrated antibacterial activity against GNB, including <i>P. aeruginosa</i> strains and <i>A. baumannii</i> isolates, with MIC ranging between 2.0 and 4.5 $\mu\text{g mL}^{-1}$ and 4.6 and 9.4 $\mu\text{g mL}^{-1}$ , respectively			
Defensin	Am23SK (85)	Crocodilian $\beta$ -defensin synthetic analogue			Am23SK (85) displayed antibacterial activity against <i>Salmonella enterica</i> serovar Typhimurium ATCC 14028, <i>Staphylococcus aureus</i> SAP0017, and <i>Enterobacter cloacae</i> 218R1	<i>Salmonella enterica</i> serovar Typhimurium ATCC 14028, <i>Staphylococcus aureus</i> SAP0017, and <i>Enterobacter cloacae</i> 218R1	150	
Apolipoprotein	Apo5 (87), Apo6 (88), and A1P (89)				Apo5 and Apo6 induced membrane disruption	<i>S. aureus</i> , <i>Escherichia coli</i> , and <i>P. aeruginosa</i>	87, 88, and 89 inhibited <i>A. baumannii</i> ATCC 9955 and <i>A. baumannii</i> ATCC BAA-1794 with EC <sub>50</sub> values of 0.644 and 0.234 $\mu\text{g mL}^{-1}$ , 0.233 and 0.126 $\mu\text{g mL}^{-1}$ , and 224.0 and 23.6 $\mu\text{g mL}^{-1}$ , respectively	151
Linear peptide	2K4L (90) 2K2L (91)	Temporin-1CEc analogs derived from <i>Rana chensinensis</i> skin secretion		2K4L demonstrated interactions with lipopolysaccharides	They cause membrane disruption		2K4L (90) and 2K2L (91) showed activity against <i>A. baumannii</i> MRAB 0227 and <i>A. baumannii</i> 22.933 with MIC values of 6.25 and 3.13 $\mu\text{M}$ and 25 and 12.5 $\mu\text{M}$ , respectively	152

Table 2 (continued)

Category	Compound name	Source	Mode of action	Morphological changes	Targeted <i>A. baumannii</i>	Other targeted bacteria	Ref.
	Hylin a1-11K (93) Hylin a1-15K (94)	Hylin a1 analogue	Hylin a1-11K and Hylin a1-15K bind to the lipopolysaccharide	These peptides disrupt the membrane	Hylin a1-11K (93) and hylin a1-15K (94) exhibited broad-spectrum antimicrobial activity and anti-biofilm activity against carbapenem-resistant <i>A. baumannii</i>		153
AP19 (95)	A hybrid of cathelicidin (P7) and aurein (A3)			The d-form of AP19 causes membrane disruption and leakage of cytoplasmic contents	The AP19 (95) d-form exhibited antibacterial activity against MDR and XDR clinical isolates of <i>A. baumannii</i>		154
Esculentin-1a (96)			Esculentin-1a, in combination with colistin, colistin, enhanced the membrane perturbation effects	Mp1a and its derivatives demonstrated potent cell membrane binding and disrupted the cytoplasmic membrane	Esculentin-1a, in combination with colistin, demonstrated synergistic activity against MDR <i>A. baumannii</i> clinical isolates 97-104 MIC <i>A. baumannii</i> ATCC 19606 = 0.025, 0.015-0.03, 0.015-0.03, 0.015-0.03, 0.05-0.1, 0.025-0.1, 0.2, and 0.4-0.8 $\mu$ M, respectively		155
$\Delta$ -Myrtotoxin-Mp1a (97) and its analogues (98-104)	Mp1a is obtained from the venom of <i>Myrmecia pilosula</i>			LyetTx I mn $\Delta$ K is derived from LyetTx I AMP	LyetTx I mn $\Delta$ K disrupts the bacterial cell membrane and causes leakage of cell contents, reducing the preformed biofilms.	LyetTx I mn $\Delta$ K (106) MIC carapenem-resistant <i>A. baumannii</i> AC10 = 2 $\mu$ M	156
LyetTx I mn $\Delta$ K (106)					Cec4 treatment of <i>A. baumannii</i> led to the destruction of the bacterial membrane and caused leakage of the cytoplasmic contents	Cec4 (108) demonstrated activity against <i>A. baumannii</i> (ATCC 19606), Multidrug-resistance <i>A. baumannii</i> and extensive drug-resistant <i>A. baumannii</i> (PRAB) with the same MIC value of 4 $\mu$ g mL $^{-1}$	160, 161
Cecropin	Cec4 (108)		Cec4 is derived from cecropin, a peptide from <i>Musca domestica</i>		Cec4 (108) demonstrated activity against <i>A. baumannii</i> (ATCC 19606), Multidrug-resistance <i>A. baumannii</i> and extensive drug-resistant <i>A. baumannii</i> (PRAB) with the same MIC value of 4 $\mu$ g mL $^{-1}$	Pap12-6 (109) inhibited <i>E. coli</i> , <i>P. aeruginosa</i> , <i>S. typhimurium</i>	162
Cecropin	Pap12-6 (109)		Pap12-6 derived from papillocin		Pap12-6 (109) inhibited <i>E. coli</i> , <i>P. aeruginosa</i> , <i>A. baumannii</i> , and <i>S. typhimurium</i> , with MIC values of 4, 4, 4, and 8 $\mu$ M, respectively	OMN6 (110) inhibited <i>A. baumannii</i> with a 4 $\mu$ g mL $^{-1}$ MIC value	163
OMN6 (110)					OMN6 causes membrane disruption and leakage of cellular contents in <i>E. coli</i>		

Table 2 (continued)

Category	Compound name	Source	Mode of action	Morphological changes	Targeted <i>A. baumannii</i>	Other targeted bacteria	Ref.
	L6 (111) and L8 (112)	L6 and L8 are formed from the <i>l</i> -form of D6 and D8. Notably, D6 and D8 are derived from cecropin-melittin hybrids	D6 and D8 bind to the LPS of the bacterial membrane		L6 (111) and L8 (112) synergized with vancomycin in <i>A. baumannii</i>		164
Defensin	Pro9-3 (114), Pro9-3D (115), R-Pro9-3 (116), and R-Pro9-3D (117)	Pro9-3, Pro9-3D, R-Pro9-3, and R-Pro9-3D are derived from protaecitamycin	These peptides interact with LPS in the outer membrane, causing permeabilization	mCM11 disrupts the membrane	114–117 MIC <i>A. baumannii</i> = 16, 8, 16, and 8 $\mu$ M, respectively		165
	mCM11 (119)	mCM11 is derived from CM11			mCM11 (119) inhibited MDR <i>A. baumannii</i> 31, PDR <i>A. baumannii</i> 71, XDR <i>A. baumannii</i> 23, and XDR <i>A. baumannii</i> 59, with MIC values of <4, <4, 4, and 4 $\mu$ g $\text{mL}^{-1}$ , respectively		166
	Bicarinalin (120)	Bicarinalin is obtained from the venom of <i>Tetramorium bicarinatum</i>			Bicarinalin and BP100 demonstrated morphological changes in the cells, with pronounced blebbing, variable cell shape, and shrinkage. Also, they induces membrane disruption		167
	BP100 (121)	BP100 is a hybrid of cecropin A and melittin			HPME (123), HPMA (124), CAME (125), and CAMA (126) exhibited antibacterial activity with MIC values ranging from 3.12–12.5 $\mu$ M in <i>A. baumannii</i> strains		168
	HPME (123)	HPME is derived from HP 2–9, and ME 1–12, HPMA is from HP 2–9 and MA 1–12, CAME is from CA 1–8 and ME 1–12, and CAMA is from CA 1–8 and MA 1–12, respectively			Mastoparan and its analogs cause structural damage to the bacterial membrane and cause dye leakage in dye-assay experiments		169
	HPMA (124)				Mastoparan (127), H-inlkalaalakkil-NH <sub>2</sub> (128), and Gu-INLKALAALAKKL-NH <sub>2</sub> (129) inhibit <i>A. baumannii</i> Ab113 with MIC values of 2.7, 2.7, and 2.6 $\mu$ M, respectively		169
	CAME (125)				Lycosin-II (140) competes with the bacterial membrane		170
	CAMA (126)				From venom of <i>Lycosa singoriensis</i> Lycosin-II (130) showed broadspectrum antibacterial activity against <i>E. coli</i> , <i>K. pneumoniae</i> , <i>Streptococcus pyogenes</i> , <i>Staphylococcus saprophyticus</i> , <i>Staphylococcus epidermidis</i> , <i>Pseudomonas aeruginosa</i> , <i>Viridans</i>		
Linear peptide	Lycosin-II (130)						



Table 2 (continued)

Category	Compound name	Source	Mode of action	Morphological changes	Targeted <i>A. baumannii</i>	Other targeted bacteria	Ref.
					<i>Staphylococcus epidermidis</i> , <i>Pseudomonas aeruginosa</i> , <i>Viridans streptococci</i> , <i>S. aureus</i> , and <i>A. baumannii</i> with MIC values of 12.5, 50, 50, 3.1, 3.1, 12.5, 3.1, 3.1, and 3.1–6.3 $\mu$ M, respectively	<i>Streptococci</i> , and <i>S. aureus</i>	172
DvAMP (131)			It showed 100% homology to <i>drosophila virilis</i>	It binds to exogenous lipopolysaccharides and phospholipids of <i>A. baumannii</i>	It enhanced membrane permeability, causing the dissipation of proton motive force, reducing intracellular ATP, and increasing ROS levels, ultimately leading to bacterial death	<i>pneumoniae</i> ATCC70060, <i>S. aureus</i> ATCC25923, <i>A. baumannii</i> ATCC19606, <i>A. baumannii</i> CRAB 01, <i>A. baumannii</i> CRAB 02, <i>A. baumannii</i> CRAB 03, <i>A. baumannii</i> CRAB 04, and <i>A. baumannii</i> CRAB 05, with MIC values of 8, 16, 16, 64, 8, 8, 8, and 8 $\mu$ g mL <sup>-1</sup> , respectively	<i>E. coli</i> ATCC 25922, <i>K. pneumoniae</i> BAA-2146 (NDM-1)
Arenicin	AA139 (133)	Derived from arenicin-3			It causes membrane disruption and leakage of cytoplasmic contents in <i>P. aeruginosa</i>	<i>E. coli</i> ATCC 25922, <i>K. pneumoniae</i> BAA-2146 (NDM-1), non-MDR <i>A. baumannii</i> , MDR <i>A. baumannii</i> , and XDR <i>A. baumannii</i> with MIC values of 0.125, 1, 2, 1, and 0.5 $\mu$ g mL <sup>-1</sup> , respectively	173
					These peptides cause bacterial membrane destruction and inhibition of biofilm formation.	<i>Hp1404</i> (134) also inhibits the growth of <i>Staphylococcus aureus</i> 409081, <i>A. baumannii</i> 719705, and <i>A. baumannii</i> 907233 with MIC values of 3.13, 6.25, 3.13, 3.13, and 3.13 $\mu$ g mL <sup>-1</sup> , and 3.13, 12.5, 3.13, 6.25, 3.13, and 3.13 $\mu$ g mL <sup>-1</sup> , respectively	174, 175
	Im5 (146)					<i>Acinetobacter baumannii</i> ATCC19606 = 2.5 $\mu$ g mL <sup>-1</sup>	175

Table 2 (continued)

Category	Compound name	Source	Mode of action	Morphological changes	Targeted <i>A. baumannii</i>	Other targeted bacteria	Ref.
	Octopromycin [147]	<i>Octopus minor</i>		Octopromycin causes severe cell wall damage. It forms irregularly shaped cells and increases ROS generation inside the cells	Octopromycin (147) MIC <i>Acinetobacter baumannii</i> = 50 $\mu\text{g mL}^{-1}$		177
Octoprohibitin [148]	Synthesized from the prohibitin-2 gene			It causes severe damage with opening and shrinkage of cells	Octoprohibitin (148) MIC <i>Acinetobacter baumannii</i> = 50 $\mu\text{g mL}^{-1}$		178
TP2-5 [150] and TP2-6 [151]	Derived from tilapia piscidin 2 (TP2)			These peptides cause membrane depolarization with deformed cells	TP2-5 (150) and TP2-6 (151) inhibited sensitive and MDR isolates, including <i>A. baumannii</i> 10 591, <i>A. baumannii</i> 14B0091, <i>A. baumannii</i> 2088, <i>A. baumannii</i> 921, <i>A. baumannii</i> 1019, and <i>A. baumannii</i> 1033 with the same MIC value of 3.125 $\mu\text{g mL}^{-1}$		
LysMK34 (eLysMK34) [152]	A chimeric protein having a fusion of lysin and cecropin A			It causes peptidoglycan degradation and pressure-induced osmotic lysis	eLysMK34 (152) inhibited sensitive and resistant strains <i>A. baumannii</i> MK34, <i>A. baumannii</i> RUH134, <i>A. baumannii</i> Greek46, <i>A. baumannii</i> Greek47, and <i>A. baumannii</i> NCTC13423 with MIC values of 0.76, 0.76, 0.76, 1.2, and 0.45 $\mu\text{M}$ , respectively	<i>P. aeruginosa</i> , <i>E. coli</i>	183
PlyA [153]	It is derived from cecropin A, and OBP <sub>gp279</sub>				PlyA (153) showed potent antibacterial activities against <i>A. baumannii</i> eAbEndolysin (154)	<i>P. aeruginosa</i>	184
eAbEndolysin [155]	A chimeric protein derived from cecropin A fusion with the AbEndolysin N-terminus				showed potent antibacterial activity against MDR <i>A. baumannii</i>		185
LysAB2 P3 [156]	Derived from LysAB2			LysAB2 P3 causes damage to bacterial cell walls and the collapse of the cellular structure	LysAB2 P3 (156) showed antibacterial activity against MDR and colistin-resistant strains. It inhibited <i>A. baumannii</i> ATCC17978, <i>A. baumannii</i> ATCC19606, <i>A. baumannii</i> M3237, <i>A. baumannii</i> M6337, <i>A. baumannii</i> M105656, <i>A. baumannii</i> M2925, and <i>A. baumannii</i>		186

Table 2 (continued)

Category	Compound name	Source	Mode of action	Morphological changes	Targeted <i>A. baumannii</i>	Other targeted bacteria	Ref.
	P307 (158), and P307 <sub>AE-8</sub> (159)	Derived from LysAB2			MI17720, with MIC and MBC values of 4 and 8, 8 and 16 and 16, 4 and 4, 8 and 8, 8 and 8, and 8 and 8 $\mu$ M, respectively P307 (158) and P307 <sub>SQ-8</sub> (159) exhibited antibacterial activity against <i>A. baumannii</i>	<i>P. aeruginosa</i> , <i>K. pneumoniae</i> , and <i>E. coli</i>	187
	LysP53 (160)	Derived from <i>A. baumannii</i> phage 53			LysP53 (100 $\mu$ g mL <sup>-1</sup> ) caused a 4-log reduction in <i>A. baumannii</i> in 15 minutes of exposure	<i>P. aeruginosa</i>	182
	Artilysin Art-175 (161)	This is an engineered fusion of endolysin KZ144 linked to SMAP-29			Artilysin Art-175 (161) inhibits MDR <i>A. baumannii</i> with MIC values ranging between 4 and 20 $\mu$ g mL <sup>-1</sup> . Lys1S-19P (162) showed potent activity against MDR <i>A. baumannii</i>	<i>P. aeruginosa</i>	188
	Lys1S-19P (162)				Guavanin 2 (163) inhibited <i>Escherichia coli</i> ATCC 25922, <i>Pseudomonas aeruginosa</i> ATCC 27853, <i>Acinetobacter baumannii</i> ATCC 19606, and <i>Klebsiella pneumoniae</i> with 6.25, 25, 6.25, and 80 $\mu$ g mL <sup>-1</sup> , respectively	<i>E. coli</i> ATCC 191	191
	Guavanin 2 (163)	Derived from glycine-rich peptide Pg-AMP1			T7 causes membrane disruption activity in bacterial cells	<i>P. aeruginosa</i>	194–196
Dendrimer	G3KL (164) T7 (165)				G3KL (164) inhibited <i>A. baumannii</i> (10 OXA-23, 7 OXA-24, and 11 OXA-58 carbapenemase producers) and <i>P. aeruginosa</i> (18 VIM and 3 IMP carbapenemase producers) strains with MIC values ranging from 4–16 and 4–32 $\mu$ g mL <sup>-1</sup> , and MBC values ranging from 4–16 and 4–128 $\mu$ g mL <sup>-1</sup> , respectively T7 (165) showed broadspectrum activity against Gram-negative MDR strains. It inhibited <i>A. baumannii</i> ATCC 19606, <i>E. coli</i> bla OXA-48, <i>E. coli</i> W3110, <i>P. aeruginosa</i> ZEM-9A, <i>P. aeruginosa</i> ZEM-1A, <i>E. cloacae</i> bla NCCTC 418, <i>K. pneumoniae</i> Bla OXA-48	<i>E. coli</i> bla OXA-48, <i>E. coli</i> W3110, <i>P. aeruginosa</i> ZEM-9A, <i>P. aeruginosa</i> ZEM-1A, <i>E. cloacae</i> bla NCCTC 418, <i>K. pneumoniae</i> Bla OXA-48	



Table 2 (continued)

Category	Compound name	Source	Mode of action	Morphological changes	Targeted <i>A. baumannii</i>	Other targeted bacteria	Ref.
Chimeric peptide	TAT-RasGAP <sub>317-326</sub> (166)	A hybrid of TAT <sub>48-57</sub> and Src homology 3 domain	Biofilm inhibition		<i>P. aeruginosa</i> PA14		197
	SA4 (167) SPO (168)	Membrane perturbation					198, 199
	Paenipeptin hexanoyl (169) Paenipeptin carboxybenzyl (170)	Derived from paenipeptin					200
	Ω76 (171)			It causes rapid membrane disruption, leakage, and bacterial death	<i>E. coli</i>		201
	MSI-78-ADCA (172) and MSI-78-ACA (173)				<i>K. pneumoniae</i> and <i>P. aeruginosa</i>		202
	B2 (174)						203
	RO7075573 (176), RO7055137 (177), and zosurabalin (179)	Zosurabalin inhibited the inner membrane LptB2FGC complex to block the LPS transport in <i>A. baylyi</i>					204

*A. baumannii*. Further analysis suggests that the mode of binding of peptide B2 is by forming a complex with BamA.<sup>203</sup>

**2.2.3. Tethered macrocyclic peptide (MCP).** Zampaloni *et al.* carried out screenings of macrocyclic peptides of Tranzyme Pharma. From the initial screenings, they identified compounds with a tripeptide subunit tethered to diphenylsulfide with a closed ring-like structure. Among them, the compounds RO7036668 (175, Fig. 13), RO7075573 (176, Fig. 13), RO7055137 (177, Fig. 13), and RO7202110 (178, Fig. 13) showed antibacterial activity against *A. baumannii*. RO7075573 is a potent antibacterial compound; however, it demonstrated poor plasma compatibility by causing the formation of aggregated low-density lipoprotein and aggregated high-density lipoprotein vesicles through an unknown mechanism. Later, this problem was solved by forming the compound zwitterionic tethered macrocyclic peptide zosurabalpin (179, Fig. 13), which showed reduced plasma precipitation. RO7075573, RO7055137, and zosurabalpin were found to be active against sensitive and MDR *A. baumannii* isolates. Moreover, zosurabalpin effectively reduced the infections caused by drug-resistant contemporary isolates of CRAB both *in vitro* and in mouse disease models. Zosurabalpin exhibited antibacterial activity by inhibiting the bacterial inner membrane LptB2FGC complex to block the LPS transport in *A. baylyi*.<sup>204</sup> AMPs with their source, mode of action, and antibacterial activity are summarised in Table 2.

### 3. Conclusion

*A. baumannii* is on the list of nosocomial ESKAPE pathogens of the WHO, and there is an urgent need for research to discover antibiotics to tackle its infections. Several antibiotics, including carbapenems, aminoglycosides, fluoroquinolones, cephalosporins, and  $\beta$ -lactamase inhibitors, are used to treat *A. baumannii* infections. However, in recent decades, abuse and misuse of antibiotics to treat other diseases other than the mentioned use led to the rapid emergence of MDR *A. baumannii*, consequently leading to an increase in the MICs of prescribed antibiotics. The emergence of MDR *A. baumannii*, XDR *A. baumannii*, and PDR *A. baumannii* strains significantly affect health, and it is a threat to human life and health and is responsible for a significant economic burden to society. Several targets, including ribosomes, DNA gyrase, and the cell wall, have already been explored in *A. baumannii* to control its growth. However, targeting the cell wall and its components is one of the primary focuses of antibiotics research, and it continues to hold the center stage in antibiotics discovery, as cell wall targeting antibiotics are less likely to acquire mutation-based resistance. Moreover, membrane-targeting antibiotics do not have to cross the plasma membrane to exhibit their activity. Among them, AMPs are next-generation membrane-targeting antibiotics and exhibit broad-spectrum activity against GNB, GPB, and related clinical-resistant strains. Moreover, most AMPs act on the membrane targets and other generalized

Table 2 (continued)

Category	Compound name	Source	Mode of action	Morphological changes	Targeted <i>A. baumannii</i>	Other targeted bacteria	Ref.
			of $\leq 0.06$ , 0.12, and 0.5 ( $\leq 0.06$ –0.5) mg L <sup>-1</sup> , $\leq 0.06$ , $\leq 0.06$ , and 0.12 ( $\leq 0.06$ –0.12) mg L <sup>-1</sup> , and $\leq 0.06$ , 0.25, and 0.25 (0.12–1) mg L <sup>-1</sup> , respectively				



cytoplasmic targets, and some of them activate the human immune response for the effective eradication of pathogens from the body. This paper discussed AMPs from natural or synthetic origins and their congeners acting through membrane disruption of *A. baumannii*.

## Abbreviations

AbaR	Antibiotic resistance island
Acb	<i>Acinetobacter calcoaceticus</i> – <i>Acinetobacter baumannii</i>
ADC	Acinetobacter-derived cephalosporinase
AMPs	Antimicrobial peptides
ApoE	Apolipoprotein E
BAP	Biofilm-associated protein
CecA	Cecropin A
CLSM	Confocal laser scanning microscopy
CRAB	Carbapenem-resistant <i>A. baumannii</i>
Dab, L-2	4-Diaminobutyric acid
Dpa	Diaminopropane acetyltransferase
ELISA	Enzyme-linked immunosorbent assays
ESKAPE	( <i>Enterococcus faecium</i> , <i>Staphylococcus aureus</i> , <i>Klebsiella pneumoniae</i> , <i>Acinetobacter baumannii</i> , <i>Pseudomonas aeruginosa</i> , and <i>Enterobacter</i> spp.)
GlcNAc	N-Acetylglucosamine
hBD-1	Human $\beta$ -defensin-1
hBD-2	Human $\beta$ -defensin-2
hBD-3	Human $\beta$ -defensin-3
hBD-4	Human $\beta$ -defensin-4
HD5	Human defensin 5
Hst5	Histatin 5
Kdo	Ketodeoxyoctanoic acid
LPS	Lipopolysaccharides
LpsB	Glycosyltransferase
LOS	Lipoooligosaccharides
LPLATs	Lysophospholipid acyltransferase
MBEC	Minimum biofilm eradication concentration
MBIC <sub>90</sub>	Minimum biofilm inhibition concentration
MCP	Tethered macrocyclic peptide
MDR	Multidrug-resistant
MICs	Minimum inhibitory concentrations
MurNAc	N-Acetylmuramic acid
OMP	Outer membrane protein
OMR	Outer membrane receptors
OMVs	Outer membrane vesicles
PBPs	Penicillin-binding proteins
PDR	Pan-drug-resistant
PMR	Polymyxin-resistant
Pr-AMPs	Proline-rich peptides
qPCR	Quantitative polymerase chain reaction
SEM	Scanning electron microscopy
SPase	Signal peptidase
syn-BNP	Synthetic-bioinformatic natural product
TCA	Tricarboxylic acid cycle
TLR4	Toll-like receptor 4
WHO	World Health Organization
XDR	Extensively drug-resistant

XDR-ABC Drug-resistant *Acinetobacter baumannii*–*calcoaceticus* complex

## Data availability

No primary research results, software or code have been included and no new data were generated or analysed as part of this review.

## Conflicts of interest

There are no conflicts of interest to declare.

## Acknowledgements

GK thanks the Director of Birla Institute of Technology and Science Pilani, Pilani Campus, Rajasthan for providing the necessary facilities to carry out the research work.

## References

- 1 A. Gedefie, W. Demsis, M. Ashagrie, Y. Kassa, M. Tesfaye, M. Tilahun, H. Bisetegn and Z. Sahle, *Infect. Drug Resist.*, 2021, **14**, 3711–3719.
- 2 A. Nemec, L. Krizova, M. Maixnerova, O. Sedo, S. Brisse and P. G. Higgins, *Int. J. Syst. Evol. Microbiol.*, 2015, **65**, 934–942.
- 3 N. Bagińska, M. Cieślik, A. Górska and E. Jończyk-Matysiak, *Antibiotics*, 2021, **10**, 1–15.
- 4 T. Ballouz, J. Aridi, C. Afif, J. Irani, C. Lakis, R. Nasreddine and E. Azar, *Front. Cell. Infect. Microbiol.*, 2017, **7**, 1–8.
- 5 M. Asif, I. A. Alvi and S. U. Rehman, *Infect. Drug Resist.*, 2018, **11**, 1249–1260.
- 6 N. Pakharukova, M. Tuittila, S. Paavilainen, H. Malmi, O. Parilova, S. Teneberg, S. D. Knight and A. V. Zavialov, *Proc. Natl. Acad. Sci. U. S. A.*, 2018, **115**, 5558–5563.
- 7 C. M. Harding, S. W. Hennon and M. F. Feldman, *Nat. Rev. Microbiol.*, 2018, **16**, 91–102.
- 8 R. Vázquez-López, S. G. Solano-Gálvez, J. J. Juárez Vignon-Whaley, J. A. Abello Vaamonde, L. A. Padró Alonzo, A. Rivera Reséndiz, M. Muleiro Álvarez, E. N. Vega López, G. Franyuti-Kelly, D. A. Álvarez-Hernández, V. Moncaleano Guzmán, J. E. Juárez Bañuelos, J. Marcos Felix, J. A. González Barrios and T. Barrientos Fortes, *Antibiotics*, 2020, **9**, 1–22.
- 9 C.-R. Lee, J. H. Lee, M. Park, K. S. Park, I. K. Bae, Y. B. Kim, C.-J. Cha, B. C. Jeong and S. H. Lee, *Front. Cell. Infect. Microbiol.*, 2017, **7**, 1–35.
- 10 F. C. Morris, C. Dexter, X. Kostoulias, M. I. Uddin and A. Y. Peleg, *Front. Microbiol.*, 2019, **10**, 1–20.
- 11 J. M. Boll, A. T. Tucker, D. R. Klein, A. M. Beltran, J. S. Brodbelt, B. W. Davies and M. S. Trent, *MBio*, 2015, **6**, 1–11.
- 12 C. Y. Chin, K. A. Tipton, M. Farokhyfar, E. M. Burd, D. S. Weiss and P. N. Rather, *Nat. Microbiol.*, 2018, **3**, 563–569.
- 13 L. Semenec, A. K. Cain, C. J. Dawson, Q. Liu, H. Dinh, H. Lott, A. Penesyan, R. Maharjan, F. L. Short, K. A. Hassan and I. T. Paulsen, *Nat. Commun.*, 2023, **14**, 1–18.
- 14 B. Shin, C. Park and W. Park, *Appl. Microbiol. Biotechnol.*, 2020, **104**, 1259–1271.



15 J. Armalytė, A. Čepauskas, G. Šakalytė, J. Martinkus, J. Skerniškytė, C. Martens, E. Sužiedėlienė, A. Garcia-Pino and D. Jurėnas, *Nat. Commun.*, 2023, **14**, 1–11.

16 S. Roy, G. Chowdhury, A. K. Mukhopadhyay, S. Dutta and S. Basu, *Front. Med.*, 2022, **9**, 1–32.

17 E. De Gregorio, E. Roscetto, V. D. Iula, M. Martinucci, R. Zarrilli, P. P. Di Nocera and M. R. Catania, *New Microbiol.*, 2015, **38**, 251–257.

18 C.-H. Su, M.-H. Tsai, C.-Y. Lin, Y.-D. Ma, C.-H. Wang, Y.-D. Chung and G.-B. Lee, *Biosens. Bioelectron.*, 2020, **159**, 1–7.

19 J. Luo, M. Jiang, J. Xiong, J. Li, X. Zhang, H. Wei and J. Yu, *Anal. Chim. Acta*, 2018, **1044**, 147–153.

20 C. Ayoub Moubareck and D. Hammoudi Halat, *Antibiotics*, 2020, **9**, 1–29.

21 G. Kumar and S. Kapoor, *Bioorg. Med. Chem.*, 2023, **81**, 117212.

22 K. B. Steinbuch and M. Fridman, *MedChemComm*, 2016, **7**, 86–102.

23 M. Zahn, S. P. Bhamidimarri, A. Baslé, M. Winterhalter and B. van den Berg, *Structure*, 2016, **24**, 221–231.

24 L. M. VanOtterloo, L. A. Macias, M. J. Powers, J. S. Brodbelt and M. S. Trent, *MBio*, 2024, **15**, 1–20.

25 E. Geisinger, W. Huo, J. Hernandez-Bird and R. R. Isberg, *Annu. Rev. Microbiol.*, 2019, **73**, 481–506.

26 J. M. Boll, A. A. Crofts, K. Peters, V. Cattoir, W. Vollmer, B. W. Davies and M. S. Trent, *Proc. Natl. Acad. Sci. U. S. A.*, 2016, **113**, E6228–E6237.

27 B. W. Simpson, M. Nieckarz, V. Pinedo, A. B. McLean, F. Cava and M. S. Trent, *MBio*, 2021, **12**, 1–19.

28 D. Dovala, C. M. Rath, Q. Hu, W. S. Sawyer, S. Shia, R. A. Elling, M. S. Knapp and L. E. Metzger, *Proc. Natl. Acad. Sci. U. S. A.*, 2016, **113**, E6064–E6071.

29 M. J. Powers and M. S. Trent, *Mol. Microbiol.*, 2018, **107**, 47–56.

30 D. Nie, Y. Hu, Z. Chen, M. Li, Z. Hou, X. Luo, X. Mao and X. Xue, *J. Biomed. Sci.*, 2020, **27**, 1–8.

31 C. Whiteway, A. Breine, C. Philippe and C. Van der Henst, *Trends Microbiol.*, 2022, **30**, 199–200.

32 W. F. Penwell, A. B. Shapiro, R. A. Giacobbe, R.-F. Gu, N. Gao, J. Thresher, R. E. McLaughlin, M. D. Huband, B. L. M. DeJonge, D. E. Ehmann and A. A. Miller, *Antimicrob. Agents Chemother.*, 2015, **59**, 1680–1689.

33 Y. Doi, G. Murray and A. Peleg, *Semin. Respir. Crit. Care Med.*, 2015, **36**, 085–098.

34 H. Chen, Q. Liu, Z. Chen and C. Li, *J. Infect. Chemother.*, 2017, **23**, 278–285.

35 T. F. Durand-Réville, S. Guler, J. Comita-Prevoir, B. Chen, N. Bifulco, H. Huynh, S. Lahiri, A. B. Shapiro, S. M. McLeod, N. M. Carter, S. H. Moussa, C. Velez-Vega, N. B. Olivier, R. McLaughlin, N. Gao, J. Thresher, T. Palmer, B. Andrews, R. A. Giacobbe, J. V. Newman, D. E. Ehmann, B. de Jonge, J. O'Donnell, J. P. Mueller, R. A. Tommasi and A. A. Miller, *Nat. Microbiol.*, 2017, **2**, 1–10.

36 M. I. El-Gamal, I. Brahim, N. Hisham, R. Aladdin, H. Mohammed and A. Bahaaeldin, *Eur. J. Med. Chem.*, 2017, **131**, 185–195.

37 M. Nguyen and S. G. Joshi, *J. Appl. Microbiol.*, 2021, **131**, 2715–2738.

38 J. Fishbain and A. Y. Peleg, *Clin. Infect. Dis.*, 2010, **51**, 79–84.

39 E.-T. Piperaki, L. S. Tzouvelekis, V. Miriagou and G. L. Daikos, *Clin. Microbiol. Infect.*, 2019, **25**, 951–957.

40 C. H. Rodríguez, M. Nastro and A. Famiglietti, *Rev. Argent. Microbiol.*, 2018, **50**, 327–333.

41 M. R. Galac, E. Snesrud, F. Lebreton, J. Stam, M. Julius, A. C. Ong, R. Maybank, A. R. Jones, Y. I. Kwak, K. Hinkle, P. E. Waterman, E. P. Lesho, J. W. Bennett and P. Mc Gann, *Antimicrob. Agents Chemother.*, 2020, **64**, 1–11.

42 E. Rando, S. L. Cutuli, F. Sangiorgi, E. S. Tanzarella, F. Giovannenze, G. De Angelis, R. Murri, M. Antonelli, M. Fantoni and G. De Pascale, *JAC Antimicrob. Resist.*, 2023, **5**, 1–9.

43 W. Ni, Y. Han, J. Zhao, C. Wei, J. Cui, R. Wang and Y. Liu, *Int. J. Antimicrob. Agents*, 2016, **47**, 107–116.

44 P. Fragkou, G. Poulakou, A. Blizou, M. Blizou, V. Rapti, D. Karageorgopoulos, D. Koulenti, A. Papadopoulos, D. Matthaiou and S. Tsiodras, *Microorganisms*, 2019, **7**, 1–20.

45 W. Deng, T. Fu, Z. Zhang, X. Jiang, J. Xie, H. Sun, P. Hu, H. Ren, P. Zhou, Q. Liu and Q. Long, *Emerging Microbes Infect.*, 2020, **9**, 639–650.

46 M. C. Phillips, N. Wald-Dickler, K. Loomis, B. M. Luna and B. Spellberg, *Open Forum Infect. Dis.*, 2020, **7**, 1–9.

47 M. L. Gil-Marqués, P. Moreno-Martínez, C. Costas, J. Pachón, J. Blázquez and M. J. McConnell, *J. Antimicrob. Chemother.*, 2018, **73**, 2960–2968.

48 F. L. Gordillo Altamirano, X. Kostoulias, D. Subedi, D. Korneev, A. Y. Peleg and J. J. Barr, *EBioMedicine*, 2022, **80**, 104045.

49 M. Y. Cruz-Muñiz, L. E. López-Jacome, M. Hernández-Durán, R. Franco-Cendejas, P. Licona-Limón, J. L. Ramos-Balderas, M. Martínez-Vázquez, J. A. Belmont-Díaz, T. K. Wood and R. García-Contreras, *Int. J. Antimicrob. Agents*, 2017, **49**, 88–92.

50 Y. Yu, H. Zhao, J. Lin, Z. Li, G. Tian, Y. Y. Yang, P. Yuan and X. Ding, *Int. J. Antimicrob. Agents*, 2022, **59**, 1–6.

51 S. Garneau-Tsodikova and K. J. Labby, *MedChemComm*, 2016, **7**, 11–27.

52 C. O. Vrancianu, I. Gheorghe, I. B. Czobor and M. C. Chifiriu, *Microorganisms*, 2020, **8**, 1–40.

53 M. S. Ramirez, R. A. Bonomo and M. E. Tolmisky, *Biomolecules*, 2020, **10**, 1–32.

54 L. L. Maragakis and T. M. Perl, *Clin. Infect. Dis.*, 2008, **46**, 1254–1263.

55 S. N. Abdi, R. Ghatalou, K. Ganbarov, A. Mobed, A. Tanomand, M. Yousefi, M. Asgharzadeh and H. S. Kafil, *Infect. Drug Resist.*, 2020, **13**, 423–434.

56 Z. A. Qureshi, L. E. Hittle, J. A. O'Hara, J. I. Rivera, A. Syed, R. K. Shields, A. W. Pasculle, R. K. Ernst and Y. Doi, *Clin. Infect. Dis.*, 2015, **60**, 1295–1303.

57 S. Ibrahim, N. Al-Saryi, I. M. S. Al-Kadmy and S. N. Aziz, *Mol. Biol. Rep.*, 2021, **48**, 6987–6998.

58 X. Wu, J. D. Chavez, D. K. Schweppe, C. Zheng, C. R. Weisbrod, J. K. Eng, A. Murali, S. A. Lee, E. Ramage, L. A. Gallagher, H. D. Kulasekara, M. E. Edrozo, C. N.

Kamischke, M. J. Brittnacher, S. I. Miller, P. K. Singh, C. Manoil and J. E. Bruce, *Nat. Commun.*, 2016, **7**, 1–14.

59 Y. Zhu, J. Lu, M. Han, X. Jiang, M. A. K. Azad, N. A. Patil, Y. Lin, J. Zhao, Y. Hu, H. H. Yu, K. Chen, J. D. Boyce, R. A. Dunstan, T. Lithgow, C. K. Barlow, W. Li, E. K. Schneider-Futschik, J. Wang, B. Gong, B. Sommer, D. J. Creek, J. Fu, L. Wang, F. Schreiber, T. Velkov and J. Li, *Adv. Sci.*, 2020, **7**, 1–13.

60 L. Zhang and R. L. Gallo, *Curr. Biol.*, 2016, **26**, R14–R19.

61 S. Li, Y. Wang, Z. Xue, Y. Jia, R. Li, C. He and H. Chen, *Trends Food Sci. Technol.*, 2021, **109**, 103–115.

62 Q. Wu, J. Patočka and K. Kuča, *Toxins*, 2018, **10**, 1–17.

63 M. Mahlapuu, C. Björn and J. Ekblom, *Crit. Rev. Biotechnol.*, 2020, **40**, 978–992.

64 A. Peschel and H. G. Sahl, *Nat. Rev. Microbiol.*, 2006, **4**, 529–536.

65 H. Q. Ning, Y. Q. Li, Q. W. Tian, Z. S. Wang and H. Z. Mo, *LWT–Food Sci. Technol.*, 2019, **99**, 62–68.

66 M. Magana, M. Pushpanathan, A. L. Santos, L. Leanse, M. Fernandez, A. Ioannidis, M. A. Giulianotti, Y. Apidianakis, S. Bradfute, A. L. Ferguson, A. Cherkasov, M. N. Seleem, C. Pinilla, C. de la Fuente-Nunez, T. Lazaridis, T. Dai, R. A. Houghten, R. E. W. Hancock and G. P. Tegos, *Lancet Infect. Dis.*, 2020, **20**, 1–15.

67 E. F. Haney, S. C. Mansour and R. E. W. Hancock, in *Methods in Molecular Biology*, 2017, vol. 1548, pp. 3–22.

68 A. Panjla, G. Kaul, S. Chopra, A. Titz and S. Verma, *ACS Chem. Biol.*, 2021, **16**(12), 2731–2745.

69 C. Chen, J. Shi, D. Wang, P. Kong, Z. Wang and Y. Liu, *Crit. Rev. Microbiol.*, 2024, **50**, 267–284.

70 J. M. Sierra, E. Fusté, F. Rabanal, T. Vinuesa and M. Viñas, *Expert Opin. Biol. Ther.*, 2017, **17**, 663–676.

71 W. C. Wimley and K. Hristova, *J. Membr. Biol.*, 2011, **239**, 27–34.

72 Q.-Y. Zhang, Z.-B. Yan, Y.-M. Meng, X.-Y. Hong, G. Shao, J.-J. Ma, X.-R. Cheng, J. Liu, J. Kang and C.-Y. Fu, *Mil. Med. Res.*, 2021, **8**, 1–25.

73 H. X. Luong, T. T. Thanh and T. H. Tran, *Life Sci.*, 2020, **260**, 118407.

74 A. M. van der Does, P. S. Hiemstra and N. Mookherjee, in *Advances in Experimental Medicine and Biology*, Springer New York LLC, 2019, vol. 1117, pp. 149–171.

75 N. Mookherjee, M. A. Anderson, H. P. Haagsman and D. J. Davidson, *Nat. Rev. Drug Discovery*, 2020, **19**, 311–332.

76 R. E. W. Hancock, E. F. Haney and E. E. Gill, *Nat. Rev. Microbiol.*, 2016, **14**, 321–334.

77 S. Biswas, J. M. Brunel, J. C. Dubus, M. Reynaud-Gaubert and J. M. Rolain, *Expert Rev. Anti-Infect. Ther.*, 2012, **10**, 917–934.

78 J. H. Moffatt, M. Harper and J. D. Boyce, in *Advances in Experimental Medicine and Biology*, Springer New York LLC, 2019, vol. 1145, pp. 55–71.

79 J. Zhu, S. Wang, C. Wang, Z. Wang, G. Luo, J. Li, Y. Zhan, D. Cai and S. Chen, *Synth. Syst. Biotechnol.*, 2023, **8**, 314–322.

80 G. Pavithrra and R. Rajasekaran, *Int. J. Pept. Res. Ther.*, 2020, **26**, 191–199.

81 M. Heidary, A. D. Khosravi, S. Khoshnood, M. J. Nasiri, S. Soleimani and M. Goudarzi, *Daptomycin*, *J. Antimicrob. Chemother.*, 2018, **73**, 1–11.

82 C. H. Lee, C. Y. Tsai, C. C. Li, C. C. Chien and J. W. Liu, *J. Antimicrob. Chemother.*, 2015, **70**, 257–263.

83 J. A. Karlowsky, K. Nichol and G. G. Zhan, *Clin. Infect. Dis.*, 2015, **61**, S58–S68.

84 K. D. Brade, J. M. Rybak and M. J. Rybak, *Infect. Dis. Ther.*, 2016, **5**, 1–15.

85 J. R. Smith, K. D. Roberts and M. J. Rybak, *s, Infect. Dis. Ther.*, 2015, **4**, 245–258.

86 R. Álvarez, L. E. L. Cortés, J. Molina, J. M. Cisneros and J. Pachón, *Antimicrob. Agents Chemother.*, 2016, **60**, 2601–2609.

87 G. D. Marena, M. A. dos Santos Ramos, T. M. Bauab and M. Chorilli, *Crit. Rev. Anal. Chem.*, 2021, **51**, 312–328.

88 J. C. Song and D. A. Stevens, *Crit. Rev. Microbiol.*, 2016, **42**, 813–846.

89 H. Pang, Z. Qu, V. Kumar, Y. Wang, Y. Wu, M. H. Lin, D. Harrich and F. Y. Han, *Adv. Ther.*, 2024, **7**, 2300439.

90 N. V. Hentig, *HIV/AIDS*, 2016, **8**, 1–16.

91 H. B. Koo and J. Seo, *Pept. Sci.*, 2019, **111**, e24122.

92 S. Baron, L. Hadjadj, J.-M. Rolain and A. O. Olaitan, *Expert Rev. Anti-Infect. Ther.*, 2012, **10**, 917–934.

93 M. H. Rigatto, D. R. Falci and A. P. Zavascki, in *Advances in Experimental Medicine and Biology*, 2019, vol. 1145, pp. 197–218.

94 J. H. Moffatt, M. Harper and J. D. Boyce, in *Advances in Experimental Medicine and Biology*, 2019, vol. 1145, pp. 55–71.

95 K. D. Roberts, Y. Zhu, M. A. K. Azad, M. Han, J. Wang, L. Wang, H. H. Yu, A. S. Horne, J. Pinson, D. Rudd, N. H. Voelcker, N. A. Patil, J. Zhao, X. Jiang, J. Lu, K. Chen, O. Lomovskaya, S. J. Hecker, P. E. Thompson, R. L. Nation, M. N. Dudley, D. C. Griffith, T. Velkov and J. Li, *Nat. Commun.*, 2022, **13**, 1–15.

96 P. Nasr, *J. Hosp. Infect.*, 2020, **104**, 4–11.

97 T. C. Menegucci, J. Albiero, L. B. Migliorini, J. L. B. Alves, G. F. Viana, J. Mazucheli, F. E. Carrara-Marroni, C. L. Cardoso and M. C. B. Tognim, *Int. J. Antimicrob. Agents*, 2016, **47**, 380–385.

98 K. Kengkla, K. Kongpakkattana, S. Saokaew, A. Apisarnthanarak and N. Chaiyakunapruk, *J. Antimicrob. Chemother.*, 2018, **73**, 22–32.

99 K. D. Roberts, M. A. K. Azad, J. Wang, A. S. Horne, P. E. Thompson, R. L. Nation, T. Velkov and J. Li, *ACS Infect. Dis.*, 2015, **1**, 568–575.

100 A.-L. Cui, X.-X. Hu, Y. Gao, J. Jin, H. Yi, X.-K. Wang, T.-Y. Nie, Y. Chen, Q.-Y. He, H.-F. Guo, J.-D. Jiang, X.-F. You and Z.-R. Li, *J. Med. Chem.*, 2018, **61**, 1845–1857.

101 C. Xie, P. Wang, H. Wu, X. Hu, T. Nie, X. Li, P. Pang, G. Li, Y. Lu, X. Yang, X. Wang, C. Li and X. You, *Biomed. Pharmacother.*, 2023, **164**, 1–11.

102 J. M. Tyrrell, A. F. Aboklaish, T. R. Walsh, T. Vaara and M. Vaara, *Peptides*, 2019, **112**, 149–153.



103 Z. Wang, B. Koirala, Y. Hernandez, M. Zimmerman, S. Park, D. S. Perlin and S. F. Brady, *Nature*, 2022, **601**, 606–611.

104 P. A. Smith, M. F. T. Koehler, H. S. Grgis, D. Yan, Y. Chen, Y. Chen, J. J. Crawford, M. R. Durk, R. I. Higuchi, J. Kang, J. Murray, P. Paraselli, S. Park, W. Phung, J. G. Quinn, T. C. Roberts, L. Rougé, J. B. Schwarz, E. Skippington, J. Wai, M. Xu, Z. Yu, H. Zhang, M.-W. Tan and C. E. Heise, *Nature*, 2018, **561**, 189–194.

105 M. Jangra, M. Kaur, R. Tambat, R. Rana, S. K. Maurya, N. Khatri, A. Ghafur and H. Nandanwar, *Antimicrob. Agents Chemother.*, 2019, **63**, 1–16.

106 S. J. Bann, R. D. Ballantine and S. A. Cochrane, *RSC Med. Chem.*, 2021, **12**, 538–551.

107 S. A. Cochrane, C. T. Lohans, J. R. Brandelli, G. Mulvey, G. D. Armstrong and J. C. Vederas, *J. Med. Chem.*, 2014, **57**, 1127–1131.

108 S. A. Cochrane and J. C. Vederas, *Int. J. Antimicrob. Agents*, 2014, **44**, 493–499.

109 S. A. Cochrane, C. T. Lohans, M. J. van Belkum, M. A. Bels and J. C. Vederas, *Org. Biomol. Chem.*, 2015, **13**, 6073–6081.

110 S. A. Cochrane, B. Findlay, A. Bakhtiyari, J. Z. Acedo, E. M. Rodriguez-Lopez, P. Mercier and J. C. Vederas, *Proc. Natl. Acad. Sci. U. S. A.*, 2016, **113**, 11561–11566.

111 R. D. Ballantine, C. E. McCallion, E. Nassour, S. Tokajian and S. A. Cochrane, *MedChemComm*, 2019, **10**, 484–487.

112 M. Jangra, V. Raka and H. Nandanwar, *Molecules*, 2020, **25**, 3255.

113 V. M. Thomas, R. M. Brown, D. S. Ashcraft and G. A. Pankey, *Int. J. Antimicrob. Agents*, 2019, **53**, 663–668.

114 Q. Li, M. Montalban-Lopez and O. P. Kuipers, *Appl. Environ. Microbiol.*, 2018, **84**, 1–15.

115 C. Nord, J. Bjerketorp, J. J. Levenfors, S. Cao, A. A. Strömstedt, B. Guss, R. Larsson, D. Hughes, B. Öberg and A. Broberg, *ACS Chem. Biol.*, 2020, **15**, 2937–2944.

116 X. Zhong, K. Deng, X. Yang, X. Song, Y. Zou, X. Zhou, H. Tang, L. Li, Y. Fu, Z. Yin, H. Wan and X. Zhao, *Front. Microbiol.*, 2023, **14**, 1–14.

117 D. Palpal-latoc, A. J. Horsfall, A. J. Cameron, G. Campbell, S. A. Ferguson, G. M. Cook, V. Sander, A. J. Davidson, P. W. R. Harris and M. A. Brimble, *J. Nat. Prod.*, 2024, **87**, 764–773.

118 Y.-X. Li, Z. Zhong, W.-P. Zhang and P.-Y. Qian, *Nat. Commun.*, 2018, **9**, 1–9.

119 C. E. Seyfert, C. Porten, B. Yuan, S. Deckarm, F. Panter, C. D. Bader, J. Coetzee, F. Deschner, K. H. M. E. Tehrani, P. G. Higgins, H. Seifert, T. C. Marlovits, J. Herrmann and R. Müller, *Angew. Chem., Int. Ed.*, 2023, **62**, 1–11.

120 S. Patel, S. Ahmed and J. S. Eswari, *World J. Microbiol. Biotechnol.*, 2015, **31**, 1177–1193.

121 M. Heidary, A. D. Khosravi, S. Khoshnood, M. J. Nasiri, S. Soleimani and M. Goudarzi, *J. Antimicrob. Chemother.*, 2018, **73**, 1–11.

122 A. Raja, J. LaBonte, J. Lebbos and P. Kirkpatrick, *Nat. Rev. Drug Discovery*, 2003, **2**, 943–944.

123 J. E. Page and S. Walker, *Curr. Opin. Microbiol.*, 2021, **61**, 16–24.

124 M. Ghosh, P. A. Miller, U. Möllmann, W. D. Claypool, V. A. Schroeder, W. R. Wolter, M. Suckow, H. Yu, S. Li, W. W. Huang, J. Zajicek and M. J. Miller, *J. Med. Chem.*, 2017, **60**, 4577–4583.

125 M. Ghosh, Y.-M. Lin, P. A. Miller, U. Möllmann, W. C. Boggess and M. J. Miller, *ACS Infect. Dis.*, 2018, **4**, 1529–1535.

126 A. S. Lee, H. De Lencastre, J. Garau, J. Kluytmans, S. Malhotra-Kumar, A. Peschel and S. Harbarth, *Nat. Rev. Dis. Primers*, 2018, **4**, 1–23.

127 E. Breukink and B. de Kruijff, *Nat. Rev. Drug Discovery*, 2006, **5**, 321–323.

128 V. Yarlagadda, G. B. Manjunath, P. Sarkar, P. Akkapeddi, K. Paramanandham, B. R. Shome, R. Ravikumar and J. Haldar, *ACS Infect. Dis.*, 2016, **2**, 132–139.

129 P. Sarkar, S. Samaddar, V. Ammanathan, V. Yarlagadda, C. Ghosh, M. Shukla, G. Kaul, R. Manjithaya, S. Chopra and J. Haldar, *ACS Chem. Biol.*, 2020, **15**, 884–889.

130 D. Guan, F. Chen, Y. Qiu, B. Jiang, L. Gong, L. Lan and W. Huang, *Am. Ethnol.*, 2019, **131**, 6750–6754.

131 D. Sanderink, V. Cassisa, R. Chenouard, R. Mahieu, M. Kempf, V. Dubée and M. Eveillard, *Future Microbiol.*, 2019, **14**, 581–586.

132 X. Vila-Farres, J. Chu, M. A. Ternei, C. Lemetre, S. Park, D. S. Perlin and S. F. Brady, *mSphere*, 2018, **3**, 1–10.

133 Q. Lu, X. Wu, Y. Fang, Y. Wang and B. Zhang, *Synth. Syst. Biotechnol.*, 2024, **9**, 312–321.

134 E. S. Jayawant, J. Hutchinson, D. Gašparíková, C. Lockey, L. Prúñonosa Lara, C. Guy, R. L. Brooks and A. M. Dixon, *ChemBioChem*, 2021, **22**, 2430–2439.

135 M. F. Lin, P. W. Tsai, J. Y. Chen, Y. Y. Lin and C. Y. Lan, *PLoS One*, 2015, **10**, 1–19.

136 Y. Guo, L. Wang, J. Lei, J. Xu and L. Han, *Jundishapur J. Microbiol.*, 2017, **10**, 1–7.

137 H. Memariani and M. Memariani, *World J. Microbiol. Biotechnol.*, 2023, **39**, 1–28.

138 M. Safari, R. Rafiei Tabatabaei, H. Abtahi, S. Fahimirad and A. Alimoradian, *Jundishapur J. Microbiol.*, 2023, **15**, 1–8.

139 A. Jahangiri, A. Neshani, S. A. Mirhosseini, K. Ghazvini, H. Zare and H. Sedighian, *Microb. Pathog.*, 2021, **150**, 1–7.

140 M. Dai, P. Pan, H. Li, S. Liu, L. Zhang, C. Song, Y. Li, Q. Li, Z. Mao, Y. Long, X. Su and C. Hu, *Exp. Cell Res.*, 2018, **364**, 95–103.

141 M.-J. Kang, A.-R. Jang, J.-Y. Park, J.-H. Ahn, T.-S. Lee, D.-Y. Kim, D.-H. Jung, E.-J. Song, J. J. Hong and J.-H. Park, *Immune Netw.*, 2020, **20**, 1–13.

142 M. Amerikova, I. Pencheva El-Tibi, V. Maslarska, S. Bozhanov and K. Tachkov, *Biotechnol. Biotechnol. Equip.*, 2019, **33**, 671–682.

143 J. G. Routsias, P. Karagounis, G. Parvulesku, N. J. Legakis and A. Tsakris, *Peptides*, 2010, **31**, 1654–1660.

144 B. Wang, F.-W. Zhang, W.-X. Wang, Y.-Y. Zhao, S.-Y. Sun, J.-H. Yu, M. P. Vitek, G. F. Li, R. Ma, S. Wang, Z. Hu and W. Chen, *Front. Microbiol.*, 2022, **13**, 1–16.



145 Y. Guo, M. Xun and J. Han, *Medicine*, 2018, **97**, 1–7.

146 L. Dolzani, A. Milan, M. Scocchi, C. Lagatolla, R. Bressan and M. Benincasa, *J. Med. Microbiol.*, 2019, **68**, 1253–1265.

147 M. Mardirossian, R. Sola, B. Beckert, D. W. P. Collis, A. Di Stasi, F. Armas, K. Hilpert, D. N. Wilson and M. Scocchi, *ChemMedChem*, 2019, **14**, 2025–2033.

148 C. Liu, B. Shan, J. Qi and Y. Ma, *Front. Cell. Infect. Microbiol.*, 2017, **7**, 1–11.

149 J. Mwangi, Y. Yin, G. Wang, M. Yang, Y. Li, Z. Zhang and R. Lai, *Proc. Natl. Acad. Sci. U. S. A.*, 2019, **116**, 26516–26522.

150 F. L. Santana, I. Arenas, E. F. Haney, K. Estrada, R. E. W. Hancock and G. Corzo, *Peptides*, 2021, **141**, 1–11.

151 S. M. Barksdale, E. J. Hrifko, E. M.-C. Chung and M. L. van Hoek, *BMC Microbiol.*, 2016, **16**, 189.

152 F. Ji, G. Tian, D. Shang and F. Jiang, *Front. Microbiol.*, 2023, **14**, 1–18.

153 H. J. Park, H. K. Kang, E. Park, M. K. Kim and Y. Park, *Eur. J. Pharm. Sci.*, 2022, **175**, 1–13.

154 P. Jariyaratthanach, N. Klubthawee, M. Wongchai, S. Roytrakul and R. Aunpad, *Sci. Rep.*, 2022, **12**, 15852.

155 F. Sacco, C. Bitossi, B. Casciaro, M. R. Loffredo, G. Fabiano, L. Torrini, F. Raponi, G. Raponi and M. L. Mangoni, *Antibiotics*, 2022, **11**, 1–12.

156 Z. Dekan, S. J. Headley, M. Scanlon, B. A. Baldo, T. Lee, M. Aguilar, J. R. Deuis, I. Vetter, A. G. Elliott, M. Amado, M. A. Cooper, D. Alewood and P. F. Alewood, *Angew. Chem., Int. Ed.*, 2017, **56**, 8495–8499.

157 W. G. Lima, J. C. M. Brito, M. E. de Lima, A. C. S. T. Pizarro, M. A. M. de M. Vianna, M. C. de Paiva, D. C. S. de Assis, V. N. Cardoso and S. O. A. Fernandes, *J. Antibiot.*, 2021, **74**, 425–434.

158 A. L. Carboni, M. A. Hanson, S. A. Lindsay, S. A. Wasserman and B. Lemaitre, *Genetics*, 2022, **220**, 1–10.

159 M. Wang, J. Lin, Q. Sun, K. Zheng, Y. Ma and J. Wang, *Appl. Microbiol. Biotechnol.*, 2019, **103**, 1765–1775.

160 J. Peng, H. Long, W. Liu, Z. Wu, T. Wang, Z. Zeng, G. Guo and J. Wu, *Infect. Drug Resist.*, 2019, **12**, 2417–2428.

161 W. Liu, Z. Wu, C. Mao, G. Guo, Z. Zeng, Y. Fei, S. Wan, J. Peng and J. Wu, *Front. Microbiol.*, 2020, **11**, 1–13.

162 J. Kim, B. Jacob, M. Jang, C. Kwak, Y. Lee, K. Son, S. Lee, I. D. Jung, M. S. Jeong, S.-H. Kwon and Y. Kim, *Sci. Rep.*, 2019, **9**, 1–13.

163 S. Mandel, J. Michaeli, N. Nur, I. Erbetti, J. Zazoun, L. Ferrari, A. Felici, M. Cohen-Kutner and N. Bachnoff, *Sci. Rep.*, 2021, **11**, 1–22.

164 G. Schouten, F. Paulussen, O. Kuipers, W. Bitter, T. Grossmann and P. van Ulzen, *Antibiotics*, 2022, **11**, 1–16.

165 M. Krishnan, J. Choi, A. Jang, Y. K. Yoon and Y. Kim, *Int. J. Mol. Sci.*, 2021, **22**, 1–22.

166 S. Eshtiaghi, R. Nazari and M. Fasihi-Ramandi, *Curr. Microbiol.*, 2023, **80**, 1–13.

167 M. G. Eales, E. Ferrari, A. D. Goddard, L. Lancaster, P. Sanderson and C. Miller, *Res. Microbiol.*, 2018, **169**, 296–302.

168 R. Gopal, Y. G. Kim, J. H. Lee, S. K. Lee, J. D. Chae, B. K. Son, C. H. Seo and Y. Park, *Antimicrob. Agents Chemother.*, 2014, **58**, 1622–1629.

169 X. Vila-Farrés, R. López-Rojas, M. E. Pachón-Ibáñez, M. Teixidó, J. Pachón, J. Vila and E. Giralt, *Eur. J. Med. Chem.*, 2015, **101**, 34–40.

170 Y. Wang, L. Wang, H. Yang, H. Xiao, A. Farooq, Z. Liu, M. Hu and X. Shi, *Toxins*, 2016, **8**, 1–9.

171 L. Yang, Z. Tian, W. Zhao, J. Zhang, C. Tian, L. Zhou, Z. Jiao, J. Peng and G. Guo, *Bioorg. Chem.*, 2023, **138**, 1–16.

172 L. Yang, Y. Gao, J. Zhang, C. Tian, F. Lin, D. Song, L. Zhou, J. Peng and G. Guo, *Int. J. Antimicrob. Agents*, 2024, **63**, 1–12.

173 A. G. Elliott, J. X. Huang, S. Neve, J. Zuegg, I. A. Edwards, A. K. Cain, C. J. Boinett, L. Barquist, C. V. Lundberg, J. Steen, M. S. Butler, M. Mobli, K. M. Porter, M. A. T. Blaskovich, S. Locuero, M. Strandh and M. A. Cooper, *Nat. Commun.*, 2020, **11**, 1–13.

174 M. J. Hong, M. K. Kim and Y. Park, *Int. J. Mol. Sci.*, 2021, **22**, 1–18.

175 X. Luo, X. Ye, L. Ding, W. Zhu, Z. Zhao, D. Luo, N. Liu, L. Sun and Z. Chen, *Microb. Pathog.*, 2021, **157**, 1–7.

176 D. C. Rajapaksha, E. H. T. T. Jayathilaka, S. L. Edirisinghe, C. Nikapitiya, J. Lee, I. Whang and M. De Zoysa, *Fish Shellfish Immunol.*, 2021, **117**, 82–94.

177 D. C. Rajapaksha, S. L. Edirisinghe, C. Nikapitiya, I. Whang and M. De Zoysa, *Antibiotics*, 2023, **12**, 1–13.

178 E. H. T. T. Jayathilaka, D. C. Rajapaksha, C. Nikapitiya, J. Lee, M. De Zoysa and I. Whang, *Pharmaceuticals*, 2022, **15**, 1–19.

179 P. K. Hazam, C.-C. Cheng, C.-Y. Hsieh, W.-C. Lin, P.-H. Hsu, T.-L. Chen, Y.-T. Lee and J.-Y. Chen, *Int. J. Mol. Sci.*, 2022, **23**, 1–12.

180 M. T. P. Gontijo, P. M. P. Vidigal, M. E. S. Lopez and M. Brocchi, *Res. Microbiol.*, 2021, **172**, 1–9.

181 W. C. B. Lai, X. Chen, M. K. Y. Ho, J. Xia and S. S. Y. Leung, *Int. J. Pharm.*, 2020, **589**, 1–17.

182 C. Li, M. Jiang, F. M. Khan, X. Zhao, G. Wang, W. Zhou, J. Li, J. Yu, Y. Li, H. Wei and H. Yang, *ACS Infect. Dis.*, 2021, **7**, 3336–3344.

183 K. Abdelkader, D. Gutiérrez, H. Tamés-Caunedo, P. Ruas-Madiedo, A. Safaan, A. S. Khairalla, Y. Gaber, T. Dishisha and Y. Briers, *Appl. Environ. Microbiol.*, 2022, **88**, 1–15.

184 H. Yang, M. Wang, J. Yu and H. Wei, *Front. Microbiol.*, 2015, **6**, 1–9.

185 M. M. Islam, D. Kim, K. Kim, S.-J. Park, S. Akter, J. Kim, S. Bang, S. Kim, J. Kim, J. C. Lee, C.-W. Hong and M. Shin, *Front. Microbiol.*, 2022, **13**, 1–13.

186 S. Y. Peng, R. I. You, M. J. Lai, N. T. Lin, L. K. Chen and K. C. Chang, *Sci. Rep.*, 2017, **7**, 1–12.

187 M. Thandar, R. Lood, B. Y. Winer, D. R. Deutsch, C. W. Euler and V. A. Fischetti, *Antimicrob. Agents Chemother.*, 2016, **60**, 2671–2679.

188 V. Defraigne, J. Schuermans, B. Grymonprez, S. K. Govers, A. Aertsen, M. Fauvert, J. Michiels, R. Lavigne and Y. Briers, *Antimicrob. Agents Chemother.*, 2016, **60**, 3480–3488.

189 I. Rázquin-Olazarán, H. Shahrou and G. Martínez-De-Tejada, *J. Biomed. Sci.*, 2020, **27**, 1–19.



190 S. M. Son, J. Kim and S. Ryu, *Front. Microbiol.*, 2023, **14**, 1–11.

191 W. F. Porto, L. Irazazabal, E. S. F. Alves, S. M. Ribeiro, C. O. Matos, Á. S. Pires, I. C. M. Fensterseifer, V. J. Miranda, E. F. Haney, V. Humblot, M. D. T. Torres, R. E. W. Hancock, L. M. Liao, A. Ladram, T. K. Lu, C. de la Fuente-Nunez and O. L. Franco, *Nat. Commun.*, 2018, **9**, 1–12.

192 S. Paul, S. Verma and Y.-C. Chen, *ACS Infect. Dis.*, 2024, **10**, 1034–1055.

193 M. Stach, T. N. Siriwardena, T. Köhler, C. van Delden, T. Darbre and J. Reymond, *Angew. Chem.*, 2014, **126**, 13041–13045.

194 J. Pires, T. N. Siriwardena, M. Stach, R. Tinguely, S. Kasraian, F. Luzzaro, S. L. Leib, T. Darbre, J.-L. Reymond and A. Endimiani, *Antimicrob. Agents Chemother.*, 2015, **59**, 7915–7918.

195 T. N. Siriwardena, A. Lüscher, T. Köhler, C. van Delden, S. Javor and J. Reymond, *Helv. Chim. Acta*, 2019, **102**, 1–11.

196 T. N. Siriwardena, A. Capecci, B. Gan, X. Jin, R. He, D. Wei, L. Ma, T. Köhler, C. van Delden, S. Javor and J. Reymond, *Angew. Chem.*, 2018, **130**, 8619–8623.

197 T. Heinonen, S. Hargraves, M. Georgieva, C. Widmann and N. Jacquier, *J. Global Antimicrob. Resist.*, 2021, **25**, 227–231.

198 S. Joshi, G. S. Bisht, D. S. Rawat, A. Kumar, R. Kumar, S. Maiti and S. Pasha, *Biochim. Biophys. Acta, Biomembr.*, 2010, **1798**, 1864–1875.

199 D. Sharma, M. Choudhary, J. Vashist, R. Shrivastava and G. S. Bisht, *Biochem. Biophys. Res. Commun.*, 2019, **518**, 472–478.

200 S. H. Moon and E. Huang, *Antimicrob. Agents Chemother.*, 2018, **62**, 1–5.

201 D. Nagarajan, N. Roy, O. Kulkarni, N. Nanajkar, A. Datey, S. Ravichandran, C. Thakur, S. T, I. V. Aprameya, S. P. Sarma, D. Chakravortty and N. Chandra, *Sci. Adv.*, 2019, **5**, 1–19.

202 W. Li, N. M. O'Brien-Simpson, J. A. Holden, L. Otvos, E. C. Reynolds, F. Separovic, M. A. Hossain and J. D. Wade, *Pept. Sci.*, 2018, **110**, 1–9.

203 Q. He, L. Zhao, G. Li, Y. Shen, Y. Hu and Y. Wang, *New J. Chem.*, 2022, **46**, 6577–6586.

204 C. Zampaloni, P. Mattei, K. Bleicher, L. Winther, C. Thäte, C. Bucher, J.-M. Adam, A. Alanine, K. E. Amrein, V. Baidin, C. Bieniossek, C. Bissantz, F. Boess, C. Cantrill, T. Clairfeuille, F. Dey, P. Di Giorgio, P. du Castel, D. Dylus, P. Dzygiel, A. Felici, F. García-Alcalde, A. Haldimann, M. Leipner, S. Leyn, S. Louvel, P. Misson, A. Osterman, K. Pahil, S. Rigo, A. Schäublin, S. Scharf, P. Schmitz, T. Stoll, A. Trauner, S. Zoffmann, D. Kahne, J. A. T. Young, M. A. Lobritz and K. A. Bradley, *Nature*, 2024, **625**, 566–571.

